University of Washington
Department of Orthopaedics and Sports Medicine

2005 Research Report

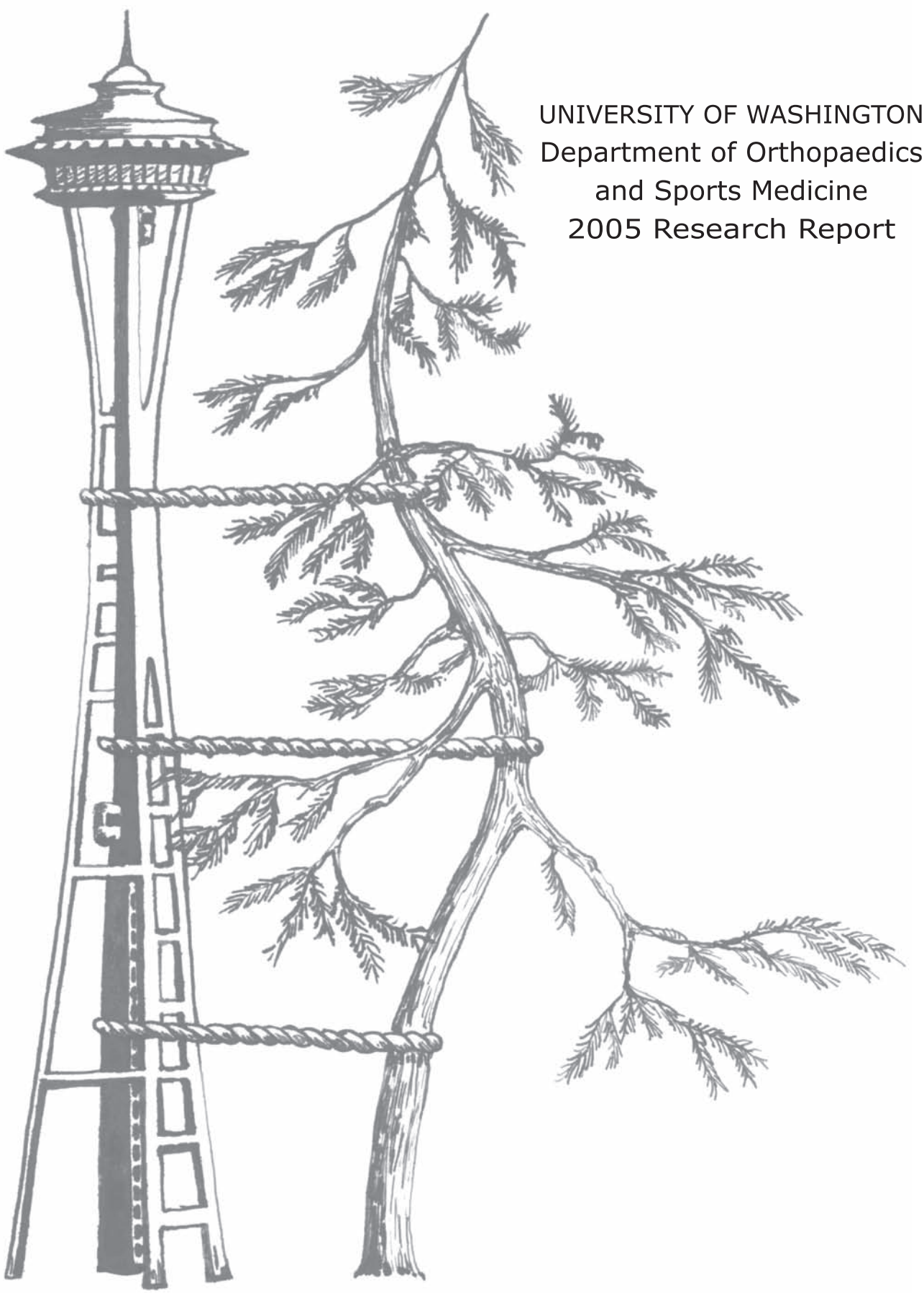

UNIVERSITY OF WASHINGTON

Department of Orthopaedics and Sports Medicine 2005 Research Report

UW Medicine
SCHOOL OF MEDICINE

Department of Orthopaedics and Sports Medicine
University of Washington
Seattle, WA 98195

Editor:
Frederick A. Matsen III, M.D.
Fred Westerberg

Design & Layout:
Fred Westerberg

Cover Illustration: "The Club-Footed Boy" by Jusepe de Ribera
1642. Oil on canvas.
Photograph: Erich Lessing
Louvre, Paris, France.
Photo Credit: Erich Lessing / Art Resource, NY

Contents

Foreword

This year's Research Report is covered by one of the last major paintings of Jusepe de Ribera (1591-1652), titled the Club-Footed Boy (1642). This 1.6 X .9 meter canvas can be seen at the Louvre in Paris. Like many physicians, painter de Ribera was able to see the strength, calm and inner beauty in individuals who were deformed and those who were suffering. Whether your diagnosis in this person is club foot, or, as I tend to think, right spastic hemiplegia, we cannot escape the fact that the young Spanish boy is smiling and sports the martial stance of a hidalgo, his crutch over his shoulder like a musket. Yet his pride does not keep him from asking for assistance; the note in his hand reads, "Give me help for the love of God". De Ribera was born in Jativa, moving to Rome as a teenager. He survived by begging in the streets and working as a lackey. He became a prolific artist, painting the entire spectrum of human existence, from the unsettling Bearded Women, to the unfortunate Blind Sculptor, to the pugnacious Match of Women, to the realistic Martyrdom of St. Bartholomew and to the grace of Rapture of St. Magdalen. As his career became successful, he was able to move to Naples where he lived like a nobleman and carried the title of "Roman Academician". Yet, like the best of physicians, he never lost his ability to understand and treat those who were poor, deformed or suffering. He knew personal sorrow as well: his daughter was one of the 'victims' of Don Juan of Austria.

In keeping with the theme of the foot, introduced by our cover, this Report features several important articles on the foot – a particular area of expertise of our faculty. The first two deal with the surgical management of fractures of the calcaneous, or heel bone. It is of note that when I began my residency in 1971, these fractures, no matter how severe, were essentially ignored because of the inadequacy of fixation methods and the high complication rates when surgery was attempted. In those days, the painful and deformed foot was managed by having special shoes made to accommodate it. Now, as the articles demonstrate, our surgeons have developed methods for reducing and stabilizing these fractures so that structure and comfort are restored. Our foot and ankle faculty continue to make advances, thanks both to their expertise and to the support of the Jerome Debs Endowed Chair for Foot and Ankle Reconstruction, held by Steven Benirschke, and to the Veterans Affairs Center Grant, headed by Bruce Sangeorzan.

I have arranged the next group of articles anatomically, moving up from the foot to fractures of the knee, to fractures of the hip in the young, and finally to fractures of the pelvis (including a novel car seat system to reduce the risk of these injuries in "T-Bone" auto accidents). The upper extremity section starts with the work on restoring stability in dislocating surgery (supported by the Harryman/DePuy Endowed Chair), fixation of elbow fractures, restoration of movement to the stiff elbow, and finally to the management of wrist arthritis and the thumb injury known as "game keeper's thumb", an injury I personally sustained and from which I've made a full recovery thanks to the authors of this article.

Frederick A. Matsen III, M.D.
Professor and Chairman

The next two articles demonstrate our ongoing work in understanding the genesis of bone tumors and also on the restoration of function of the knee after resection of large malignant tumors.

What do Botox and crab skeletons have to do with Orthopaedics? To find out you'll just have to read the next two articles to find out. The Botox study was supported by the Hansen Endowed Chair and the chitosan study by the Washington Women's Foundation.

We conclude with two articles from the laboratories supported by the Burgess Endowed Chair for Orthopaedic Investigation, one on basic science related to the exciting field of cartilage tissue engineering (which holds promise for the treatment of arthritis) and one on the collagen structure of the intervertebral disc (which enhances our understanding of the structure most commonly implicated in low back pain).

From this Report you can see that the Department is tackling the key problems in Orthopaedics, those that take away the pleasure of healthy form and function from so many individuals. We are most grateful to those who support our investigative programs. To assure the future of our efforts to improve quality of life for those at risk for bone and joint problems, we have identified four priority areas where support would substantially enhance our ability to discover new solutions:

(1) Regenerative Orthopaedics. We are convinced that the solutions of the future for bone and joint problems such as arthritis, osteoporosis, degenerative spine disease, tendon failure, and problems with fracture healing will lie in harnessing the body's ability to regenerate itself. We have active programs in exploring the signals that turn on the body's ability to make bone, to make fibrocartilage, and to develop other new musculoskeletal tissues. We are seeking $1.5 million to establish a novel program in regenerative orthopaedics and tissue engineering.

(2) Pelvic and acetabular surgery. Our Department has been a world leader in the development of techniques that preserve life and function after these fractures, which are an all too common result of motor vehicle, climbing and skiing accidents. We hope to raise $1.5 million to permanently endow a chair to perpetuate this program.

(3) Amputations and prosthetics. Our Department has pioneered new techniques in amputation surgery and in restoring limb function with comfortable, cosmetic, and energy returning prostheses. We hope to raise $1.5 million to permanently endow a chair to perpetuate this program.

(4) Health of the student athlete. Our Department has a distinguished track record of research and practice to enable participation in sports and athletics safe for student athletes and to enable rapid restoration of function and ability to play after injury. We hope to raise $1.5 million to permanently endow a chair to perpetuate this program.

These four foundational programs will join our other endowed research programs in enabling us to aggressively pursue new methods for a wide range of individuals who today are seriously compromised by bone and joint injuries and degeneration.

If you would like to learn more about any of these programs, just drop me a note, a call or an email.

Best wishes,

Frederick A. Matsen III, M.D.
University of Washington Medical Center
Department of Orthopaedics and Sports Medicine
1959 NE Pacific Street, Box 356500
Seattle, WA 98195
Office Phone (206) 543-3690
Email: matsen@u.washington.edu

Department of Orthopaedics and Sports Medicine Faculty

Frederick A. Matsen III, M.D.
Professor and Chair

Christopher H. Allan, M.D.
Assistant Professor

Dheera Ananthakrishnan, M.D.
Assistant Professor

David P. Barei, M.D.
Assistant Professor

Carlo Bellabarba, M.D.
Assistant Professor

Stephen K. Benirschke, M.D.
Professor

Stanley J. Bigos, M.D.
Professor Emeritus

Richard J. Bransford, M.D.
Assistant Professor

Howard A. Chansky, M.D.
Associate Professor

Jens R. Chapman, M.D.
Professor

John M. Clark, M.D., Ph.D.
Professor

Ernest U. Conrad III, M.D.
Professor

David R. Eyre, Ph.D.
Professor

Russell J. Fernandes, Ph.D.
Research Assistant Professor

John R. Green III, M.D.
Associate Professor

Theodore K. Greenlee, Jr., M.D.
Associate Professor Emeritus

Ted S. Gross, Ph.D.
Associate Professor

Douglas P. Hanel, M.D.
Professor

Sigvard T. Hansen, Jr., M.D.
Professor

Dennis A. Hanson, Ph.D.
Research Assistant Professor

M. Bradford Henley, M.D.
Professor

Nancy J. Kadel, M.D.
Assistant Professor

Leonid I. Katolik, M.D.
Assistant Professor

Roger V. Larson, M.D.
Associate Professor

Seth S. Leopold, M.D.
Associate Professor

Sohail K. Mirza, M.D.
Associate Professor

Vincent S. Mosca, M.D.
Associate Professor

Sean E. Nork, M.D.
Assistant Professor

John W. O'Kane, M.D.
Associate Professor

Milton L. Routt, Jr., M.D.
Professor

Bruce J. Sangeorzan, M.D.
Professor

Gregory A. Schmale, M.D.
Assistant Professor

John A. Sidles, Ph.D.
Professor

Douglas G. Smith, M.D.
Associate Professor

Kevin L. Smith, M.D.
Associate Professor

Kit M. Song, M.D.
Associate Professor

Sundar Srinivasan, Ph.D.
Research Assistant Professor

Lynn T. Staheli, M.D.
Professor Emeritus

Lisa A. Taitsman, M.D., M.P.H.
Assistant Professor

Carol C. Teitz, M.D.
Professor

Allan F. Tencer, Ph.D.
Professor

Thomas E. Trumble, M.D.
Professor

Christopher J. Wahl, M.D.
Assistant Professor

Jiann-Jiu Wu, Ph.D.
Research Associate Professor

Liu Yang, Ph.D.
Research Assistant Professor

Adjunct Faculty

Basia R. Belza, R.N., Ph.D.
Associate Professor, Physiological Nursing

Jack W. Berryman, Ph.D.
Professor, Medical History & Ethics

Charles H. Chesnut, M.D.
Professor, Nuclear Medicine

Randal P. Ching, Ph.D.
Associate Professor, Mechanical Engineering

Richard A. Deyo, M.D.
Professor, Medicine

Gregory C. Gardner, M.D.
Associate Professor, Rheumatology

Thurman Gillespy III, M.D.
Associate Professor, Radiology

Daniel O. Graney, Ph.D.
Professor, Biological Structure

Frederick A. Mann, M.D.
Professor, Radiology

Arshad R. Muzaffar, M.D.
Assistant Professsor, Surgery

Susan M. Ott, M.D.
Associate Professor, Division of Metabolism

Wendy Raskind, M.D., Ph.D.
Professor, General Internal Medicine

Michael L. Richardson, M.D.
Professor, Radiology

Peter A. Simkin, M.D.
Professor, Medicine

Tony J. Wilson, M.D.
Professor, Radiology

Miqin Zhang, Ph.D.
Assistant Professor, Materials Science and Engineering

Joint Faculty

Mark A. Harrast, M.D.
Assistant Professor, Rehabilitation Medicine

John E. Olerud, M.D.
Professor, Division of Dermatology

Nathan J. Smith, M.D.
Professor Emeritus, Pediatrics

Michael D. Strong, Ph.D.
Research Professor, Surgery

Nicholas B. Vedder, M.D.
Professor, Plastic Surgery

Clinical Faculty

Sarah E. Jackins, R.P.T.
Assistant Professor, Rehabilitation Medicine

University of Washington

UW Medicine
SCHOOL OF MEDICINE

University of Washington School of Medicine

Department of Orthopaedics and Sports Medicine

1959 N.E. Pacific Street
Box 356500
Seattle, Washington 98195-6500
Phone: (206) 543-3690
Fax: (206) 685-3139

Affiliated Institutions

Children's Hospital and
Regional Medical Center
4800 Sand Point Way NE
Seattle, WA 98105
(206) 987-1776

Harborview Medical Center
325 Ninth Avenue
Seattle, WA 98104
(206) 731-3466

University of Washington
Medical Center
Bone and Joint Center
4245 Roosevelt Way NE
Seattle, WA 98105
(206) 598-4288

VA Puget Sound Health Care System
1660 South Columbian Way
Seattle, WA 98108
(206) 764-2215

Visiting Lecturers

Emil Schemitsch, M.D.
2005 LeCocq Lecturer

Richard A. Brand, M.D.
2005 OREF Hark Lecturer, Residents' Research Days

This year at our annual LeCocq Lecture on January 20 and 21st, we were honored to have Dr. Emil Schemitsch as our 2005 LeCocq Lecturer. Dr. Schemitsch is currently the Head of the Division of Orthopaedic Surgery at St. Michael's Hospital, a position he has held since 2001. He is also a Professor of Surgery at the University of Toronto. Dr. Schemitsch received his M.D. degree from the University of Toronto as well as his orthopedic training. Dr. Schemitsch completed a research fellowship at the University of Washington, Harborview Medical Center in 1992 and a fellowship at the Brigham and Women's Hospital in Boston in 1993. He has received numerous awards including the North American Traveling Fellowship, the ABC Traveling Fellowship, the Samson Award from the Canadian Orthopaedic Association for lifetime achievement in research, the RB Salter teaching award, the Founders medal for research from the COA , as well as the Bovill Award from the OTA. He is also the Deputy Editor for research for the *Journal of Orthopedic Trauma* and has been active in numerous orthopaedic associations.

His primary clinical interests are in trauma and joint replacement. His research interests are in the systemic response to trauma, fracture healing and biomechanics as well as clinical trials and outcome studies. His publications and grants in these areas are numerous. The faculty, residents, and community physicians were treated to 3 innovating lectures from Dr. Schemitsch during the 2 days: "Femoral Fracture Management in the Poly Trauma Patient: From Bench to Bedside," "The Use of Bone Substitutes in Orthopaedic Trauma," and "Current Concepts in the Treatment of Open Tibial Fractures."

This year at our annual Residents' Research Days on May 19 and 20th, we were honored to have Dr. Richard A. Brand, M.D. as our OREF Hark Lecturer. Dr. Brand is the current Editor-in-Chief of *Clinical Orthopaedics and Related Research* and a Clinical Professor in the Department of Orthopaedic Surgery at the University of Iowa. He has received numerous honors such as the Otto E. Aufranc Award twice from the Hip Society and also the Kappa Delta Young Investigator's award from the American Academy of Orthopaedic Surgeons. He is an active member in many societies, including the Hip Society, History of Science Society, American Orthopaedic Association, European Society of Biomechanics, American Society of Biomechanics of which he became president in 1984-1985 and the Orthopaedic Research Society, serving as president in 1997-1998. Prior to becoming Editor-in-Chief for *Clinical Orthopaedics and Related Research*, he served as Editor-in-Chief for the *Journal of Biomechanics* from 1987-2002 and he has served on the Board of Trustees for the Orthopaedic Research and Education Foundation in 2002 and the Hospital for Special Surgery beginning in 2004.

Dr. Brand has authored more than 200 journal articles, book chapters and abstracts. Some of Dr. Brand's current research interests include cell mechanics and connective tissue adaptation as well as receiving a grant in 2001-2002 from the American Academy of Orthopaedic Surgeons/ Orthopaedic Research Society to explore the incidence and scope of activity of Orthopaedic clinicians-scientists in the US. During the 2 days of lectures, the faculty, residents, and community physicians were treated to 2 lectures from Dr. Brand: "Clinician-Scientists: An Endangered Species?' and "Writing for Keeps: How to Prepare an Archival Manuscript." In addition to Dr. Brand's lectures, the R3's and the R4's presented the progress of their research, while the R5's presented the completion of their research projects.

Surgical Dynamics Endowed Chair
Sohail K. Mirza, M.D.

Dr. Sohail K. Mirza has been named as the first holder of the Surgical Dynamics Endowed Chiar for Spine Research as of October 1, 2004. Dr. Mirza received his medical postgraduate training at the University of Washington and Harvard University. He completed his Masters in Public Health at the University of Washington in March of 2005. Dr. Mirza has been a member of the UW faculty since 1995 and has held the title of Associate Professor since 2001. In addition to his faculty positions in orthopaedics and neurological surgery, he is a member of the Faculty Council on Research and the Medical Quality Assurance Committee. In September 2002, Dr. Mirza received a major grant from the National Institute of Arthritis and Musculoskeletal and Skin Diseases on the Safety of Lumbar Fusion Surgery for Chronic Back Pain. He was also awarded the American Orthopaedic Association's ABC Fellowship in 2003. We are delighted to recognize Dr. Mirza's expertise, dedication, and contributions with his appointment to the Surgical Dynamics Endowed Chair.

Is Delayed Open Reduction Internal Fixation Of Calcaneal Fractures Effective?

John R. Shank, M.D., Michael P. Swords, D.O., Stephen K. Benirschke, M.D., and Patricia A. Kramer, Ph.D.

Although multiple studies support open reduction internal fixation (ORIF) of calcaneus fractures, no current study supporting delayed open reduction and internal fixation (ORIF) exists. Judet theorized that fractures involving the posterior facet were, by definition, injuries to the subtalar joint. Because these injuries disrupt the subtalar articular surface, reduction that is short of anatomic can lead to complications. ORIF within the first several weeks following injury is preferable because obtaining a reduction is easier prior to consolidation of fracture callous. Secondly, restoring the normal gastrocnemius-soleus working length via restoration of height becomes considerably more difficult as the delay between fracture and surgery increases. For these reasons, many surgeons elect to not attempt anatomic reduction, instead opting for closed treatment or primary subtalar arthrodesis for those injuries presenting late. Closed treatment and subtalar arthrodesis are not optimal choices, however, because they not only sacrifice motion in the hindfoot, but also alter the mechanics of the forefoot and midfoot, leading to further stress on these joints. Studies indicate that up to 50% of patients continue to have pain following subtalar arthrodesis for calcaneal fracture. The purpose of the present study was to examine the outcome of a group of calcanal fractures treated with ORIF > 25 days after injury. Twenty five days was selected as a time when many surgeons would elect other treatment than formal open reduction internal fixation. Results were evaluated with measurement of Böhler's angle, calcaneal height and the Musculoskeletal Function Assessments (MFA).

Materials and Methods

This study was performed with the approval of Harborview's Human Subjects Internal Review Board. Twenty patients sustaining calcaneal fracture that were treated with ORIF > 25 days after injury were retrospectively identified over an 8-year period (January 1994 – January 2002). Preoperative lateral and axial radiographs of the involved and contralateral extremity were obtained for all patients along with coronal and axial CT scans of the involved limb. Both joint depression and tongue-type injuries were represented.

All patients were treated by the senior author (SKB) with ORIF using a extensile lateral approach with standard AO fixation techniques. An extensile lateral approach was performed over the lateral aspect of the hindfoot and taken sharply down to bone. A thick flap was formed by subperiosteal exposure protecting the sural nerve and peroneal tendons within the flap. Care was taken to protect the critical branch of the peroneal artery in all cases. The goal of each operative procedure was anatomic reduction with restoration of calcaneal height, length and alignment with stable internal fixation. Allograft bone graft was used in most cases. Hemovac drainage and splinting were used to protect the soft tissues postoperatively. Early subtalar and ankle range of motion were emphasized when incisional drainage ceased.

Radiographic and clinical followup was performed at regularly scheduled intervals postoperatively. Weightbearing was instituted no earlier than three months, with the specific time to weightbearing dependent on clinical and radiographic evidence of healing. Böhler's angle and calcaneal height of the injured calcaneus were measured using standard techniques from radiographs obtained at the time of initial presentation, following operative fixation and at final followup (Figure 1A & 1B). Böhler's angle and calcaneal height of the contralateral calcaneus were measured on radiographs taken at the time of the initial presentation. Musculoskeletal Function Assessments (MFA) were conducted on those patients who were available for interview. Statistical analysis was performed using STATA (College Station, TX) with significance set at $p > 0.05$

Results

Two patients were lost to followup leaving 18 patients for data analysis. Eleven patients were male (61%), seven female (39%) with an average age of 39.8 years (range 27 – 59 yr). Mechanism of injury was a fall in 13 and a motor vehicle accident in 5. There was one open fracture. Eleven injuries were joint depression with 7 tongue-type fracture patterns. Mean operative time including nerve block was 382 minutes (range 240 – 640 min) with a mean estimated blood loss of 575 milliliters (range 150 – 3500 ml). The mean time from injury to fixation was 33.4 days. (range 26-58 days) The treatment of the majority of patients (n = 15, 83%) was either delayed as a result of a late referral from an outside institution or until the patient was hemodynamically stable following treatment of other traumatic or musckuloskeletal injury. Two patients (11%) had delayed treatment secondary to fracture blisters. One patient (6%) underwent ORIF at 31 days following sepsis after operative treatment of a tibial plateau fracture. Two patients (11%) had preoperative evidence of deep venous thrombosis (DVT), both detected by ultrasound and treated with preoperative Greenfield filter with no long-term sequelae. None of the isolated calcaneal fractures required blood transfusion following ORIF. There were no cases of wound dehiscence or postoperative infection. No patient underwent gastrocnemius recession or percutaneous tendoachilles lengthening at the index operation. Eight patients (44%) developed symptomatic hardware requiring removal. There were 4 secondary operative procedures performed after the index operation including one claw toe correction, one ankle cheilectomy with percutaneous tendo-achilles lengthening and one gastrocnemius slide with extra-

a.

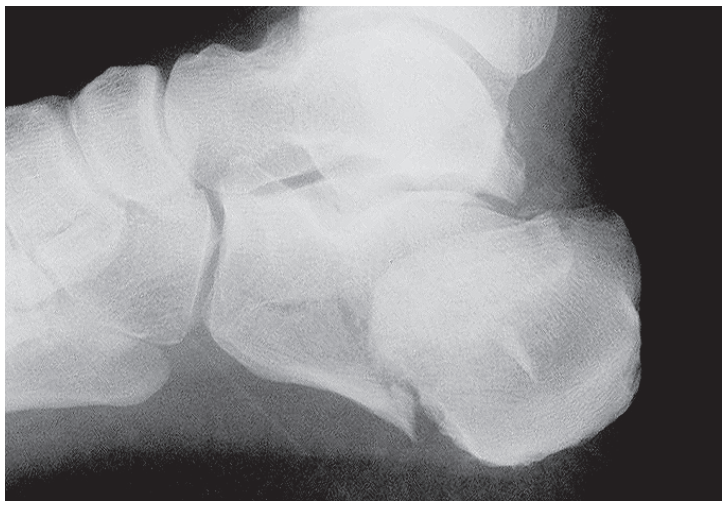

b.

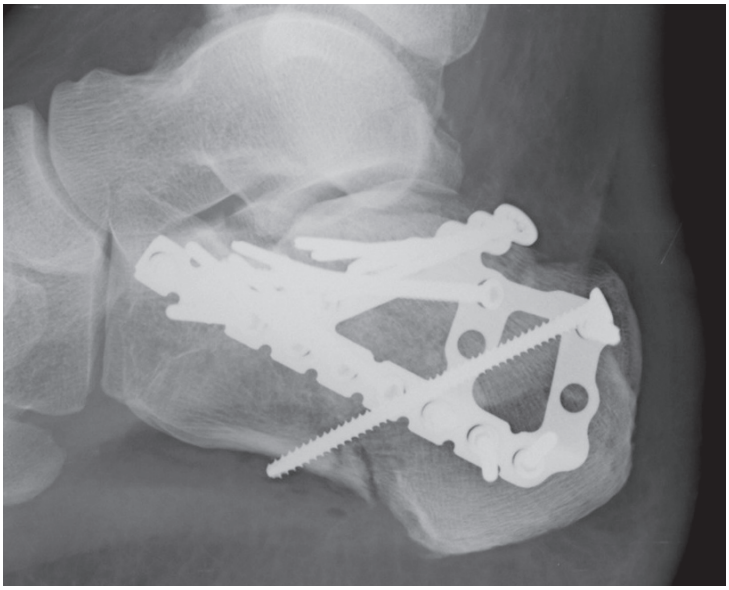

Figure 1a. Injury radiograph. 1b. Post-surgical radiograph

articular calcaneal osteotomy. One patient did require an extra-articular osteotomy at 1.5 years following ORIF secondary to a tuberosity malunion. All of these procedures were delayed until there was clinical and radiographic evidence of calcaneal healing. No patient required subtalar arthrodesis at final followup.

Mean Böhler's angle at the time of injury was 10.9 degrees (SD +/- 18.4) which corrected to a mean of 33.3 degrees (SD +/- 8.5) degrees following operative fixation. Mean followup Böhler's angle decreased to 28.1 degrees (SD +/- 9.0) degrees at final followup. Mean contralateral Böhler's angle was 32.3 degrees (SD +/- 3.3). Mean calcaneal height at the time of injury was 46.2 mm which increased to a mean value of 56.9 mm following operative fixation. The mean calcaneal height on final followup radiographs was 55.5 mm. The mean contralateral calcaneal height was 57.5 mm. Mean MFA score was 16.5. Individual MFA scores were not correlated with Böhler's angle or height, although only 6 patients had both MFA scores and a complete set of radiographs.

Discussion

Anatomic reduction and rigid internal fixation has been advocated as the treatment of choice for virtually all displaced calcaneal fractures. While superior results with operative treatment have been demonstrated, the effect of delayed treatment on outcome has been undocumented. Benefits of anatomic reduction include decreased incidence of subtalar arthrosis, re-establishment of length and height of the calcaneus, prevention of anterior tibiotalar abutment, decompression of the peroneal tendons and narrowing of the hindfoot. Studies indicate that nonoperative care is six times more likely to require subtalar arthrodesis than when ORIF is performed.

Essex Lopresti stated that calcaneal fractures treated late may take a longer time to unite, require a more extensive local exposure and be technically more difficult to reduce and maintain reduction. While more effort is required to precisely reduce these injuries, the additional effort is worthwhile as closed treatment can lead to many problem, including an incongruous subtalar joint, decreased calcaneal body height which results in a shortened Achilles lever arm, lateral calcaneal wall expansion with fibular impingement, hindfoot varus/valgus, midfoot malalignment, flattening of the longitudinal arch, decreased talocalcaneal angle resulting in tibiotalar impingement, and talonavicular subluxation. The aberrant spatial relationships between the calcaneus, talus, navicular and cuboid can disrupt the normal harmonic motion of these joints necessary for the complex motion of the hindfoot. Salvage procedures to correct these problems are difficult. In situ subtalar arthrodesis is unable to restore physiologic heel height, talocalcaneal angle or talar inclination in injuries involving collapse of the subtalar joint. Furthermore, subtalar arthrodesis leads to loss of motion in the hindfoot and further stress on the midtarsal joints. Procedures such as distraction subtalar bone block arthrodesis may become necessary.

Mean MFA at final followup was determined to be 16.5 which is comparable to MFA scores on patients with hindfoot injuries treated on a more acute basis.

Our data suggest that formal ORIF is a viable and safe surgical option for

patients with delayed presentation of calcaneal fractures, although the delay in treatment may increase the interval between surgery and a return to full activities and work. Formal anatomic operative reduction is successful in treating these injuries with a low incidence of complications. Primary subtalar arthrodesis should be reserved for late pain and deformity of calcaneal fractures following open reduction internal fixation.

Recommended Reading

Bezes H, Massart P, Delvaux D, Fourquet JP, Tazi F. The operative treatment of intraarticular Calcaneal fractures. Clin Orthop. 1993;290:55-59.

Buch BD, Myerson MS, Miller SD. Primary subtalar arthrodesis for the treatment of comminuted Calcaneal fractures. Foot Ankle Int. 1996;17:61-70.

Kundel K, Funk E, Brutcher M, Bickel R. Calcaneal fractures: operative versus nonoperative Treatment. J Trauma.1996;41:839-845.

Letournel E. Open treatment of acute calcaneal fractures. Clin Orthop. 1993;290:60-67.

Myerson MS. Primary subtalar arthrodesis for the treatment of comminuted fractures of the Calcaneus. Orthop Clin North Am. 1995;26:215-227.

Prospective Comparison of Extensile vs. Minimally Invasive Reduction and Small Fragment Fixation of Tongue-type Calcaneus Fractures

Bruce J. Sangeorzan, M.D., Sarah K. Holt, M.P.H., Stephen K. Benirschke, M.D., and Sean E. Nork, M.D.

Fractures of the calcaneus account for approximately 60 percent of fractures of the large bones of the foot. They tend to occur in males in the prime working years and as a result, have substantial economic impact. Non-surgical treatment is associated with poor functional outcomes, primarily due to the residual hindfoot deformity. However operative treatment has a relatively high complication rate, primarily due to soft tissue problems with the extensile lateral approach. The literature suggests that open reduction produces improved patient outcomes when compared to nonoperative treatment if complications can be avoided. Certain fracture patterns, specifically tongue-type calcaneus fractures, may be amenable to minimally invasive reduction techniques. This minimally invasive approach may offer the advantages of surgical treatment, specifically reduction of the calcaneus morphology, without the high complication rate. We used a prospective comparison with the extensile approach to assess the results of this technique for patients with displaced, tongue-type calcaneus fractures.

Methods

We performed a prospective Surgeon-Randomized Controlled Trial of two treatment strategies for patients with displaced tongue-type calcaneus fractures (OTA class 73C1.3) who were treated Harborview Medical Center over a 5-year period. Patients were included in the study if they had an isolated displaced, tongue type fracture of the calcaneus, were over 18 years of age and were able to communicate. The study was designed as a Surgeon randomized trial so that each surgeon could perform the operative procedure that he felt was best for the patient. Two surgeons with more than 10 years experience treating the fractures did the surgery. Each surgeon was experienced in the extensile (traditional) approach.

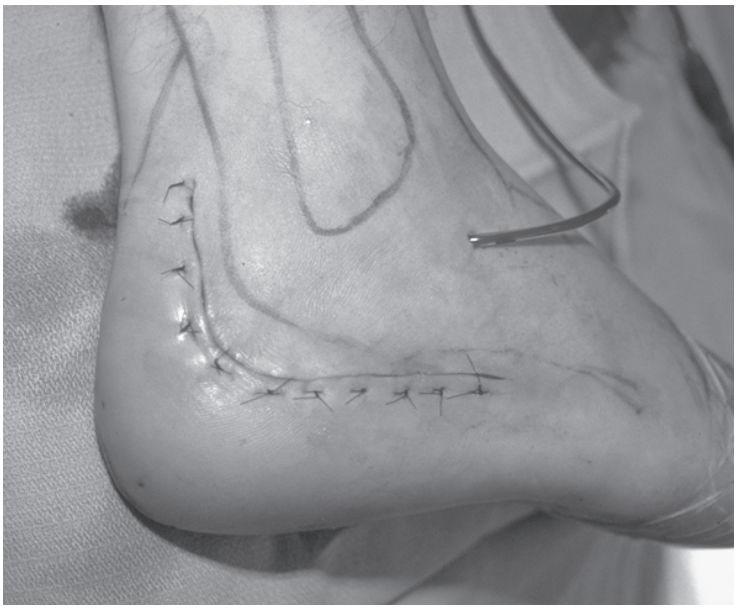

Figure 1: Traditional surgical incision.

The extensile approach involves an incision pioneered at Harborview that is "L" shaped with a vertical limb parallel to the Achilles tendon and a horizontal limb along the body of the Calcaneus (see Figure 1). One of the surgeons also had used the small incision approach for 7 years before the study was initiated. This approach uses a series of small incisions (less than 1 cm) combined with a Schanz pin in the tongue fragment to manipulate the fragments under fluoroscopy (see Figure 2). Both approaches attempt to restore the fracture to its pre injury position particularly in regard to the joint (cartilage) surface, the height of the bone (Bohlers angle) and width of the calcaneus (see Figure 3 and 4).

Clinical outcome was measured using two questionnaires. The Musculoskeletal Functional Assessment (MFA) instrument is a validated outcome tool used for assessing disability and "bother" after bone and joint injuries. There are scales for emotional function, relationship, mobility, work, hand and arm function, self-care, cognition, home activity and sleep. The AOFAS outcome instrument is a widely used but not validated tool with presumed sensitivity to change in foot and ankle disorders. These instruments were given at 6 weeks, 3 months, 6 months, and 12 months after treatment. We also measured time from injury to surgery, hospital length of stay (LOS), time to unassisted full weight-bearing (FWB), and self assessed pain at each interval. We also tracked complications including loss of fixation; implant failure, infection, deep vein thrombosis (DVT), sural nerve irritation, and hardware removal.

Radiographic outcome was measured using Bohler's angle before surgery, after surgery and at final follow up.

Results

Study period was 54 months. During that time, there were 522

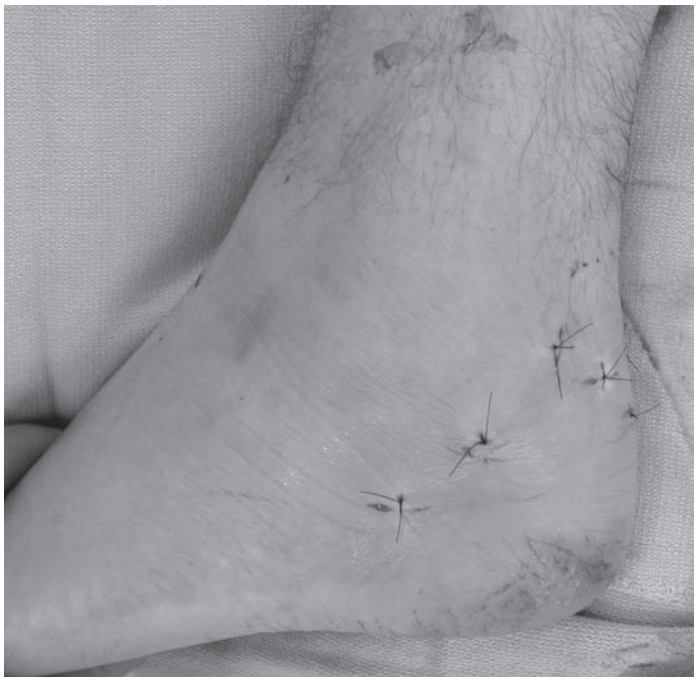

Figure 2: Small incisions of the minimally invasive approach.

calcaneus fractures treated by surgical reduction. There were 80 patients with tongue type fractures, of whom 20 had associated musculoskeletal injuries. Of the 60 eligible patients, 14 refused participation. Of the 46 patients who were successfully enrolled, 5 were lost to follow up and 5 were within one year of treatment at the time of review. The remaining 36 patients formed the study group. The average age of the 16 patients in the small incision group was 40 (range, 21 to 56 years). The average age of the 20 patients in the traditional incision group was 36.4 (range, 18 to –57 years). Twenty-six of the patients were male with a comparable distribution in each group.

When the treatment groups were compared, several differences were identified. The patients in the small incision group had a shorter LOS (1.6 days vs. 3.4 days, $p < 0.05$). The MFA subsections revealed that the small incision patients were significantly more active at 6 months ($p < 0.01$), were more active at 1 year both in the community ($p < 0.059$) and at home ($p < 0.03$), and had less sleep disturbance at 1 year ($p < 0.006$). The AOFAS evaluation also showed significant differences between the two groups. Patients treated with the small incision approach had less pain at 6 weeks ($p < 0.05$), more function at 6 weeks ($p < 0.002$) and improved range of motion at 3 months ($p < 0.03$). The patients in the small incision group also walked earlier without walking aids (13 weeks vs. 21 weeks). There were no differences in complication rates between the two groups.

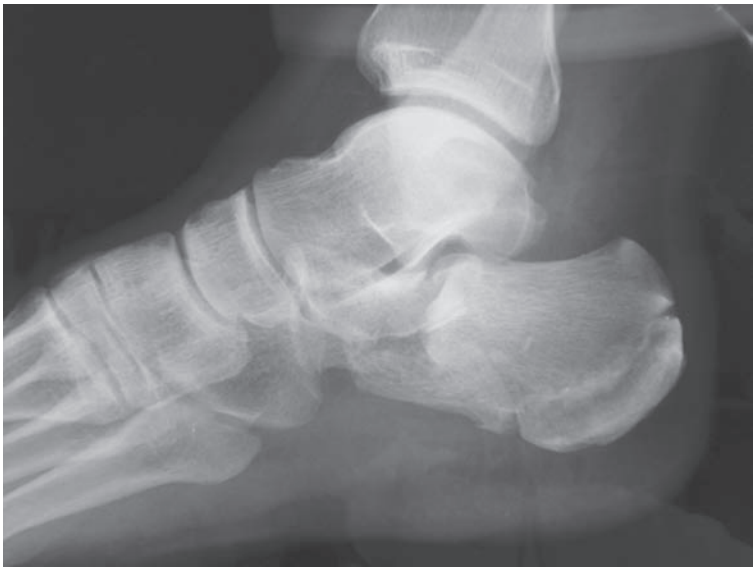

Figure 3: A lateral radiograph of a tongue type calcaneus fracture with reversal of Bohler's angle.

The shortcomings of the study include a small sample size. The majority of calcaneus fractures are not amenable to this technique, and the majority of patients at our institution have other associated fractures. However, several differences were statistically significant using these outcome tools. A second shortcoming is the short follow up period. It is possible that the differences in outcome will not continue with increasing time, or that the results will reverse with increased follow-up. Given the presumed improved articular reduction in the patients treated with an extensile approach, it is possible that time dependent changes in outcomes could occur. Finally, we have no baseline function for these patients. We don't know if the function of the patients in the two groups were equivalent before injury or if the fractures were of similar severity. The only radiographic measure (Bohlers angle) was similar in the two groups, but it does not have a validated association with fracture outcome.

Summary

It appears that the small incision technique leads to a shorter length of stay, earlier weight bearing, less pain and greater function in the first year after injury when compared to similar fractures treated with an extensile exposure without a difference in complication rates. Though not specifically measured, it is expected

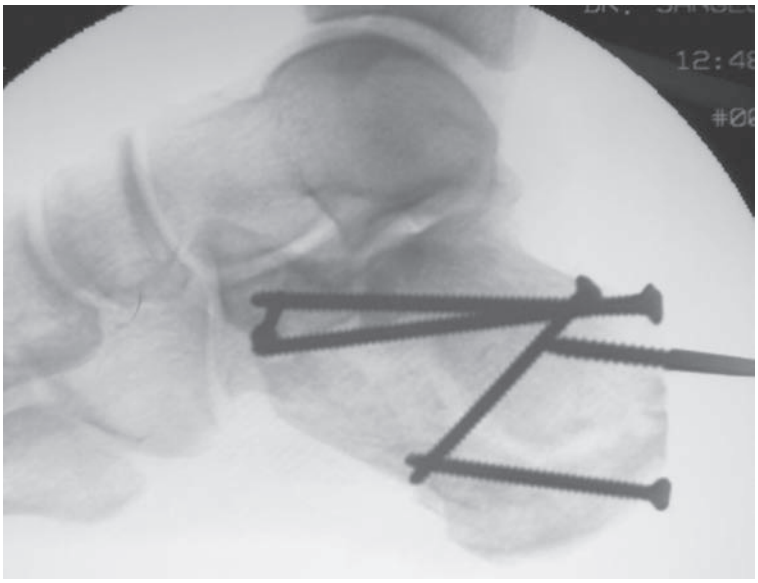

Figure 4: In this lateral radiograph, the facets have been reduced and the height restored. Small fragment screws maintain rigid fixation. The Shanz pin is removed after reduction. The patients begin active range of motion on post operative day one.

that the cost of treatment will be less in patients treated with the small incision technique given the shorter hospital stay and the early return to weight bearing. In experienced hands the small incision technique holds promise in a small number of appropriately selected calcaneus fractures.

Recommended Reading

Barei DP, Bellabarba C, Sangeorzan BJ, Benirschke SK. Fractures of the calcaneus. Orthop Clin North Am. 2002 Jan;33(1):263-85.

Kitaoka, H. B., E. J. Schaap, et al. (1994). "Displaced intra-articular fractures of the calcaneus treated non-operatively. Clinical results and analysis of motion and ground-reaction and temporal forces." J Bone Joint Surg Am 76(10): 1531-40.

Ma, Y. Z., Z. Z. Chen, et al. (1984). "Os calcis fracture treated by percutaneous poking reduction and internal fixation." Chin Med J (Engl) 97(2): 105-10.

Tornetta, P., 3rd (1998). "The Essex-Lopresti reduction for calcaneal fractures revisited." J Orthop Trauma 12(7): 469-73.

The Effect of Foot Type on Plantar Pressure

William R. Ledoux, Ph.D., Eric S. Rohr, M.S., Randal P. Ching, Ph.D., and Bruce J. Sangeorzan, M.D.

It has long been held that foot structure can affect foot function. Foot type is a means of structurally describing the foot. Feet can be classified as pes cavus (PC, high arch), neutrally aligned (NA, normal arch), and pes planus (PP, low arch). Pes planus feet may be further subdivided into asymptomatic (PPA) and symptomatic (PPS) groups. Plantar pressure is considered a measure of foot function. It has been retrospectively and prospectively associated with ulceration (Boulton et al. 1983; Veves et al. 1992) and it has been correlated to measures of foot shape (Morag and Cavanagh 1999). The purpose of this study was to explore how foot type (structure) affects plantar pressure (function).

Methods

A total of 40 subjects were enrolled with ten in each of four foot type groups: PC, NA, PPA, and PPS. Each subject contributed one foot to this analysis. Foot type was determined via clinical examination by an orthopaedic surgeon (Figure 1). Each foot was X-rayed (AP and lateral, Figure 2) and a weight-bearing CT scan was performed. The X-ray and the CT measurements of foot shape were both used to support the determination of foot type (i.e., there were significant differences between foot types, data not shown). Age, weight, height and gender were recorded. Ten trials of barefoot plantar pressure data were collected with an EMED-SF system. Velocity was recorded with two infrared emitter-reflector-detector systems placed a fixed distance apart on either side of the pressure plate. Stance phase was divided into contact phase (heel strike to foot-flat), mid-stance phase (foot-flat to heel-off) and propulsion phase (heel-off to toe-off). Peak pressure and the pressure-time integral (PTI, i.e., a measure of high pressure dosage) was determined over the entire foot as well as 10 subdivisions: the hallux, lesser toes, first through fifth metatarsal heads, medial midfoot, lateral midfoot and heel. These subdivisions were obtained by overlaying the AP X-ray on top of an actual-size composite peak plantar pressure print out. The Center of Pressure Excursion Index (CPEI), a measure of dynamic foot function, was also determined, as was foot angle (the angle of the foot bisection with the sagittal plane). Adjusting for age, body mass index, and velocity, a linear mixed effects model was used to explore differences between foot types.

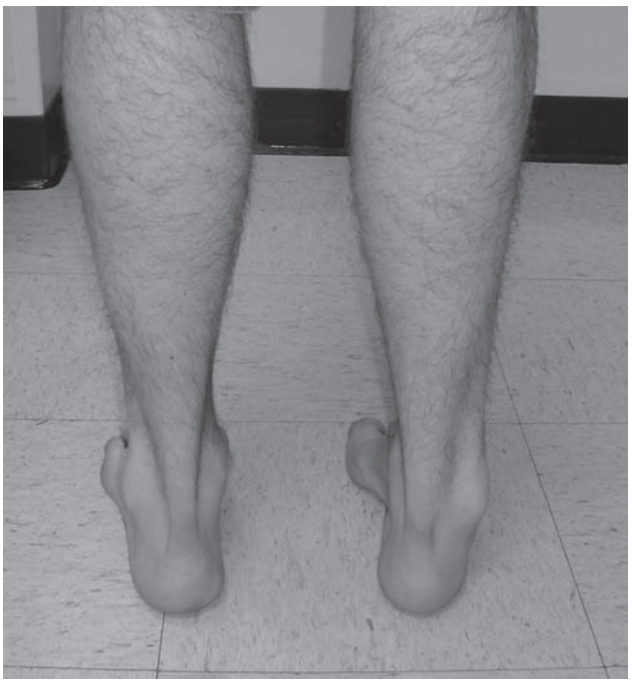

Figure 1: A patient with pes cavus foot (right) viewed from behind. Note the inward slant of the heel compared to the other side.

Results

There were no significant differences in age, BMI or gender between the four groups, but PC subjects walked significantly slower than all other foot types (Table 1, $p<0.0001$). PC subjects spent significantly more time in midstance ($p<0.0001$) and less time in propulsion ($p=0.002$) than all other foot types. They also spent less time in contact phase than NA feet ($p=0.003$). There were no significant differences in CPEI or foot angle. Over the entire foot, PC feet had higher peak pressures than NA or PPA feet (Figures 3 and 4), while the PPS had higher peak pressures than NA feet ($p=0.001$). The PC feet had less pressure beneath the hallux ($p=0.0004$) and second metatarsal ($p=0.002$) than all other foot types, and less pressure under the toes ($p=0.002$) than the PP feet, but higher peak pressure at the fifth metatarsal than either pes planus group ($p=0.008$). PPS feet had higher peak pressures beneath the first metatarsal compared to the PPA and NA feet ($p=0.012$). The PC feet also had a higher PTI over the entire foot compared to the PPA and NA feet ($p=0.001$).

Discussion

Subjects with PC feet walked slower and with more time in midstance than the other foot types. PC and PPS foot types are considered pathologic, and thus several differences in peak pressure and PTI from the more benign NA and PPA foot types were seen, indicating aberrant foot function.

	PC (n=10)	NA (n=10)	PPA (n=10)	PPS (n=10)	p*
Velocity (m/s)	0.93 ± 0.05	1.26 ± 0.04	1.20 ± 0.04	1.17 ± 0.05	.0001[abc]
Contact (%)	6.9 ± 0.7	11.0 ± 0.6	9.3 ± 0.6	9.3 ± 0.6	.003[a]
Midstance (%)	69.4 ± 2.7	51.4 ± 2.4	54.1 ± 2.4	52.6 ± 2.6	.0001[abc]
Propulsion (%)	24.0 ± 2.6	37.6 ± 2.4	36.6 ± 2.3	38.1 ± 2.5	.002[abc]
PeP - total	89.2 ± 6.2	53.6 ± 5.4	63.5 ± 5.7	77.7 ± 5.9	.001[abe]
PeP - hallux	13.3 ± 6.9	41.2 ± 6.4	55.6 ± 6.8	55.0 ± 7.0	.0004[abc]
PeP - 1st metatarsal	31.5 ± 7.4	24.4 ± 7.0	20.2 ± 7.3	53.9 ± 7.4	.012[de]
PeP - 2nd metatarsal	22.1 ± 3.9	39.7± 3.7	43.8 ± 3.9	42.2 ± 3.9	.002[abc]
PeP - 5th metatarsal	47.6 ± 6.5	25.2 ± 5.8	22.6 ± 6.1	14.5 ± 6.1	.008[bc]
PeP - toes	7.7 ± 2.3	13.1 ± 2.1	19.9 ± 2.2	19.0 ± 2.3	.002[bc]
PTI - total	32.7 ± 2.3	20.2 ± 2.1	20.4 ± 2.1	25.4 ± 2.2	.001[ab]

Table 1: Significantly different gait measures (mean ± SE adjusted for age, BMI, and velocity) Adjusting for age, body mass index, and velocity. PeP = peak pressure, PTI = pressure time integral, [a]PC v. NA, [b]PC v. PPA, [c]PC v. PPS, [d]PPS v. PPA, [e]PPS v. NA *A linear mixed effects model was used to explore differences between foot types.

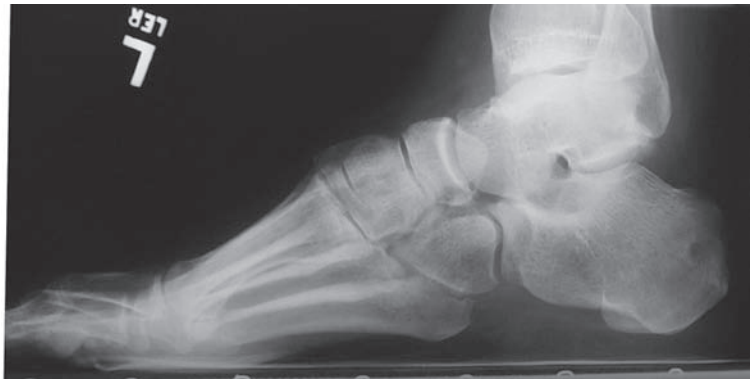

Figure 2: A lateral X-ray of a pes cavus foot.

Figure 3: The peak pressure distribution of a neutrally aligned foot.

Figure 4: The peak pressure distribution of a pes cavus foot.

Recommended Reading

Boulton, A. J., et al. (1983). Diabetes Care 6, 26-33.

Morag, E., Cavanagh P. R. (1999). Journal of Biomechanics 32, 359-70.

Veves, A. et al. (1992). Diabet. 35, 660-3.

Acknowledgements

This work was supported by the Department of Veteran Affairs project #A2180R. Jane Shofer performed the statistical analysis and Charles Harp assisted with the data analysis.

Patterns of Injury and Fracture Morphology in Displaced Medial Tibial Plateau Fractures

Robert P. Dunbar, M.D., Sean E. Nork, M.D., David P. Barei, M.D., and William J. Mills, M.D.

Tibial plateau fractures are common lower extremity injuries, with fracture patterns and treatment options for isolated lateral plateau fractures and bicondylar fractures previously described. Conversely, medial tibial plateau fractures occur less commonly and have been less fully characterized, with few studies specifically focusing on medial sided proximal tibial injuries. Proper identification and understanding of these fracture patterns and their associated soft tissue injuries may decrease the predisposition of these fractures to late displacement and poor outcome. The purpose of this study is to clarify and characterize the displacement patterns and associated injuries observed in medial tibial plateau fractures.

We reviewed data from a prospectively designed orthopaedic trauma database to identify 785 patients who had sustained a tibial plateau fracture during the 60 month period from January 1998 through December 2002. From this group we identified 45 patients who had sustained a displaced medial tibial plateau fracture. Medial tibial plateau fractures were defined as fractures which entered the proximal tibial articular surface and exited through the medial metaphysis or metadiaphysis but not the lateral metaphysis or metadiaphysis. Pure depression fractures of the medial plateau, which did not exit the medial metaphysis or metadiaphysis were also included.

The 45 medial tibial plateau fractures were sustained by 42 patients (30 male, 12 female), with three patients sustaining bilateral injuries. The average age of these patients was 35.1 years (range, 16 to 66 years). Mechanisms of injury included 11 pedestrians struck by moving vehicles, 11 falls from height, 10 motor vehicle collisions, 5 motorcycle accidents, 3 falls from standing and 5 other mechanisms (2 skateboard crashes, 2 assaults and 1 plane crash).

Lateral and medial condylar widening were measured on anteroposterior pre-reduction injury radiographs. Medial condylar widening was measured by drawing a line perpendicular to the medial femoral articular surface and tangential to the most medial point of the medial femoral articular surface. The point at which this line crossed the tibial plateau was measured to the most medial point on the tibial plateau. A similar measurement was made on the lateral side. Patients injured in 2001 and 2002 had computerized radiographs in the PAC System (Centricity® Programmable Automation Controller, General Electric, Inc.). These films were measured using the system software. The radiographs of patients who sustained their injuries from 1998-2000 were measured manually using calipers and a ruler with 1.15 magnification correction. Computerized tomography scans were obtained on 38 of 45 fractures (84.4%). Axial images were used to clarify fracture patterns.

Associated osseous injuries including tibial eminence fractures, proximal fibular fractures, and Segond capsular avulsions were identified from plain radiographs and CT scans. Soft tissue injuries including open wounds, neurologic deficits, ligamentous disruptions, meniscal tears, vascular injuries and cases of compartmental syndrome were recorded.

In 43 of 45 fractures (95.6%) medial condylar widening measured ≤5 mm. The remaining two patients had medial condylar widening measuring 8 and 11mm. In 29 fractures (64.4%) medial condylar widening measured

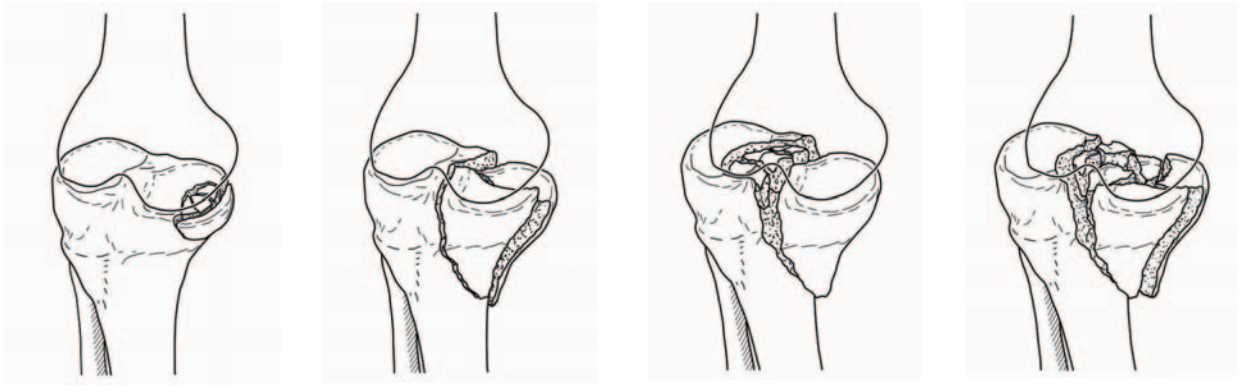

Figure 1: Type I medial tibial plateau fracture: Peripheral rim fractures. These may occur anteromedially, directly medially or posteromedially. Type II medial tibial plateau fracture: Posteromedial fracture. This fracture is shown with an associated anteromedial fragment. Type III medial tibial plateau fracture: Total condylar fracture, sparing medial articular surface, but involving intercondylar notch and medial portion of lateral articular surface. Type IV medial tibial plateau fracture: Comminuted fracture with depressed articular segment.

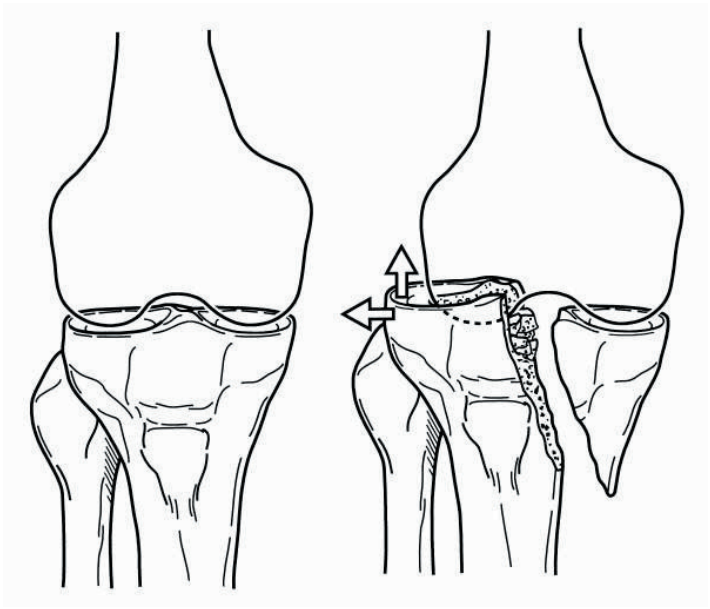

Figure 2: With many medial tibial plateau fractures, displacement is best described as lateral and proximal translation of the lateral, distal fragment.

0 mm. Conversely, 26 of 45 fractures (57.8%) demonstrated ≥5 mm lateral condylar widening (range 5-31 mm; average 10.8 mm). Medial plateau articular displacement was identified in 30/45 (66.7%) fractures. Thus, the medial articular surface was spared in one third of cases (15/45). Conversely, lateral plateau articular involvement and displacement was identified in 25 of 45 fractures (55.6%).

Consistent and definable patterns of medial tibial plateau fractures were identified. The most commonly observed patterns were those that spared the entire medial tibial plateau articular surface and those with a coronal fracture line resulting in a displaced posteromedial articular fragment. The fractures were grouped as follows:

I. Compression fractures limited to the peripheral rim of the medial tibial plateau (n = 13)
II. Coronal plane medial tibial plateau fractures with a displaced posteromedial articular fragment (n = 14)
III. Fractures exiting at either the lateral plateau articular surface of the intercondylar region, sparing the medial articular surface (n = 15)
IV. Depressed and comminuted medial tibial plateau fractures (n = 3)

Associated open traumatic wounds occurred in 5 of 45 fractures (11.1%) and were classified according to Gustilo as Type II (n = 2), Type IIIA (n = 2) and Type IIIB (n = 1). Associated osseous injuries included tibial eminence fractures in 26 (57.8%) fractures, proximal fibular fractures in 14 (31.1%) fractures, and Segond fractures in 7 (15.6%). Associated knee ligament injuries were observed commonly. Disruptions of the lateral collateral ligament were identified in 12 (26.7%) while only 1 tear of the medial collateral ligament was noted. There were 7 anterior cruciate ligament disruptions, 4 posterior cruciate ligament disruptions, and 3 disruptions of the posterolateral corner. There was one popliteal artery injury, which required surgical repair. Five patients had associated peroneal nerve injuries (11.1%). In three patients compartment syndrome of the leg was associated with the fracture, with each requiring emergent fasciotomy.

We noted that lateral condylar widening, lateral sided ligamentous injury and lateral compartment articular involvement occurs commonly while medial condylar widening and medial ligament injury is uncommon. Further, in a significant percentage of these injuries the medial articular surface is spared. The combination of lateral compartment articular involvement, lateral condylar widening, and the high incidence of lateral sided ligamentous injuries seen in this fracture pattern points to the bicondylar nature of these fractures. Further, it would appear that the medial fragment is the "stable" fragment and that the displacement pattern in most medial tibial plateau fractures is best described as lateral and proximal displacement of the lateral articular fragment, which remains contiguous with the tibial shaft. Commonly observed fracture patterns included those that spared the entire medial tibial plateau articular surface and those with a coronal fracture line resulting in a displaced posteromedial articular fragment.

While treatment of these fractures is not the specific focus of this study, a word of caution is advised. These fractures have a propensity to displacement and subsequent poor outcome. As such, aggressive treatment of all but nondisplaced fractures should be considered. Additionally, peripheral rim injuries may be small enough to not require surgical management, as they are typically submeniscal in location. Nevertheless, a high degree of suspicion should be maintained for an associated ligamentous injury on the opposite side of the knee. This suspicion should be combined with physical examination, perhaps including examination under anesthesia, as well as appropriate imaging to fully categorize the constellation of injury. Posteromedial, total condylar and comminuted medial tibial plateau fractures are typically treated with medial or posteromedial buttress/anti-glide plating, but have been treated with independent lag screws, laterally-based locked plate constructs and even external fixation. Screws placed proximally in the plate serve to compress the articular surface (buttress function) while screws placed just distal to the medial metaphyseal extent of the fracture resist the tendency of the fracture to subside (antiglide function). Anatomic reduction of the articular surface, with elevation of any depressed segments and early motion remains the goal of treatment.

Surgeons should be aware that significant lateral sided injuries in occur regularly in "medial" tibial plateau fractures and that as such, these are better considered bicondylar injuries. Therefore, when planning

a treatment strategy, evaluation of the entire knee is imperative. Toward that end, consideration of imaging pre-operatively to fully categorize soft tissue injury may be advisable.

Recommended Reading

Honkonen SE. Indications for Surgical Treatment of Tibial Condyle Fractures. Clin Orthop 1994; 302:199-205.

Mills WJ, Nork SE. High Energy Tibial Plateau Fractures. Ortho Clin N. Am. 2002;33(1):177-98.

Moore TM, Patzakis MJ, Harvey JP. Tibial Plateau Fractures: Definition, Demographics, Treatment Rationale and Long Term Results of Closed Traction, Management or Operative Reduction. J Orthop Trauma 1987;1:97-119.

Schatzker J, McBroom R, Bruce D. The Tibial Plateau Fracture: The Toronto Experience 1968-1975. Clin Orthop. 1979;138, 94-104.

Tscherne H, Lobenhoffer P. Tibial Plateau Fractures. Management and Expected Results. Clin Orthop. 1993;292:87-100.

Gustilo RB, Mendoza RM, Williams DN. Problems in the Management of Type III (Severe) Open Fractures: A New Classification of Type III Open Fractures. J Trauma. 1984;24:742-6.

Operative Treatment of Femoral Neck Fractures in Adults Younger than 50

Lisa A. Taitsman, M.D., M.P.H., Sean E. Nork, M.D., Julie Agel, M.A., and Marc F. Swiontkowski, M.D.

The treatment of high-energy femoral neck fractures in young adults remains difficult. Patient outcomes may be adversely affected by nonunion and/or aseptic necrosis. The purpose of this retrospective review is to report the results of operative fixation of femoral neck fractures in a large series of patients under the age of 50 in an effort to identify risk factors for the observed complications.

Methods

Using a prospectively designed orthopaedic trauma registry at a single level one trauma center, we retrospectively identified patients between the ages of 16 and 50 with femoral neck fractures (AO/OTA type 31B) operatively treated during an 11.75 year period. There were 125 patients (128 fractures) with an average age of 33.5 years (range, 14 to 49 years). The medical records were reviewed to identify the mechanism of injury, associated injuries, intraoperative findings, complications, and secondary surgical procedures. Radiographs were blinded and reviewed to determine the fracture displacement, fracture classification, initial reduction, and final reduction. Mechanism of injury included motor vehicle collisions in 56, falls from height in 31, motorcycle accidents in 14, sports injuries in 7, pedestrians struck in 4, gun shots in 4 and other mechanisms in 9 patients. Nine fractures were open and 4 were associated with an ipsilateral hip dislocation. Ninety-nine fractures (77%) were displaced while 29 were valgus impacted or nondisplaced. Ipsilateral femoral shaft fractures were present in 47 (37%), the majority of which (n = 32) were associated with displaced femoral neck fractures. Fixation consisted of multiple large fragment screws in 105, a dynamic hip screw (with or without a supplemental derotation screw) in 17 fractures, a reconstruction nail in four and a blade plate for two. Patients were followed until healing or documented nonunion with a minimum of three months (median, 15 months; range, 3 to 139 months).

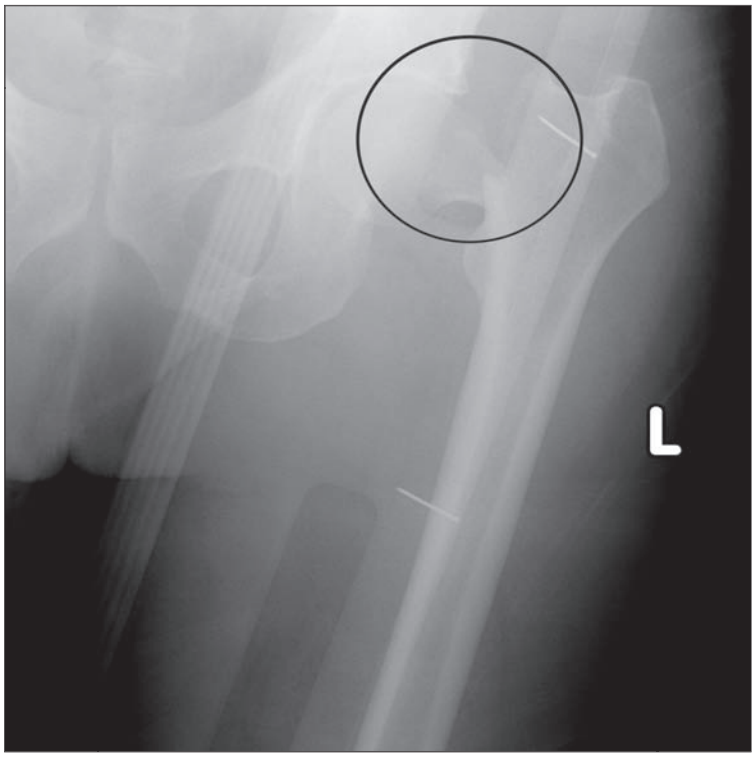

Figure 1: 43 year old male involved in a motor vehicle collision. AP radiograph of his displaced femoral neck fracture is shown.

Results

Fractures were classified as 31B1 in 9, 31B2 in 79, 31B3 in 36, and 31B in 4. Of the 29 non- or minimally displaced fractures, 23 fractures were treated with either closed reduction and fixation or in situ fixation, while six were treated with open reduction internal fixation. Of the 23 fractures treated with a closed reduction, six had a documented percutaneous capsulotomy. None of these 29 fractures were complicated by nonunion or AVN. Of the 99 displaced fractures, 80 were treated with open reduction and internal fixation while 19 were treated with closed reduction and percutaneous fixation. Thirteen of these 19 fractures underwent a percutaneous capsulotomy as well. Of the 74 displaced fractures with adequate initial and follow-up radiographs, the initial reduction was anatomical in 40 (54.1%), nearly anatomic in 21 (28.4%) and non-anatomic in 13 (17.6%).

Nonunions were observed in 18 fractures (14%). Nonunions occurred in 0% of the 31B1, 14% of 31B2, and 17% of 31B3 patterns. No association was found between the development of a nonunion and the AO/OTA classification, the type of fixation, or the presence of an ipsilateral femoral shaft fracture. However, nonunion was associated with the initial displacement ($p < .01$) and the initial reduction ($p < .01$). Nonunion was observed in 5 (13%), 5 (24%), and 7 (54%) of the anatomic, near anatomic and non-anatomic reductions (one nonunion with unknown initial reduction). Avascular

A.

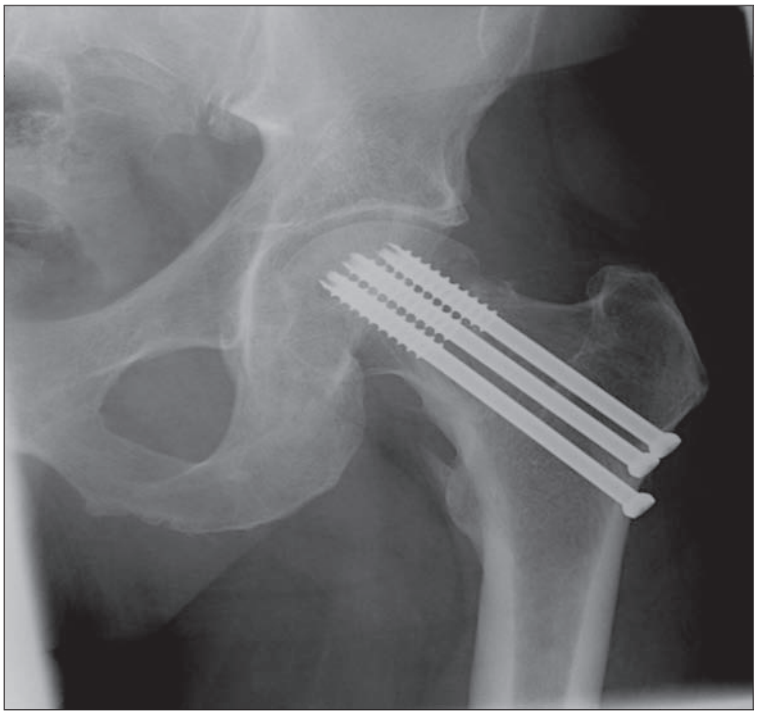

B.

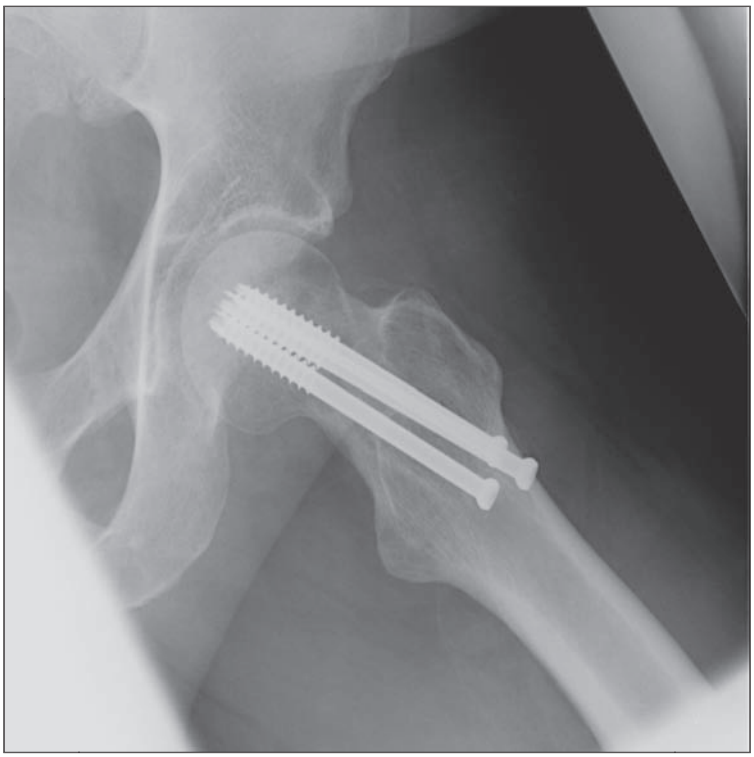

Figure 2A and B: At one year, his fracture has healed and he is asymptomatic.

necrosis was observed in 11 fractures (9%); however, the period of follow-up was short. In total, 68 (53%) fractures were followed for more than one year, while only 39 (30%) had greater than two year follow up. Avascular necrosis was identified in 8 (22%) of subcapital (31B3) fractures compared to no 31B1 and 3 (4%) of 31B2 fracture patterns. Because the vast majority of patients with displaced fractures (94%) underwent a capsulotomy (either with an open reduction or percutaneously), no relationship with AVN or nonunion could be found.

Conclusions/Significance

The treatment (open verses closed reduction) of femoral neck fractures in young patients is often driven by the injury severity and the ability to achieve an anatomical reduction. An open reduction was necessary in the majority of patients with displaced fractures; however, a perfect reduction was obtained in only half of these patients. The only factors identified that were associated with the development of a nonunion were the initial displacement and the reduction. Initial displacement was also correlated with AVN as was fracture classification. These results suggest that every effort should be made to accurately reduce displaced fractures of the femoral neck in young adults.

Recommended Reading

Haidukewych, G. J.; Rothwekk, W. S.; Jacofsky, D. J.; Torchia, M. E.; and Berry, D. J.: Operative treatment of femoral neck fractures in patients between the ages of fifteen and fifty years. JBJS, 86-A(8): 1711-1716, 2004.

Keller, C. S., and Laros, G. S.: Indications for open reduction of femoral neck fractures. Clin Orthop, 152: 131-137, 1980.

Swiontkowski, M. F.; Winquist, R. A.; and Hansen, S. T., Jr.: Fractures of the femoral neck in patients between the ages of twelve and forty-nine years. J Bone Joint Surg, 66-A(6): 837-846, 1984.

Zetterberg, C. H.; Irstam, L.; and Andersson, G.: Femoral neck fractures in young adults. Acta Orthop Scand, 53(3): 427-435, 1982.

Inguinal Abnormalities During Ilioinguinal Approaches

Paul Stafford, M.D. and M. L. Chip Routt, Jr., M.D.

The ilioinguinal surgical exposure provides access to the anterior pelvis and facilitates acetabulum fracture reduction and fixation. To safely perform the approach and to prevent post-operative inguinal hernias, one must thoroughly understand both the normal inguinal anatomy and its associated abnormalities. Potential aberrant findings include direct and indirect inguinal hernias as well as spermatic cord lesions. These abnormalities increase the complexity of the surgical exposure and/or closure. The orthopedic surgeon must detect these inguinal findings preoperatively and coordinate a surgical plan with the general surgeon.

The purpose of this study is to: 1) report the occurrence of inguinal canal and spermatic cord abnormalities in both a clinical series of adult males undergoing acetabular fracture fixation and a series of adult male cadavers, and 2) emphasize the methods and importance of detecting these inguinal abnormalities preoperatively.

Methods

Cadaveric study

We dissected eighteen embalmed male cadavers bilaterally (36 sides), and collected subject age, height, and weight from post-mortem data sheets. The dissections were performed using an ilioinguinal exposure according to Letournel. The dissections were limited to the superficial portion of the exposure. After removing all soft tissues anterior to the rectus sheath and external oblique aponeurosis, we identified the spermatic cord and the ilioinguinal nerve as they exited the external (superficial) inguinal ring. The external oblique aponeurosis was incised in line with the inguinal ligament to open the inguinal canal. We extended the incision distally through the external spermatic fascia to identify any abnormalities and fully expose the contents of the spermatic cord. We measured spermatic cord diameter and noted any local masses. Bowel hernias were identified as "direct" or "indirect" by dissecting the hernia sac and identifying their point of origin into the inguinal canal.

Clinical study

We retrospectively reviewed our series of operatively treated acetabular fractures from January 2001 through December 2003 and identified male patients with fractures treated using an ilioinguinal approach. The operative notes were reviewed to determine the incidence of inguinal canal and spermatic cord abnormalities requiring general surgery consultation. To determine the etiology of the abnormality and the details of the surgical intervention, we reviewed the corresponding general surgery operative notes. Finally, the corresponding preoperative bony CT scans were reviewed in detail. From the CT scan, we noted the radiographic characteristics of the spermatic cord abnormalities and/or hernias.

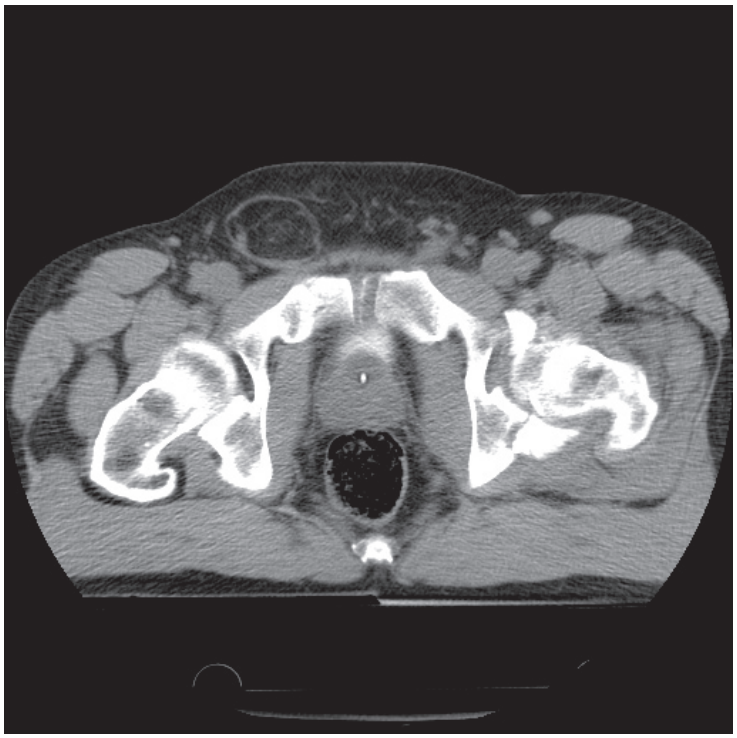

Figure 1: This patient has a left sided comminuted acetabular fracture. The pelvic computed tomography axial image identified a right sided previously undiagnosed inguinal hernia. The inguinal hernia repair can be coordinated at the same anesthetia as for the acetabular reduction and fixation, and using the ilioinguinal exposure.

Results

Cadaver Study

We dissected 18 adult male cadavers bilaterally (Table 1). The average specimen age was 80 years (range 22 to 100). The average height was 169 cm (range 152 to 191) and the average weight was 64 kg (range 34 to 114). 11 of 36 (31%) had spermatic cord and/or inguinal canal abnormalities. This included one cadaver with bilateral indirect inguinal hernias, three cadavers with bilateral spermatic cord lipomas, and three cadavers with unilateral spermatic cord lipomas. The average cord diameter in those with abnormalities was 24.9 mm (range 15 to 28). The average cord diameter in normal cords was 16 mm (range 11 to 22). The difference between normal and abnormal cord diameters was statistically significant ($p = .00001$).

Cadaver	Height (cm)	Weight (kg)	Cord Abnormality	Side	Details
1	183	77	Yes	Right	Cord Lipoma
2	175	55	No		
3	173	73	No		
4	155	98	No		
5	175	59	No		
6	191	114	Yes	Both	Cord lipomas
7	183	91	Yes	Left	Cord Lipoma
8	178	70	No		
9	183	82	No		
10	168	82	No		
11	185	82	No		
12	178	64	Yes	Both	Indirect Hernias
13	168	52	No		
14	185	82	Yes	Both	Cord Lipomas
15	178	68	No		
16	183	34	No		
17	162	57	Yes	Both	Cord Lipomas
18	178	68	Yes	Right	Cord Lipoma

Table 1: Cadaver Series.

Clinical Study

We operatively treated 277 displaced acetabular fractures from January 2001 through December 2003. Of the 120 fractures treated through an ilioinguinal exposure, 87 were males with an average age of 44 years (range 14 to 70). 5 of these 87 male patients (5.7%) had a hernia and/or spermatic cord lesion requiring general surgical intervention under the same anesthesia through the same exposure (Table 2). Two of the five had indirect inguinal hernias only. After reduction of the indirect hernia, one of these underwent repair of the inguinal canal while the other required mesh reconstruction. One of the five patients had an isolated cord lipoma without associated bowel herniation. The lipoma was resected and the inguinal canal required mesh reconstruction. The two remaining patients had both direct inguinal hernias and cord lipomas. Both patients had resection of their lipomas. One patient had a primary repair of the inguinal canal while the other required a mesh augmentation.

The preoperative pelvic CT scans of all five patients were reviewed in detail, and the abnormality was easily identified on four of the five patients. The lipomas appeared as

Age	Abnormality	CT Findings	Surgical Details
56	Indirect Hernia	Not Detected	Hernia reduction, mesh reconstruction
39	Direct Hernia, Cord Lipoma	Enlarged cord, homogeneous density	Lipoma resection, mesh reconstruction
41	Cord Lipoma	Enlarged cord, homogeneous density	Lipoma resection, mesh reconstruction
49	Indirect Hernia	Enlarged cord, heterogeneous density	Hernia reduction, repair of inguinal canal
55	Direct Hernia, Cord Lipoma	Enlarged cord, heterogeneous density	Lipoma resection, repair of inguinal canal

Table 2: Clinical Series.

spermatic cord enlargements with homogeneous density (Figure 1). The homogeneous density on the CT scan was consistent with the intraoperative finding of fat within the enlarged spermatic cord. The hernias appeared as enlargements of the spermatic cord with a heterogeneous density. This was consistent with the intraoperative findings of a bowel sac and normal cord structures within the spermatic cord. The one instance not detected on the preoperative CT scan was well documented in the preoperative history. The 39 year-old male reported a history of inguinal hernia with episodes of incarceration which he manually reduced. The hernia was confirmed and repaired during the ilioinguinal approach.

Discussion

The surgeon performing an ilioinguinal approach must understand normal inguinal anatomy and be aware of abnormalities including spermatic cord lipomas and inguinal hernias. Both cord lipomas and hernias have been described in the general surgery literature.

Hernias are defined as "direct" or "indirect" depending on point of entry into the inguinal canal and their relation to Hasselbach's Triangle. Direct inguinal hernias enter the inguinal canal by breaching through a weakened area of the inguinal floor (transverses abdominus and internal oblique muscles), medial to the inferior epigastric vessels (within Hasselbach's Triangle). Indirect hernias enter the inguinal canal through the internal (deep) inguinal ring, lateral to the epigastric vessels (out of Hasselbach's Triangle). Both types may present as a groin mass and/or bulge in the spermatic cord.

Spermatic cord lipomas may also present as enlargement of the spermatic cord. Although these abnormalities are referred to as "lipomas", they are not true lipomas. Instead, cord lipomas are actually retroperitoneal fat that has entered the inguinal canal through the internal inguinal ring. The fat protrudes through the internal (deep) inguinal ring, outside the internal spermatic fascia and lateral to the cord. They may occur in isolation or in association with a direct or indirect bowel hernia. It is important to note that their initial presentation may be indistinguishable from a bowel herniation. The spermatic cord must be opened and explored to identify the etiology of the mass.

Several previous studies report the occurrence and incidence of cord abnormalities. Heller found a discrete mass of fat (which was contiguous with the preperitoneal fat through the deep inguinal ring) within the inguinal canal in 27 of 36 (75%) of male cadavers. Six of these (16%) extended beyond the external (superficial) inguinal ring. Lilly found spermatic cord lipomas in 22.5% of patients undergoing inguinal hernia repairs. Bissada reported unusual causes of spermatic cord enlargement including three cases of sarcoma. These studies emphasize the significant incidence of hernias and cord lipomas in the adult male population.

The 31% incidence of spermatic cord and/or inguinal canal abnormalities in our cadaver study was higher than the 16% reported by Heller. While two of our twelve abnormalities consisted of indirect inguinal hernias, Heller observed no cases of inguinal hernia. Although the median age between the two groups was significantly different (80 years vs. 56 years), prior clinical studies do not support age as a factor in the development of inguinal abnormalities.

The difference in incidence between our cadaveric study and clinical series is significant (31% vs. 5.7%). The median age in our cadaver study was 80 years compared to 44 years in our clinical series. However, Carbonell did not find age to be a causative factor in the development of inguinal abnormalities.

Our definition of "inguinal abnormality" is the most likely cause of the different rates of occurrence between the cadaveric and clinical study. In our cadaveric study, we identified patients as having "inguinal abnormalities" when any size lipoma or minor disruption of the inguinal anatomy was present. This included spermatic cord lipomas which did not extend past the external (superficial) inguinal ring. In our clinical series, only inguinal abnormalities requiring general surgical intervention were included. These abnormalities were all symptomatic and/or large enough to disrupt the integrity of the inguinal canal.

Conclusions

Both our clinical and cadaveric findings emphasize the occurrence of inguinal abnormalities. The orthopedic surgeon should ask patients with acetabulum fractures about prior inguinal procedures and recent inguinal complaints. Physical exam may reveal an inguinal "bulge" and/or a mass protruding into the testes. Preoperative pelvic CT scans are highly sensitive in detecting inguinal abnormalities. Cord lipomas are visualized as enlargements of the spermatic cord with homogeneous density. Most clinically significant hernias are readily visualized as enlarged spermatic cords with heterogeneous density. Those hernias not seen on CT scans are likely revealed by clinical history. Preoperative pelvic CT scans must be carefully studied for both osseous and inguinal abnormalities. When abnormalities are detected, the orthopedic surgeon should coordinate the surgical plan with a general surgeon. The abnormalities can be treated during the same anesthesia using the same exposure.

Recommended Reading

Bissada N, Redman J. Unusual Masses in the Spermatic Cord: Report of Six Cases and Review of the Literature. Southern Medical Journal 1976;69(11):1410-1412.

Carbonell J, Sanchez J, Peris R, et al. Risk Factors Associated with Inguinal Hernias: A Case Control Study. Eur J Surg 1993;159(9):481-6.

Heller C, Marucci D, Dunn T, et al. Inguinal Canal Lipoma. Clinical Anatomy 2002;15:280-285.

Letournel E, Judet R. Fractures of the Acetabulum – 2nd edition. Berlin Springer-Verlag 1993. pp554-557.

Lilly M, Arregui M. Lipomas of the Cord and Round Ligament. Annals of Surgery 2002;235(4):586-590.

Van Wessen K, Simons M, Plaisier P, et al. The Etiology of Indirect Inguinal Hernias: Congenital and /or Acquired? Hernia 2003;7(2):76-79.

Perioperative Complications Associated with Intrapelvic Plating for Acetabular Fractures

Rob B. Molnar, Thomas A. Schildhauer, M.D., Sean E. Nork, M.D., and M. L. Chip Routt, Jr., M.D.

Operative reduction and stable fixation is the accepted treatment of most displaced acetabular fractures. Obtaining and maintaining a stable reduction can be difficult to achieve in some complex acetabular fractures, particularly those with associated quadrilateral surface displacement and comminution. Various authors have recognized this and several techniques, including the use of intrapelvic plates, have been described to address this problem. Intrapelvic plates are technically demanding and are therefore reserved for the most challenging acetabular fracture patterns. This study reports the perioperative complications associated with intrapelvic plating.

Materials and Methods

Over a 4 year period from January 2000 through December 2003, all patients sustaining an acetabular fracture were collected from a prospectively designed orthopaedic database and reviewed retrospectively. A total of 680 patients with 698 acetabular fractures were identified and included in the initial evaluation. Of these, 439 acetabular fractures were treated operatively at Harborview Medical Center, a level one trauma center in Seattle, Washington. The study group was comprised of 29 patients with 29 acetabular fractures that were treated with intrapelvic plates using a modified ilioinguinal surgical exposure.

There were 21 male and 8 female patients ranging in age from 18 to 83 years (average 40 years). Mechanisms of injury were falls in 15 patients, motor vehicle crashes in 6, bicycle accidents in 3, pedestrians struck by automobiles in 2, an all-terrain vehicle crush in 1, a skiing accident in 1, and an equestrian crush in 1 patient. The acetabular fractures were classified according to Letournel as 19 associated both column, 6 anterior column with associated posterior hemitransverse, and 4 T-type fracture patterns. Fourteen patients had traumatic medial acetabular dome crush injury noted on the preoperative radiographs and CT scans.

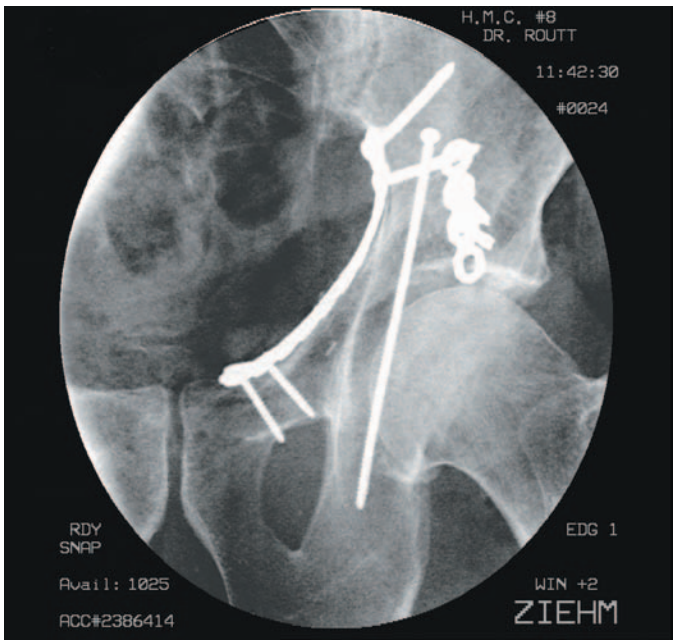

Figure 1: This intraoperative image of the acetabular fracture demonstrates the intrapelvic plate location.

Intrapelvic plates were used to secure medial quadrilateral surface or posterior column displacement at the surgeons discretion in these 29 patients (Figure 1). The plates were applied through the Stoppa or medial window of a modified ilioinguinal surgical exposure.

After surgery, all patients had pelvic plain radiographs and CT scans to assess the reductions and the safe placement of implants. Two fellowship trained orthopaedic traumatologists graded the fracture reductions as excellent, imperfect, and poor based on displacement patterns. Prior to discharge from hospital, all patients underwent duplex ultrasound examination of their lower extremities to evaluate for deep vein thromboses. Perioperative complications were documented by a review of the hospital notes, the outpatient records and from the prospective database.

Results

There were no deaths. The average surgical time was 264 minutes (range 180-468 minutes). The average blood loss for the procedure was 1297ml (range 100ml-6000ml). There were no iatrogenic visceral injuries. Postoperatively only one patient had a nerve deficit. Intraoperatively, the obturator nerve was noted to be trapped within the acetabular fracture fragments, and was sharply excised to prevent neuroma. Wound related complications occurred in 2 patients. One patient had a superficial abcess requiring two surgical debridements and intravenous antibiotics. The other patient developed an incisional hernia that required repair 7 months after the acetabular surgery.

Ten of the twenty-nine patients

(34.5%) treated with intrapelvic plates developed DVTs. Six patients had DVTs ipsilateral to the fracture, three had contralateral DVTs, and one patient had bilateral lower extremity DVTs. Two patients had their DVT diagnosed prior to surgery. Of the 680 total patients with acetabular fractures 116 (17%) had a documented DVT. Of the 409 patients with operatively treated acetabular fractures that did not have placement of an intrapelvic plate, DVTs were diagnosed in 72 (17.6%). Statistical analysis revealed that DVT was significantly more likely in the group of patients who received intrapelvic plates when compared to operatively treated patients stabilized without intrapelvic plates ($p = 0.018$, Fisher exact test). The side of the DVT was not related to side of the injury, although the study group was small. One patient had a non-fatal pulmonary embolus.

Other complications in the perioperative period included aspiration pneumonia in 2 patients, urinary retention in 2 patients, and postoperative ileus in 1 patient.

After review of the postoperative pelvic radiographs, the surgical reductions were graded as excellent in 23 and imperfect in 6. The surgical reductions based on the CT scans were excellent in 15, imperfect in 11, and poor in 3. The residual displacement was most commonly seen at the reduction of the anterior column component of the fracture. There were no screw placement errors.

Fourteen patients had traumatic medial acetabular dome crush injuries. Thirteen of these were reduced through the fracture itself. In one patient, a separate cortical window was necessary for reduction and bone grafting of the traumatic medial acetabular dome crush injury. Three patients had radiographic collapse of the femoral head into the dome defect on the postoperative radiographs. The average age of the 14 patients with medial dome crush injury in our series was 52 compared to 41 in the 15 patients without dome impaction ($p = 0.09$). Patients with subsequent medial subluxation of the femoral head into the medial dome crush defect had an average age of 61 compared to 49 years in patients without this complication ($p = 0.35$).

One patient with osteogenesis imperfecta had a juxtaarticular screw removed 4 months postoperatively. Another patient required the removal of a symptomatic screw from the anterior superior iliac spine 2.5 years after the initial surgery.

Discussion

Acetabular fractures with quadrilateral surface comminution or displacement are difficult to manage. Techniques used to address the medial quadrilateral surface displacement have included the use of screws alone, plates applied through the iliac window of an ilioinguinal exposure, and braided cables used to secure corticocancellous bone grafts to the quadrilateral surface. Intrapelvic plates function as a buttress to the quadrilateral surface. All patients treated with intrapelvic plates in our series had associated acetabular fracture types with involvement of the quadrilateral surface. Intrapelvic plating techniques were used in only 7% of operatively treated acetabular fractures in our series. The plates are technically demanding to apply, and concern exists with the amount of retraction required to insert them. Despite these concerns, we found that the use of this technique was required to maintain the reduction in this select group of patients. Intrapelvic plating did not prevent medial dome collapse demonstrating that the plate is not able to support or replace the impaction injury. While not statistically significant, there was a trend for the patients with dome impaction to be older. Perhaps supplemental bone graft would be beneficial to avoid such collapse.

This study has also confirmed that the surgical reduction can be more accurately determined on postoperative CT scans. Three reductions that would have been assessed as excellent or imperfect on plain pelvic radiographs alone were demonstrated on pelvic CT to be poor.

Overall 17 (58%) patients developed a postoperative complication. Four patients required five additional surgical procedures. None of these complications were attributed to the intrapelvic plate. The most common complication was deep vein thrombosis, and this was noted in 10 patients (34%). It is postulated that the high rate of deep vein thrombosis seen may be attributed to the mechanical effect of compression on the pelvic veins by the displaced fracture fragments at the time of injury or secondary to the retraction necessary intraoperatively.

Conclusion

Intrapelvic plating techniques for acetabular fractures are indicated infrequently. Despite the implant location and the retraction necessary to insert them an intrapelvic implant can be inserted safely. Intrapelvic plates stabilize quadrilateral surface comminution well, but are unable to support or replace medial dome acetabular impaction injuries. DVT is common when this surgical technique and fracture pattern are combined.

Recommended Reading

Cole JD, Bolhofner BR. Acetabular fracture fixation via a modified Stoppa limited intrapelvic approach: description of operative technique and preliminary treatment results. Clin Orthop. 1994; 305: 112-123.

Qureshi AA, Archdeacon MT, Jenkins MA, et al. Infrapectineal Plating for acetabular fractures: A technical adjunct to internal fixation. J Orthop Trauma. 2004; 18(3): 175-178.

Hirvensalo E, Lindahl J, Bostman O. A new approach to the internal fixation of unstable pelvic fractures. Clin Orthop. 1993 Dec; (297): 28-32.

Karunakar, MA, Le TT, Bosse, MJ. The modified ilioinguinal approach. J Orthop Trauma 2004; 18(6): 379-383.

Preliminary Testing of a System to Reduce Occupant Injury in Side Impact (T-bone) Vehicle Collisions

Allan F. Tencer, Ph.D., Philippe Huber, Robert P. Kaufman, B.S., Charles N. Mock, M.D., and M.L. Chip Routt, Jr., M.D.

Side impact crashes represented, in 2003, 32% of all fatal collisions in the US (second only to frontal crashes) with an estimated annual total of 782,000 nonfatal and 9812 fatal injuries. Injuries to the chest occurred in 40% of surviving occupants, followed by injuries to the head (25%), pelvis (12%), and abdomen (8.4%). The fundamental mechanism of injury is direct intrusion of the impacted door into the occupant space. The basic problem with protecting the occupant is lack of space in the vehicle to absorb the collision forces since the occupant sits close to the door. Several strategies have been used to increase occupant protection. Door impact beams have been mandated since 1997 in all vehicles sold in the US, to reduce door intrusion. Arm rests and door panels have more padding and arm rests have been relocated at about hip level (for the adult male) to avoid impact into the chest wall. Apart from head curtain side airbags, thoracic airbags will be available in about 40% of new vehicles in 2004. These reduce chest loads about 15%, but significant concern has been raised about the scenario in which the driver observes a vehicle coming across an intersection and in swerving away, is thrown against the door by the evasive maneuver, and has the airbag fire into his/her chest causing rib fracture and arm injury. Also, serious concern has been raised about thoracic airbags, positioned to protect the adult male chest, firing into the heads of child or short women passengers, causing neck injury.

In our study of these crashes as part of the Crash Injury Research and Engineering Network (CIREN) we observed many occupants being

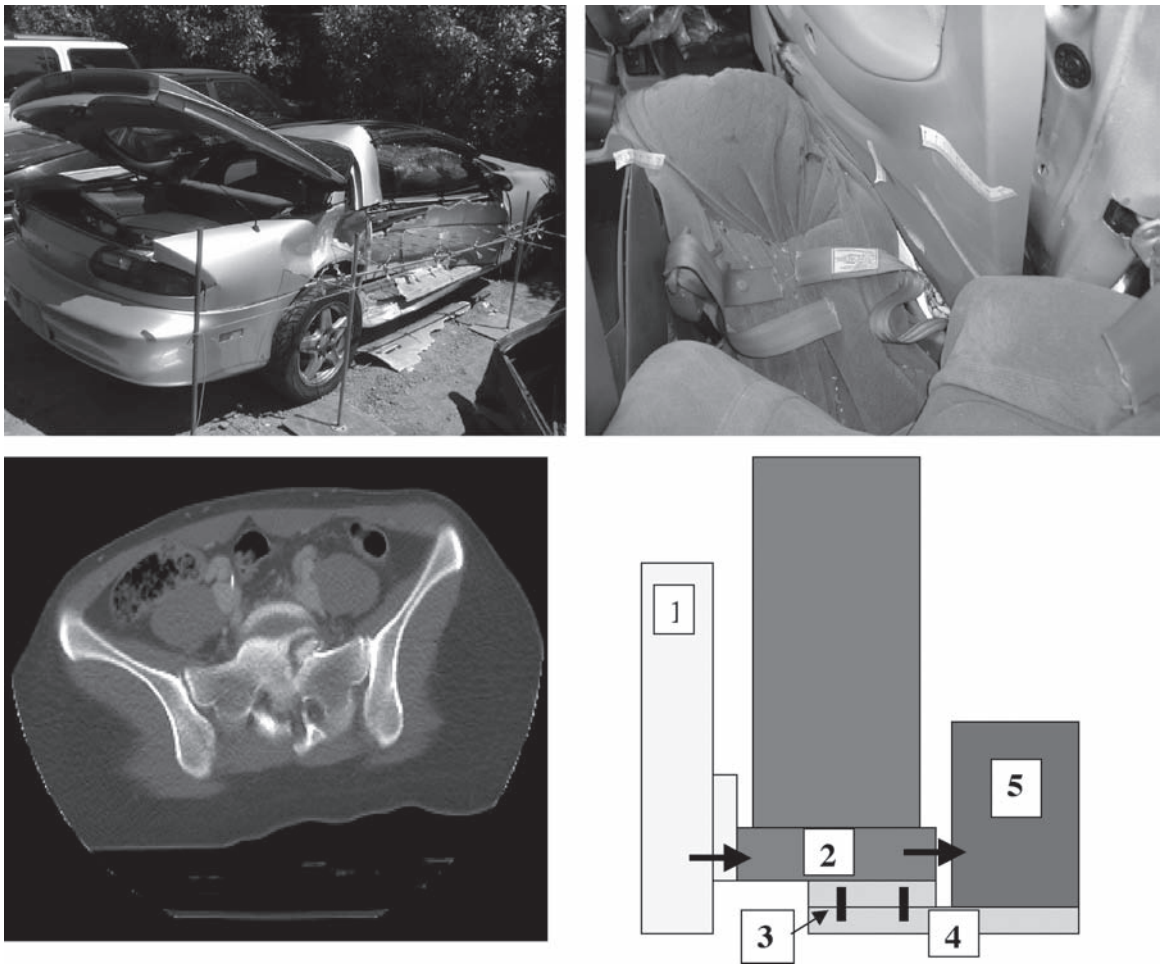

Figure 1: (upper left) CIREN crash example of a vehicle with passenger side impact, (upper right) occupant was trapped between the intruded door and the center console and (lower left) sustained a serious bilateral pelvic fracture and chest injuries. (lower right) proposal for a side impact safety system (1) door displaces inward contacting (2) rigid seat frame which shear bolts (3) and displaces along track (4) towards center of vehicle, crushing console (5) and allowing the occupant to move away from the incoming door.

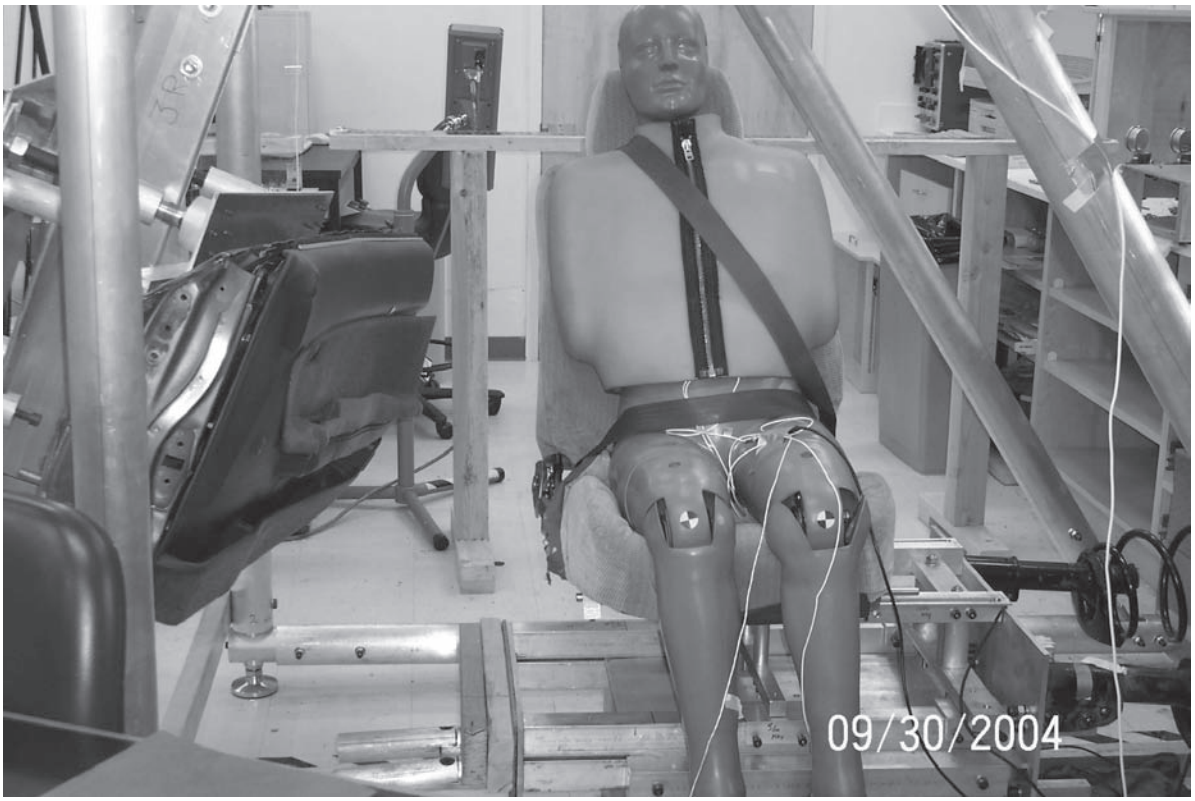

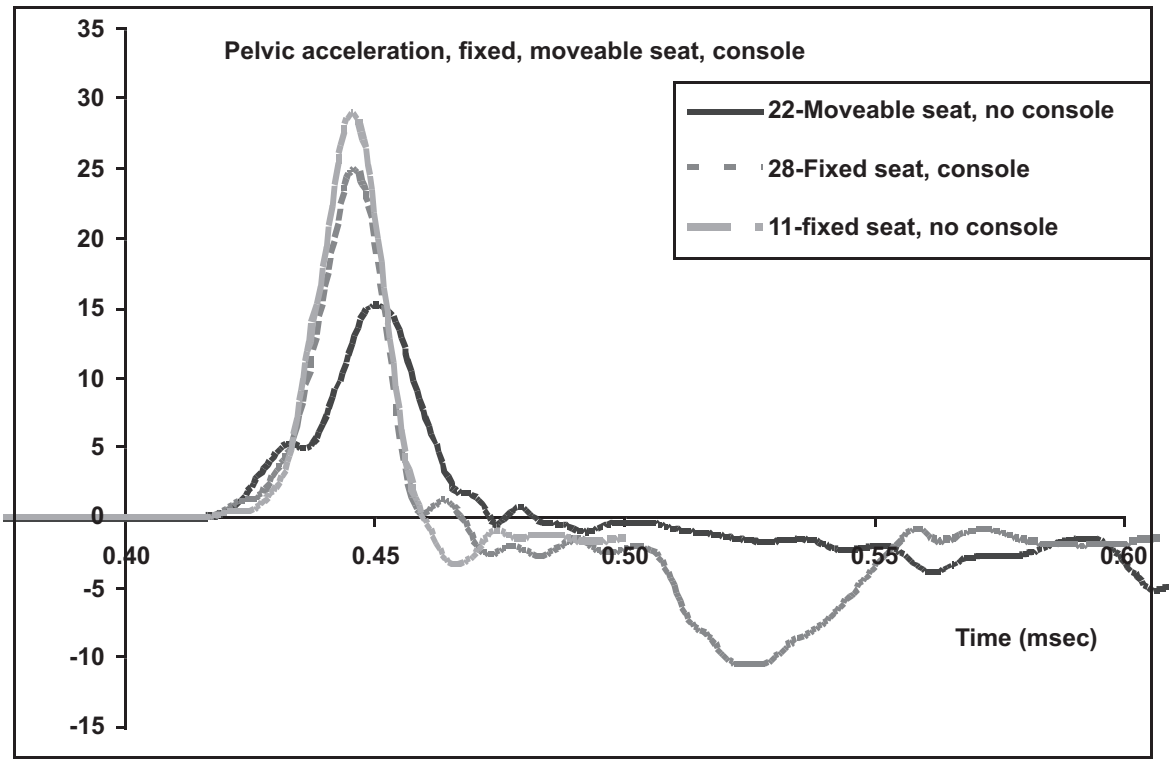

Figure 2: (Upper) Impact test apparatus showing pendulum with Toyota Celica crushed door and US DOT SID (side impact dummy). (Lower) Sample pelvic acceleration time histories from the experimental testing, with a laterally moveable seat and no console, a fixed seat with no console, and a fixed seat with a console. The Moveable seat reduced primary pelvic acceleration and eliminated the secondary (negative) acceleration.

trapped between an unyielding center console and the incoming door, Figure 1. This led to the idea of replacing the console, which has no structural purpose, with a softer, crushable console. Extending that further, we proposed a system, shown in Figure 2, in which the incoming door contacts a rigid seat (instead of directly into the occupant's chest and hip), causing the seat to displace laterally into the space occupied by the console and carrying the occupant away from the door. This report describes preliminary modeling and experimental testing of the concept.

Methods

Field Studies of Vehicle Crashes

In this phase, we tested the hypothesis that occupants in vehicles with center consoles were more likely to sustain pelvic injuries, through the mechanism described above. Crashes in the CIREN database were selected based on several criteria: (i) the occupant must have been restrained, (ii) an injury of AIS 3 (abbreviated injury score, 3 = serious) or greater (4 = severe) must have occurred, (iii) the impact was +/- 20 deg from perpendicular to the vehicle's door, and (iv) the victim was sitting on the side nearest the location of impact. Each crash scene and vehicle investigation conducted by CIREN centers follow the data collection format established by NASS (National Automotive Sampling System, US Dept of Transportation). Each crash site had scaled documentation of the roadway, traffic controls, road surface type, conditions, and road grade at both pre- and post- impact locations. Exterior, interior, and restraint system use inspections of the vehicle were performed. With Institutional Review Board approval, the injuries were assessed by examining the patient's medical records and imaging studies. For this study we identified 62 occupants in 54 crashes in vehicles between model years 1998 and 2004. Field observations were made separately to determine whether or not the types of vehicles involved had center consoles. Center consoles do not include soft or fold down arm rests, only relatively rigid center structures protruding above seat level.

Experimental testing and modeling

The test apparatus is shown in Figure 2a. The experiment was designed to simulate the contact phase of a SINCAP test (Side Impact New Car Assessment Program, the USDOT requirement for side impact safety certification). The impactor is a simple pendulum to which the door was mounted with an apparatus that could align the door vertically and change its orientation both vertically and horizontally. The top of the arm rest was level with the pelvis of the dummy. Two springs which could be pre-compressed were used to stop the forward travel of the pendulum, which approached 6.6 m/sec (equivalent to the velocity transferred to the door from a side impact by a vehicle traveling at about 30 mph). We selected a DOT SID (US Dept of Transportation Side Impact Dummy) which was fully instrumented to measure pelvic, spine, and rib accelerations. The dummy was restrained with a lap and shoulder belt fixed to the seat. The seat was designed to test the configurations of a fixed seat, with and without a console, as well as a laterally moveable seat, with 25 cm of displacement. The complete experiment was modeled mathematically in 3-D using the MADYMO system (mathematical dynamic modeling, TNO Automotive, Livonia, MI).

Results

CIREN data

There were no significant differences in age, percent drivers, percent belted, and mean delta V between the two groups (vehicles with or without consoles). In crashes with between 15 and 30 cm of door intrusion, 14 occupants in vehicles with consoles and 5 in vehicles without consoles suffered AIS 2 and 3 injuries ($p<0.05$). In crashes with 30-46 cm of door intrusion, 15 in vehicles with consoles and 4 without consoles suffered pelvic injuries ($p <0.05$).

Experimental results

The pendulum tests were reproducible with a coefficient of variation in peak pelvic acceleration of 0.074 (standard deviation / mean). With a fixed seat and no console, the maximum pelvic acceleration (due to contact from the door) was 28.5g and the minimum (due to the lap belt) was -3.3g. With a console plate added, the maximum acceleration was 24.8g (not significantly different) while the minimum acceleration (due to contact with the console) decreased to -10.5g ($p <0.05$). With a seat allowing lateral movement upon impact, with no console, the maximum pelvic acceleration decreased to 15.3g ($p< 0.05$) and minimum acceleration remained at -3.8g.

Discussion

In about 12% of side impacts the occupant suffers at least an AIS 2 pelvic injury, with unilateral pubic rami, symphysis, or SI fracture. The most likely mechanism is from direct contact of the intruding door into the pelvis. However, this mechanism does not explain the occurrence of bilateral pelvic fractures with bony injury on the side opposite the location of door contact. We reviewed CIREN crashes and found the severity of pelvic fractures was greater in vehicles with center consoles, with 15-46 cm of door intrusion. Unstable pelvic ring fractures are life threatening, due to their associated injuries. Bilateral pelvic fractures and dislocations are more difficult to treat than unilateral injuries with a greater rate of complications. Considering the severity of the resulting injury, it seems reasonable to maintain the useful function of a center console, but simply construct it so that it would yield with pelvic contact during a side impact. Further protection can be gained by allowing the seat to displace towards the center of the vehicle. In this way both maximum pelvic acceleration, produced from contact with the door, and minimum pelvic acceleration, from contact with a center console on the opposite side of the pelvis, can be reduced.

Recommended Reading

Traffic Safety Facts, 2002, NHTSA, US Department of Transportation, DOT HS 809 100, Dec, 2000, p 106.

Samaha RR, Elliott DS, NHTSA side impact research: Motivation for upgraded test procedures, Proceedings of the 18th Conference on the enhanced safety of vehicles, Nagoya, Japan, May 2003, paper 492.

Daniel RP, Biomechanical design considerations for side impact, SAE Trans 890386, 1989.

Anterior Inferior Bone Grafting Can Restore Stability In Osseous Glenoid Defects

William H. Montgomery, Jr., M.D., M.P.H., Melvin Wahl, M.D., Carolyn Hettrich, M.D., Eiji Itoi, M.D., Steven B. Lippitt, M.D., and Frederick A. Matsen III, M.D.

The glenoid fossa plays a major role in stabilizing the humeral head. Glenohumeral instability associated with a significant osseous defect of the glenoid is often treated with bone grafting to restore the glenoid concavity. The shape and positioning of the graft is critical: a graft that encroaches on the extrapolated glenoid curvature can prevent the head from seating completely in the glenoid, while a graft that is too far from the curvature does not restore the glenoid concavity. The purpose of this study is to investigate the effects on the stability provided by the glenoid of (a) a standardized anteroinferior glenoid defect and (b) different configurations of anteroinferior glenoid bone graft.

Methods

Each of four fresh cadaveric shoulders was potted in plaster in a metal frame so that the glenoid face was oriented parallel to floor facing upwards. The anteroinferior stability provided by the glenoid was quantitated by measuring the balance stability angle in that direction, that is the maximal angle that the glenoid could be tipped in the anterior inferior direction before a ball placed in the concavity dislocated over the lip. (Figure 1 A-C). The anteroinferior stability was assessed in each glenoid (1) in the unaltered state, (2) after creating a standardized defect of a magnitude reported by other investigators to be sufficient to require a bone graft, and (3) after each step of a series of procedures providing varying height and contour of bone graft.

The defect size and orientation was standardized using the parameters suggested by Itoi et al. The superior inferior glenoid length was measured for each glenoid. The length measurement was then multiplied by .21 to determine the defect size to be created along a line inclined 45 degrees from the centerline to the anteroinferior border of the glenoid with the apex at 4:30 or 7:30 depending on whether a right or left glenoid was utilized. The length of the glenoids ranged from 32 mm to 34 mm. All defects created were 7mm in maximal width (from 20.5% to 21.9% of the glenoid face length) (Figure 2 A and B).

Reconstruction of the glenoid defect with a bone block was accomplished by using a block measuring 20mm length x 25mm height x 8 mm wide. For convenience, this graft was harvested from the tip of the scapula, recognizing that in the clinical situation the graft is harvested from the iliac crest or obtained as an allograft. Each glenoid was grafted with bone harvested from its scapula. Once the stability was quantitated for the normal glenoid and for the glenoid with the standardized defect, the reconstruction was undertaken. The uncontoured bone block was secured to the defect using two 3.5mm cannulated screws placed through the graft and into the native glenoid subchondral bone (Figure 2C). The graft was initially placed at a height of 8mm above the glenoid face.

The anterior inferior balance stability angle was measured three times for each of the four glenoids for each preparation. The average of the three trials was used as the value for each specific preparation of each glenoid: native, after creation of the defect, 8 mm graft (uncontoured) (Fig 3A), 8 mm graft (contoured), 6 mm graft (contoured) (Figure 3B), 4 mm (contoured), 2 mm (contoured) and flush with the glenoid face. Contouring was performed as a surgeon would perform it in the operating room, shaping the bone graft by eye to match the curvature of the ball using

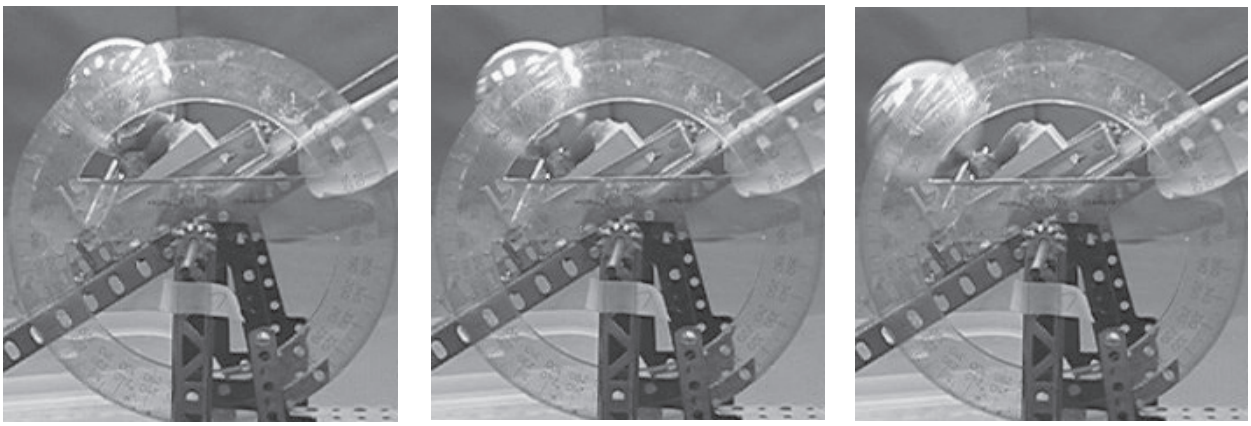

Figure 1 A, B, C: Measurement of balance stability angle. Three consecutive frames from the video recording of a glenoid being tipped at a constant rate. Note that within these three frames the ball moves from being centered (A), to moving over the lip (B), to dislocation (C). The balance stability angle is the angle of tip at which dislocation occurs.

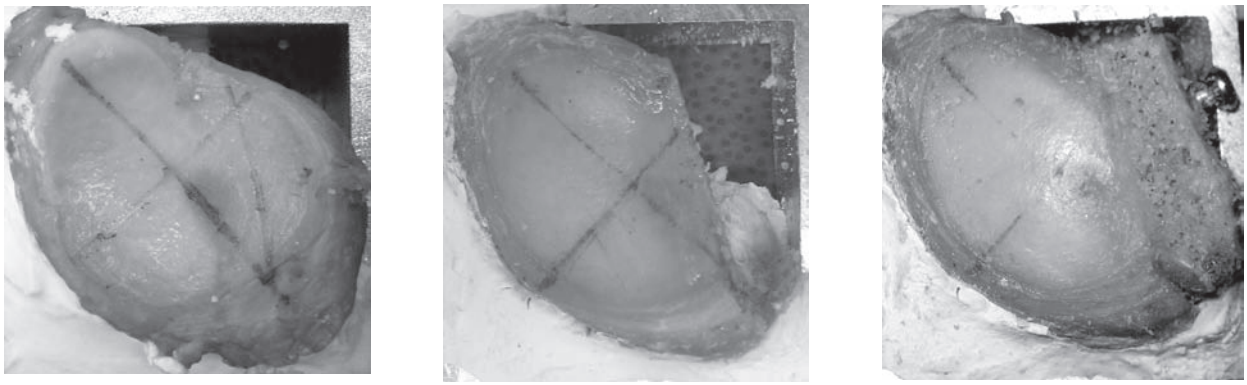

Figure 2 A, B, C: Creation of the anterior inferior glenoid defect. A. A normal glenoid. B. A glenoid with the standard defect. C. A glenoid with a graft.

a pinecone burr. The contouring of the graft was performed *in situ* without removing the screws. Physiologic saline was applied to the glenoid face between trials to prevent desiccation.

The glenoids were also observed to confirm the graft height at which contact of the ball with the graft was eliminated allowing the ball to seat in the reconstructed glenoid.

Results

The results are summarized in the Table. The balance stability angles were reproducible (within one degree) across all trials for each preparation of each glenoid. The average stability angle of the native glenoids was 26 degrees with a significant decrement to 14 degrees when the defect was created ($p = .006$). An uncontoured graft placed at 8mm had an average stability angle of 31 degrees which, when contoured, increased the average stability angle to 46 degrees. The increase in stability over the glenoid with the standardized defect was particularly marked for contoured graft heights of 6mm and 8mm, where the increases were 250% (p .001) and 330% (p .00025), respectively, while those with a graft height of 4mm approached significance (p .062). The average stability angle of the glenoids with the contoured graft placed at 4mm was almost 5 degrees greater than that of the native glenoid while a graft height of 2mm showed an average stability angle within .4 degrees of the native glenoid.

The ball was observed to be perched on the graft and posterior glenoid at graft heights of greater than or equal to 6mm. Contouring of the graft was helpful in minimizing the potential for unwanted contact between the ball and the graft.

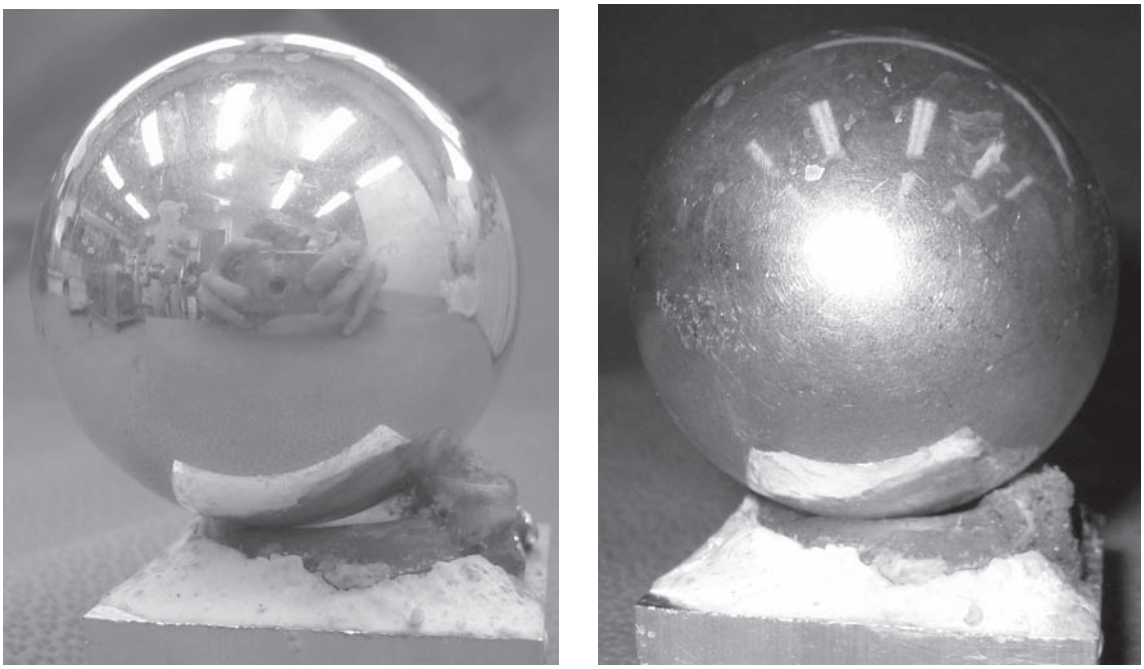

Figure 3 A, B: Relation of graft to the contour of the glenoid and the ball. A. An 8 mm uncontoured graft. B. A 6 mm contoured graft.

GLENOID #	Native	Defect	8mm Uncontoured	8mm Contoured	6mm Contoured	4mm Contoured	2mm Contoured	Flat
1	29	11	23	42	32	31	28	24
2	24	13	32	49	38	34	27	21
3	28	17	26	49	36	32	24	21
4	24	15	44	44	33	27	25	22
Ave	26	14	31	46	35	31	26	22
Std Dev	2	2	9	4	3	3	2	1
p for difference from initial		0.006	0.473	0.004	0.027	0.062	0.790	0.018
p for difference from defect			0.033	0.000	0.001	0.004	0.012	0.021

Table 1: Balance Stability Angles of Differing Glenoid States.

Conclusion

A bony defect can significantly compromise the anteroinferior instability provided by the glenoid. The lost stability can be restored by bone grafting. The effectiveness of the graft in restoring the lost stability is related to both its height and to the extent to which it is contoured as long as the graft is not so prominent that it forces the ball posteriorly from the center of the glenoid.

Recommended Reading

Itoi, E., S. B. Lee, et al. (2000). "The effect of a glenoid defect on anteroinferior stability of the shoulder after Bankart repair: A cadaveric study." J. Bone Joint Surg. 82A(1): 35-46.

Matsen, F. A., 3rd, R. M. Titelman, et al. (2004). Glenohumeral instability. The Shoulder. C. A. Rockwood, Jr., F. A. Matsen, III, M. A. Wirth and S. B. Lippitt. Philadelphia, W.B. Saunders. 1: 655-790.

Matsen, F. A., 3rd and S. B. Lippitt (2004). Procedure: Reconstruction of a deficient anterior glenoid lip using an extracapsular anatomically contoured iliac crest graft. Shoulder Surgery: Principles and Procedures. Philadelphia, Saunders: 150-174.

Weldon, E. J., III, M. M. Scarlat, et al. (2001). "Instrinsic stability of unused and retrieved polyethylene glenoid components." J. Shoulder Elbow Surg. 10(5): 474-481.

Weldon, E. J., III, R. Boorman, et al. (2004). "Optimizing the intrinsic stability of the glenoid fossa with non-prosthetic glenoid arthroplasty." J. Bone Joint Surg. (accepted for publication).

The Olecranon Osteotomy: A Six-Year Experience in the Treatment of Intra-Articular Fractures of the Distal Humerus

David P. Barei, M.D., F.R.C.S.C., Chad P. Coles, M.D., F.R.C.S.C., Sean E. Nork, M.D., Lisa A. Taitsman, M.D., M.P.H., Douglas P. Hanel, M.D., and M. Bradford Henley, M.D., M.B.A.

Open reduction and internal fixation (ORIF) remains the standard of care for the treatment of intra-articular distal humerus fractures in the physiologically active patient. The intra-articular olecranon osteotomy, can provide exceptional visualization of the distal humeral articular surface, enabling accurate articular reduction and fixation. Significant osteotomy complications, such as delayed union, nonunion, and symptomatic olecranon fixation have been reported. Alternate soft tissue mobilization exposures have been advocated, but do not offer the same degree of articular visualization. The primary purpose of this study is to review our experience with the olecranon osteotomy for the management of bicolumnar distal humerus fractures treated over a six-year period at a Level One trauma center. Secondarily we will compare the utilization, complications, and accuracy of distal humeral articular reductions treated via the olecranon osteotomy with other non-osteotomy exposures for the management of these injuries.

Materials and Methods

Over a 72-month period from January 1998 to December 2003 inclusive, 145 patients with 145 bicolumnar intra-articular distal humerus were identified from our Institution's computerized orthopaedic trauma database. Non-salvageable injuries (n=5), skeletally immature patients (n=6), patients treated non-operatively (n=6) or with primary elbow arthroplasty (n=6), and those who sustained ipsilateral intra-articular proximal ulna fractures (n=8) were excluded. The remaining 114 patients sustained 114 AO/OTA type 13-C distal humerus fractures (11) and formed the study group. Injuries were classified as: 21 C1 fractures (18.4%), 44 C2 fractures (38.6%) and 49 C3 fractures (43%). Operative management utilized either an olecranon osteotomy or a non-osteotomy soft tissue mobilizing technique at the discretion of the treating surgeon. The primary indication for using an olecranon osteotomy was to improve articular visualization, facilitating accurate articular reduction and stabilization.

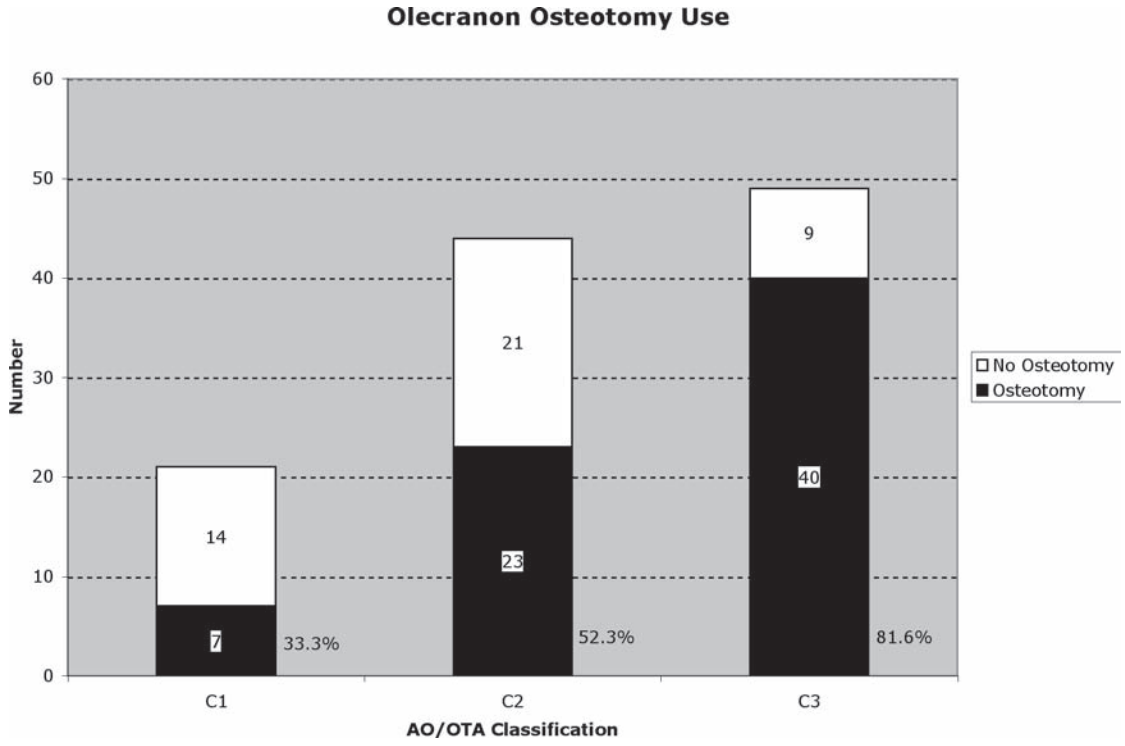

Figure 1: The distribution of the transolecranon exposure for ORIF of bicolumnar distal humerus fractures according to the AO/OTA Fracture Classification is illustrated. The increasing utilization of this exposure in distal humerus fractures that exhibit increasing amounts of metaphyseal (C2) and articular (C3) comminution is statistically significant.

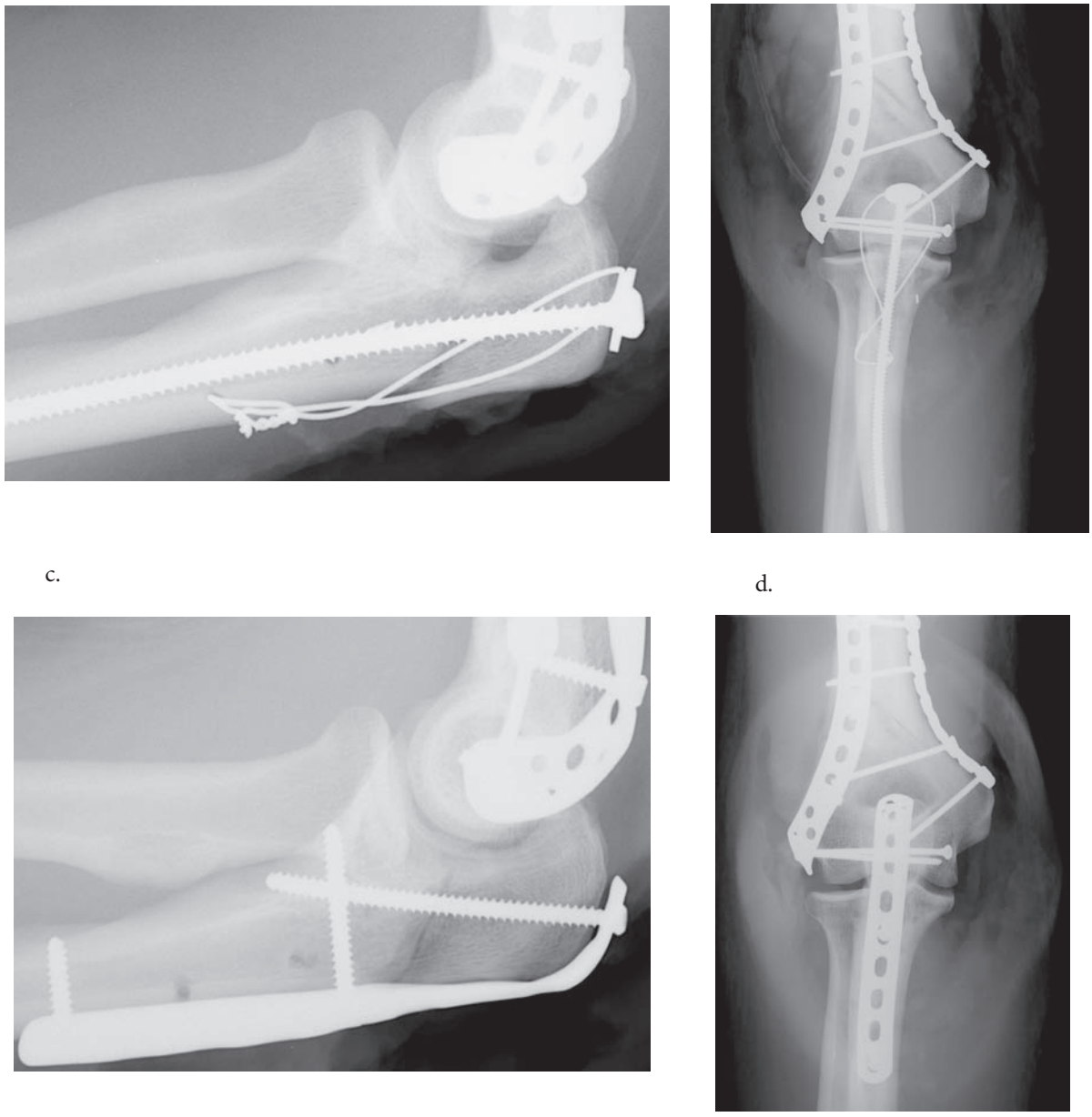

Figure 2: a. and b.) Immediate post-operative anteroposterior and lateral radiographs of a C-type distal humerus fracture treated using an olecranon osteotomy exposure. Note the oblique orientation of the osteotomy and malreduction on the lateral radiograph. The intramedullary screw and tension-band wire are unable to neutralize the shearing forces along the plane of the osteotomy, particularly when compressive loads are applied along the longitudinal axis of the ulna. This degree of displacement was considered unacceptable and was revised in the immediate post-operative period. c. and d.) Anteroposterior and lateral radiographs of the same fracture after the osteotomy fixation was revised to a plate/screw construct. Satisfactory osteotomy reduction has been obtained. The oblique nature of the osteotomy is easily identified on the lateral radiograph. Uneventful union occurred within 12 weeks of the revised fixation.

Patient records were reviewed to determine perioperative complications, union rates, and subsequent procedures, including those performed at outside institutions. Osteotomy union was defined as replacement of the radiolucent osteotomy site with bone on anteroposterior (AP) and lateral radiographs, and the initiation of resistive elbow extension exercises.

Two orthopaedic trauma surgeons assessed the accuracy of all articular reductions (distal humerus and olecranon) using the injury and immediate post-operative AP and lateral radiographs. An articular reduction of ≤ 2mm step/gap was considered satisfactory, while reductions with greater displacement were considered unsatisfactory.

Osteotomy Group

Of the 114 fractures, 70 (61.4%) were managed via an intra-articular, chevron-shaped olecranon osteotomy.

This included 47 male (67.1%) and 23 female (32.9%) patients, with a mean age of 41.1 years (range, 15 - 85). The mechanisms of injury included falls from a height (n=30), motor vehicle collisions (n=16), recreational injuries (n=12), car-pedestrian injuries (n=5), low-energy falls (n=5), and ballistic injuries (n=2).

Non-osteotomy Group

In the remaining 44 patients (38.6%), the fractures were exposed via the paratricipital approach in 28 cases (63.6%), a "triceps turndown" in 12 cases (27.4%), a modified triceps-splitting approach, specifically described by McKee et al., in two patients (4.5%), and the "triceps sparing" exposure of Bryan and Morrey in two cases (4.5%). There were 23 male (52.3%) and 21 female (47.7%) patients, with a mean age of 38.8 years (range, 14 - 86). The mechanisms of injury included motor vehicle collisions (n=13), falls from a height (n=11), recreational injuries (n=7), low-energy falls (n=6), car-pedestrian injuries (n=4), and ballistic injuries (n=3).

Osteotomy Technique

A uniform technique for the creation of the olecranon osteotomy was used. A standard posterior exposure was performed with mobilization of the ulnar nerve.

Beginning on the dorsal surface directly posterior to the deepest portion of the semilunar notch, an oscillating saw was used to create the "V"-shaped chevron osteotomy into, but not through, the subchondral bone. The osteotomy was completed with an osteotome. The osteotomized portion of the olecranon and the triceps muscle were reflected proximally.

After assuring satisfactory ORIF, an anatomic articular reduction of the osteotomy was the objective in all cases. Commonly, a long (>100mm) single intramedullary screw, washer, and a tension-band wire were employed for fixation. Infrequently, the stability of the osteotomy could not be assured with the screw and tension-band wire technique. In these situations, plate osteosynthesis was performed. However, osteotomy fixation was determined, in part, by surgeon preference, with the common goal being rigid stabilization of the osteotomy throughout a functional arc of motion. Kirschner wire (K-wire) fixations were not used during this study period.

Results

Injury Characteristics

Of the 70 patients operatively managed using an olecranon osteotomy, 42 fractures were open (60%), compared with 18 of the 44 patients (41%) treated without an olecranon osteotomy (p=0.047). All open wounds were located posteriorly and no patient required free tissue transfer. Eighteen of the 42 patients (42.9%) had substantial disruption of the triceps tendon as noted at the time of surgical fixation. The mean ISS (16, 17) was 11.5 in the osteotomy group (range 4-34) and 11.3 in the non-osteotomy group (range 4-43) (p=0.913). Eleven patients in the osteotomy group (15.7%) and eight patients in the non-osteotomy group (18.2%) were multiply injured (ISS > 18) (p=0.731).

The use of an olecranon osteotomy significantly increased in proportion to fracture complexity, particularly with distal humeral articular comminution. Specifically, 7 of 21 (33.3%) type C1 fractures, 23 of 44 (52.3%) type C2 fractures, and 40 of 49 (81.6%) type C3 fractures were treated using an olecranon osteotomy (p<0.001) (Figure 1).

Operative Characteristics

The choice of osteotomy fixation was ultimately determined by surgeon preference. Intramedullary screw and tension-band wire constructs were used in 46 patients. Fixation was achieved with a 4.5mm intramedullary screw in 29 patients, and a 6.5mm intramedullary screw in 16 patients. Three of the 6.5mm screws were placed after encountering insufficient fixation with a 4.5mm screw. Plate fixations were used in 24 patients. One-third tubular and one-quarter tubular plates were used in 15 and three patients, respectively. Five osteotomies were repaired with a commercially available, precontoured plate. A 3.5mm dynamic compression plate was used in one case.

Complications

Complications directly related to the osteotomy that required surgical interventions were considered major and occurred in 11% of patients.

In the osteotomy group, two patients died prior to three-month follow-up, and one patient was lost to follow-up prior to documented osteotomy healing. The remaining 67 patients (95.7%) had sufficient follow-up to establish osteotomy union, with a mean follow-up of 31 months (range, 3-81 months). There were no cases of osteotomy nonunion. There were two cases of early (≤ 4 weeks) osteotomy displacement (2.8%). In one of these, union occurred ten months later without further intervention, but was considered a delayed union (1.5%).

An additional six patients were lost to final follow-up, leaving sixty-one patients (87.1%) available to determine complications associated with implant prominence. The mean follow-up was 32.5 months, (range, 6-73 months). Fifty patients (82%) had greater than one-year follow-up. Of the 61 patients, five (8.2%) had symptomatic olecranon implants electively removed. Twelve patients (19.7%) had olecranon implants removed in conjunction with other surgical procedures. In total, 17 of the 61 patients (27.9%) had proximal ulna fixations removed.

In the non-osteotomy group there were two extensor mechanism failures requiring reoperations. One occurred following the "triceps turndown" approach and the other occurred following the "triceps-sparing" exposure of Bryan and Morrey.

Radiographic Assessment

Anteroposterior and lateral injury and immediate post-operative radiographs were available for review in 118 of the 121 patients. In the non-osteotomy group, there were two cases with unsatisfactory humeral articular reductions (4.1%), one through a paratricipital exposure, and one through a "triceps turndown" exposure. Both fractures were classified as type-C3. All distal humeral articular reductions performed in the osteotomy group were considered accurately reduced.

When reviewed according to the severity of articular injury, all 63 distal humerus fractures with simple articular injuries (21 type C1 and 42 type C2) demonstrated satisfactory articular reductions, regardless of whether an osteotomy or non-osteotomy exposure was used. Conversely, while all 39 type C3 fractures in the osteotomy group were accurately reduced, only seven of nine type C3 fractures in the non-osteotomy group demonstrated a satisfactory articular reduction

(p=0.03).

One olecranon osteotomy demonstrated an unsatisfactory reduction of the osteotomy (1.5%), and was revised in the immediate post-operative period.

Discussion

In this study, despite the increasingly complex articular comminution present in the olecranon osteotomy group, no articular malreductions were identified radiographically; however, two cases in the non-osteotomy group demonstrated unsatisfactory articular reductions. Both of these malreductions occurred in comminuted articular (C3 injuries. When the quality of reduction of only C3 injuries was compared, the osteotomy group demonstrated a statistically significant greater rate of satisfactory articular reductions when compared with the non-osteotomy group. These findings suggest that the olecranon osteotomy facilitates accurate reduction of the distal humeral articular surface, particularly with increasing fracture comminution (type C3 patterns).

In open fractures, injury to the triceps at the meta-diaphyseal region of the distal humerus has been noted by previous authors and has been corroborated by this study. The use of an olecranon osteotomy in 42 open fractures, of which nearly half demonstrated substantial injury to the triceps, did not result in any complications related to osteotomy union. We feel that the presence of an open injury does not preclude the use of the olecranon osteotomy, particularly in the setting of significant articular comminution.

Historically, the most frequent complications associated with an olecranon osteotomy are nonunion and symptomatic implant prominence, particularly with the use of K-wire stabilization. Comparatively, this study identified a lower percentage (11%) of patients that required additional surgical intervention related to the osteotomy. No patient developed an olecranon osteotomy nonunion, but two patients incurred early osteotomy displacement, both requiring revision to plate fixations (Figure 2). Despite the subcutaneous location, the incidence of elective symptomatic implant removal was not found to be higher with plate fixation than with intramedullary screw and wire constructs. If only patients with greater than one year follow-up are considered, the symptomatic implant removal rate remains relatively low at 10%. Other than surgeon preference, our indications for plate stabilization of the olecranon osteotomy are to secure an inadvertently oblique or comminuted osteotomy, or one that fails to demonstrate sufficient stability when placed through a functional range of motion at the conclusion of the procedure.

In conclusion, both the olecranon osteotomy and soft-tissue mobilizing exposures demonstrated satisfactory articular reductions in patients with simple articular injuries. The authors recommend ORIF via the olecranon osteotomy, however, as articular comminution increases. No osteotomy nonunions were encountered in 67 patients, over half of which were open injuries, treated with the transolecranon approach. Whether a 4.5mm or 6.5mm screw with a tension-band technique or dorsal ulnar plating is used for osteotomy fixation, rigid stabilization must be obtained.

Recommended Reading

Gofton WT, Macdermid JC, Patterson SD, Faber KJ, King GJ. Functional outcome of AO type C distal humeral fractures. J Hand Surg [Am] 2003;28(2):294-308.

Henley MB, Bone LB, Parker B. Operative management of intra-articular fractures of the distal humerus. J Orthop Trauma 1987;1(1):24-35.

Henley MB. Intra-articular distal humeral fractures in adults. Orthop Clin North Am 1987;18(1):11-23.

Jupiter JB, Neff U, Holzach P, Allgower M. Intercondylar fractures of the humerus. An operative approach. J Bone Joint Surg Am 1985;67(2):226-39.

McKee MD, Wilson TL, Winston L, Schemitsch EH, Richards RR. Functional outcome following surgical treatment of intra-articular distal humeral fractures through a posterior approach. J Bone Joint Surg Am 2000;82-A(12):1701-7.

The Use of Tensor Fascia Lata Interposition Grafts for the Treatment of Post-Traumatic Radioulnar Synostosis

Jeffrey Friedrich, M.D., Leonid I. Katolik, M.D., Heather Chilcote, B.S. and Douglas P. Hanel, M.D.

The development of a synostosis between the bones of the forearm is a relatively uncommon entity, yet one which poses a high potential for disability of the upper extremity. The formation of a bony bridge between the radius and ulna typically limits pronation and supination, but may interfere with flexion and extension to a lesser degree. Furthermore, loss of forearm rotation, particularly supination, cannot be adequately compensated for by rotation of the shoulder, and renders the positioning of the hand in space for activities of daily living difficult, if not impossible.

The goal of operative intervention following the formation of a bony bridge between the radius and ulna is both the re-establishment of a functional arc of rotation as well as the prevention of future recurrence. Currently, there is no consensus on the ideal treatment for post-traumatic radio-ulnar synostosis. Most authors advocate excision of the synostosis. These procedures are often technically difficult, pose a substantial risk to local neurovascular structures, result in an unpredictable improvement in the arc of forearm rotation, and may not prevent future recurrence.

Placement of an interpositional material at the time of synostosis resection has been proposed as a means of limiting recurrence. However, no agreement exists on the type of interpositional tissue to use, if any, and the use of adjunctive measures such as radiation or pharmaceutical therapy to potentially limit the chance of recurrence. Recommendations include synthetic material, allograft fascia, autograft fascia, or local tissue interposition.

Our study presents our management of radioulnar synostosis with synostosis excision and fascia lata interposition without the use of adjuvant pharmacologic therapy.

Patients and Methods

Patients who had undergone syostosis takedown with either autogenous or cadaveric fascia lata graft interposition were included. A retrospective chart review was conducted and patient records were analyzed for sex, age, mechanism of injury, and time to synostosis correction following injury. Measurements of preoperative, intraoperative, and postoperative range of motion including flexion, extension, pronation, and supination were all recorded. DASH scores were obtained by an investigator not directly involved in the clinical treatment of patients.

Synostosis resection and tensor fascia lata interposition is performed once forearm rotation is limited to less than 45 of supination and pronation each. The patient is administered a general anesthetic, and the entire affected upper extremity prepared

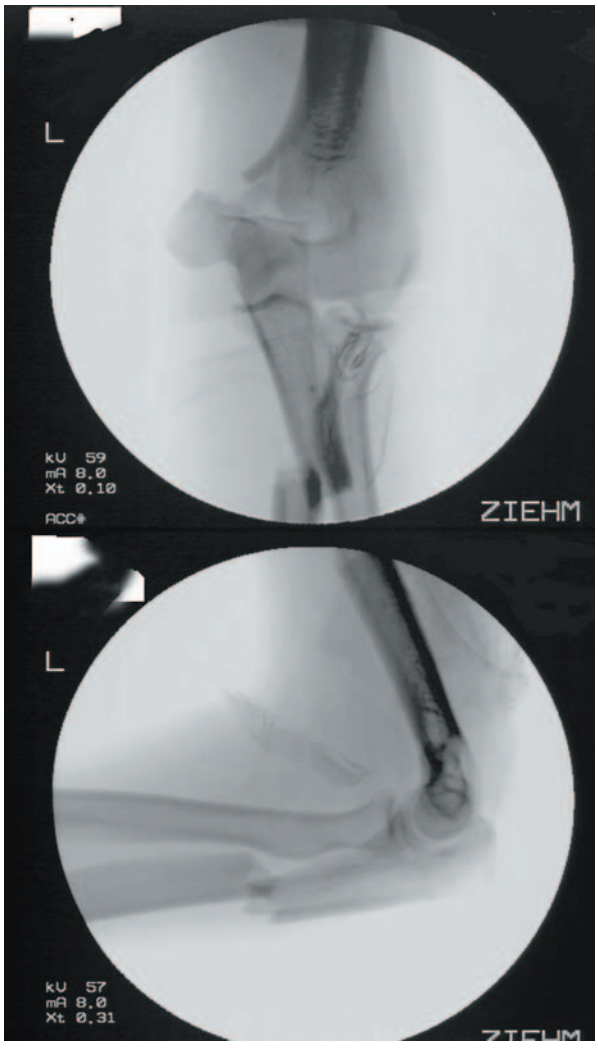

Figure 1: 35 year old male status post MVA. Intra operative films demonstrate a combined humeral fracture and Monteggia fracture.

1.

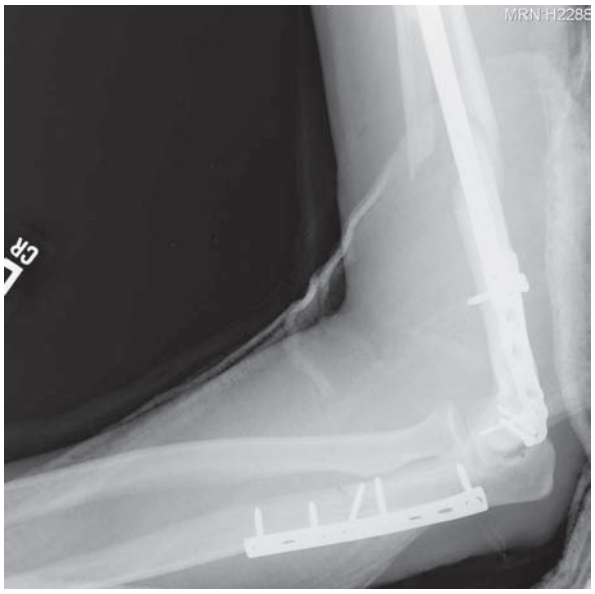

2.

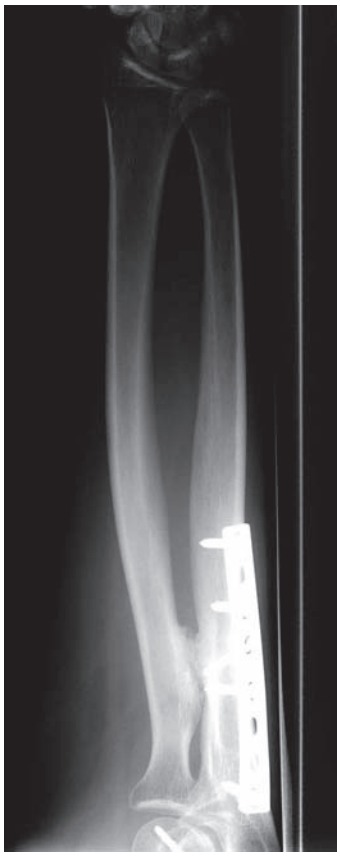

3.

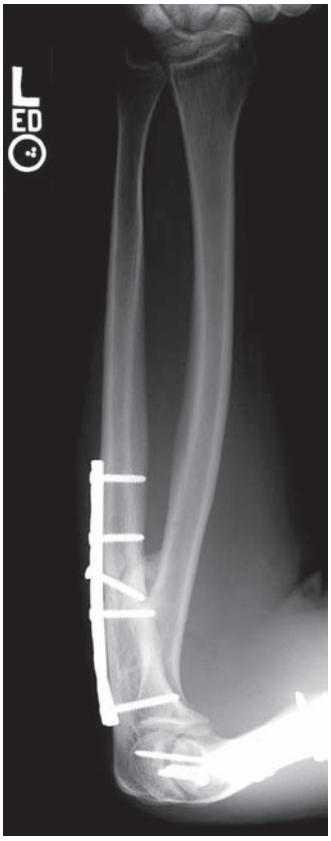

4.

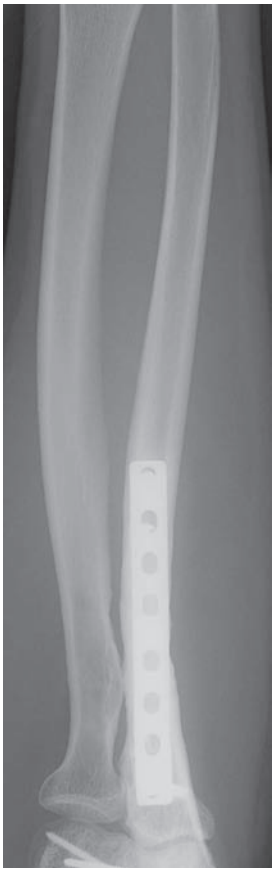

5.

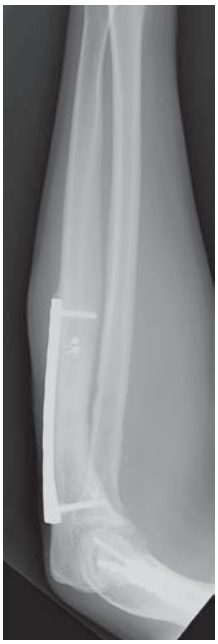

Figure 1 (cont.): 1) The ulna was operatively reduced and stabilized with a 3.5 mm LCDCP plate. 2) and 3) One year later the patient was well healed but demonstrated complete loss of forearm rotation and a well developed proximal radioulnar synostosis. 4) and 5) Synostosis resection and fascia lata interposition (note bone anchors holding graft in place) restored a functional arc of motion from 60 degrees in pronation and 50 degrees of supination.

on a standard hand surgery table. Each exposure was tailored to the individual patient, taking into account pre-existing incisions. Following careful dissection of the surrounding soft tissues, the proximal and distal extent of the synostosis was defined and resected using an oscillating saw and osteotomes. Bone was resected until full passive rotation of the forearm could be achieved. Any bleeding surfaces along the osseous margins were cauterized, and a thin layer of bone was applied with a small elevator. Fascia lata autograft was obtained from patients initially in our series, but given the large donor defect and the high potential for both early and late complications at the graft site, cadaveric graft was subsequently used in all patients. The tensor fascia lata graft was carefully wrapped around either the ulna or radius, and sutured into place using absorbable sutures. The choice of bone depended largely on the surgeon's preoperative and intraoperative perception of the origin on the synososis. This fixation method effectively formed an intact, but not water tight sleeve around one of the forearm bones. A suction drain was placed in each patient and removed when output was less than 25 cc/ 8 hours, for 3 consecutive 8-hour periods. None of the patients received nonsteroidal anti inflammatory medications largely because of their high potential for renal and gastrointestinal complications, as well as the need for strict patient compliance. Patients who had synostoses that were proximal to the radial bicipital tuberosity received a single dose of 500 cGy radiation therapy on the first postoperative day. Based on a previous study that demonstrated prevention of recurrence of heterotopic ossification when the ectopic bone is proximal to the bicipital tuberosity, we chose to utilize this therapy for these patients.

On postoperative day one a controlled therapy regimen was implemented which consisted of active, active assisted, and passive forearm rotation, with static splinted alternating between full passive pronation and full passive supination between therapy sessions.

Results

Thirteen patients were evaluated at an average follow-up of 30 months. There were 10 men and 3 women. The average age was 36.2 years (range 20-54). The average time to synostosis resection was 20.2 months after injury. The synostosis locations consisted of 9 proximal (4 of those were proximal to the bicipital tuberosity), 2 middle, and 2 distal. Four patients received a dose of postoperative radiation. Mean preoperative pronation was 13.8 degrees, and mean postoperative was 61.8 degrees ($p=0.0001$). Mean preoperative supination was 3.8 degrees, and mean postoperative was 62.4 degrees ($p=0.00002$). The mean DASH score was 29.96 (range 8.62 - 49.14).

Discussion

Published series on the operative treatment of radioulnar synostosis have largely been based on case reports involving one to three patients per series. These reports substantiate a pessimistic approach towards this entity, but are indeed based on little agreement to therapeutic approach. There is a hesitant agreement toward the necessity of surgical resection of the bony synostosis. However, recommendations regarding the timing of synostosis correction, the utility of interposition material, the type of interposition material to be used, and the use of prophylactic radiation therapy or pharmacotherapy vary widely.

Our series of patients demonstrates generally satisfactory results with forearm synostosis excision and tensor fascia lata graft interposition. Figure 1 illustrates a typical case example.

The use of this interposition material is safe, carries a negligible risk of complications, and leaves the patient with much improved range of motion. It is for these reasons that we recommend tensor fascia lata grafts as the preferred interposition material for post-traumatic radioulnar synostosis.

Recommended Reading

Jupiter J B,Ring D. Operative treatment of post-traumatic proximal radioulnar synostosis. J Bone Joint Surg Am, 1998. 80(2): p. 248-57.

Failla J M, Amadio P C,Morrey B F. Post-traumatic proximal radio-ulnar synostosis. Results of surgical treatment. J Bone Joint Surg Am, 1989. 71(8): p. 1208-13.

Vince K M, JE. Cross-union complicating fracture of the forearm. Journal of Bone and Joint Surgery, 1987. 69A: p. 640-53.

Sachar K, Akelman E,Ehrlich M G. Radioulnar synostosis. Hand Clin, 1994. 10(3): p. 399-404.

Capitate Shortening Osteotomy and Vascularized Bone Grafting for the Treatment of Kienböck's Disease in the Ulnar Positive Wrist

Leonid I. Katolik, M.D. and Thomas E. Trumble, M.D.

The loss of nutrient blood flow without an obvious traumatic cause is termed "idiopathic" avascular necrosis. While any bone can undergo idiopathic avascular necrosis, among the carpal bones the lunate is most commonly affected. The best test to demonstrate the avascular necrosis is a magnetic resonance imaging (MRI) study that shows signal change in the lunate (Figure 1). While a discrete traumatic event may indeed be the inciting factor which initiates the collapse of the microcirculatory vascular supply of the lunate, repetitive, sub-threshold trauma, may play the key role in both the initiation and propagation of the disease process.

The natural history of Kienböck's disease is progressive fragmentation and collapse of the lunate, rotation of the scaphoid, proximal migration of the capitate, and the eventual development of radiocarpal arthrosis. Prior to collapse of the carpus into an instability pattern, salvage of the lunate may help to maintain carpal kinematics.

Joint leveling procedures such as radial shortening osteotomy have found clinical applicability in the treatment of Kienbock's disease by off-loading force transmission across the radiolunate articulation. However, since Kienbock's disease certainly may occur in the ulnar neutral or ulnar positive wrist, attempted salvage of the lunate in these patients should seek to alter force transmission across the carpus rather than across the radiocarpal articulation.

In the ulnar neutral or positive wrist capitate shortening has been shown biomechanically to decrease loads across the radiolunate articulation. Furthermore, the osteotomies do not address issue of the avascular bone directly. Therefore, we describe our experience with capitate shortening and vascularized bone grafting for the treatment of Kienböck's disease.

Fourteen patients with ulnar positive wrists underwent capitate shortening osteotomy for stage II and IIIA Kienböck's disease. Average follow-up was 40.6 months. All patients underwent capitate shortening osteotomy. The capitate was approached using a midline dorsal incision. This allows for the vascularized bone graft to be harvested from the dorsal carpal arcade as crosses over the base of the third metacarpal (Figure 2). The tendons of the fourth compartment are retracted to the ulnar side and the capsule overlying the capitate is incised longitudinally. The vascularized more graft is elevated using microvascular instruments and place into the lunate after the necrotic bone has been removed with a burr (Figure 3). The location in the proximal portion of the body of the capitate for the osteotomy is confirmed using fluoroscopy. When the capitate is easily mobilized from the hamate, the capitate alone may be shorted (Figure 4). When both the

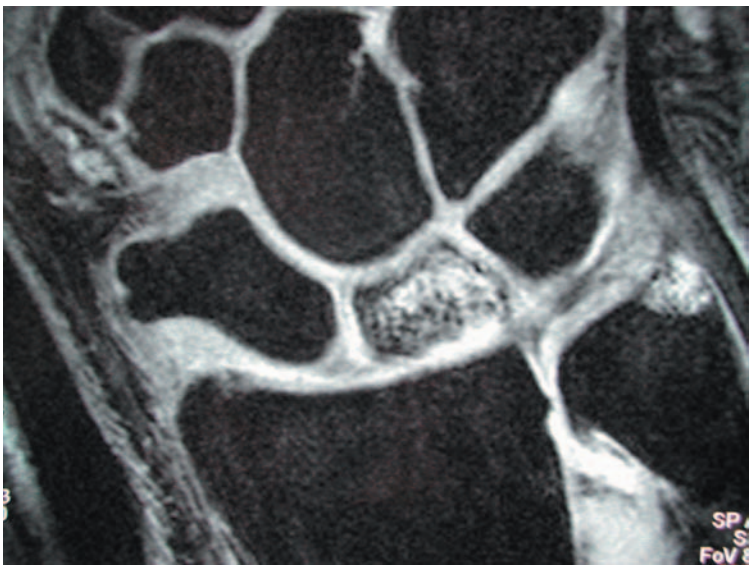

Figure 1: T2 weighted MRI of the wrist showing markedly increased signal within the lunate suggestive of Keinbock's disease.

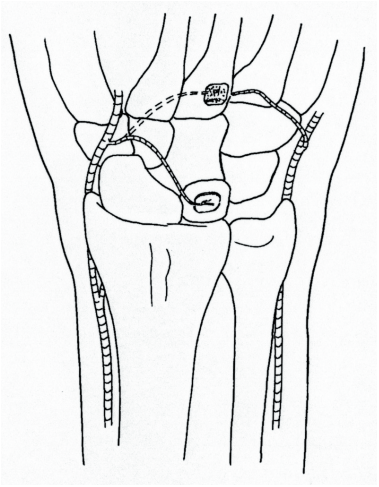

Figure 2: Schematic demonstrating pedicled bone graft based on the first or second dorsal metacarpal artery off the radial artery. Graft is generally taken from the base of the third metacarpal.

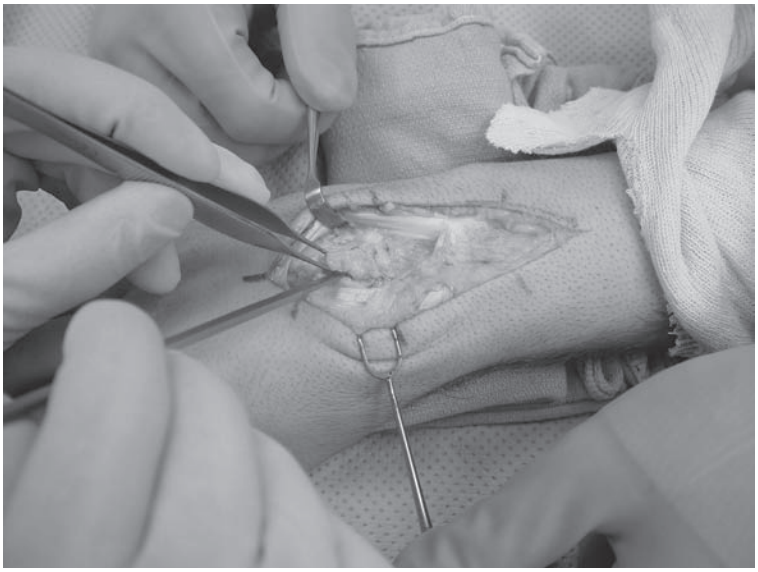

Figure 3: Surgical photograph demonstrating elevation of pedicled bone graft from the base of the third metacarpal.

capitate and the hamate articulate with the lunate and triquetrum as a single unit, we recommend shortening of both the hamate and the capitate (Figure 5). Frequently, the osteotomies can be stabilized with screw fixation to avoid the need for later Kirschner wire removal and to facilitate earlier wrist motion.

With a fine oscillating saw, a 2.0 to 3.0 mm wafer of bone is removed from the capitate (and hamate if indicated). The bone surfaces of the capitate are compressed manually and stabilized using crossed Kirschner wires or countersunk screws. For patients with evidence of lunate fracture, screw fixation was performed at the time of osteotomy.

Two weeks after surgery a removable volar resting splint is applied to protect the osteotomy while allowing some limited wrist motion until the osteotomy has healed. Active wrist motion as tolerated is allowed for the first 6 to 8 weeks. Between 8 and 12 weeks postoperatively active assisted and passive motion is added, as well as progressive resistive exercises for hand and wrist strengthening. Static progressive splinting for wrist flexion and/or extension are started if a function range of wrist motion with 60° of extension and 40° of flexion three to four weeks after the casts have been removed. Strengthening exercises are added as the swelling and discomfort subside.

Preoperatively, all patients were ulnar positive, with average length discrepancy of 1.9 mm. Mean range of motion preoperatively was a 115° arc of flexion/extension, a 40° arc of lateral deviation, and a 151° arc of forearm rotation. Grip strength was 78% of the contralateral extremity. Average time to osteotomy healing was 48 days. At follow-up, patients regained 100% of preoperative flexion-extension, 67% of preoperative lateral deviation, and 100% of preoperative rotation. Grip strength improved to 91% of the contralateral extremity. Carpal height was maintained. Thirteen of fourteen patients returned to their occupational activities at full capacity.

In earlier stages of Kienbock's disease where carpal alignment changes have not become manifest (Lichtman stages I, II, and IIIA) treatment is generally directed at salvage of the lunate to help maintain carpal kinematics. To this end, revascularization of the lunate or leveling of the joint surface has been found to be effective in the patient with ulnar-minus variance. In the situation where the radius is as short as or shorter than the ulna, and shortening the radius further is not likely to decrease loads on the lunate. Investigators have turned to other means of doing so. Capitate shortening with capitate-hamate arthrodesis has been shown to decrease loads across the radiolunate articulation. The procedure is technically straightforward, and the author who describes it reports 83 percent revascularization and healing of the lunate. Once carpal collapse has occurred, intracarpal arthrodesis becomes the treatment of choice.

Capitate shortening biomechanically serves to decrease loads across the radiolunate articulation in the ulnar positive wrist. Our study demonstrates that capitate shortening osteotomy is effective in the treatment of Kienböck's disease prior to the onset of radiocarpal arthrosis. Motion is maintained, while grip strength is substantially increased, resulting in high levels of patient satisfaction.

Recommended Reading

Viola, R.W., et al., Biomechanical analysis of capitate shortening with capitate hamate fusion in the treatment of Kienbock's disease. J Hand Surg [Am], 1998. 23(3): p. 395-401.

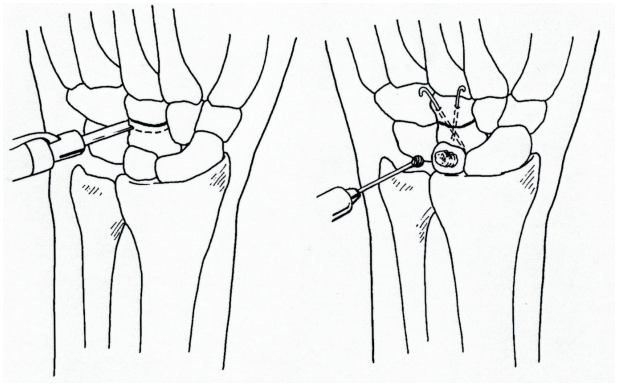

Figure 4: Schematic demonstrating wedge resection of 2-3mm of capitate waist. Osteotomy is stabilized with crossed k wires and the shortened capitate is fused to the neighboring hamate.

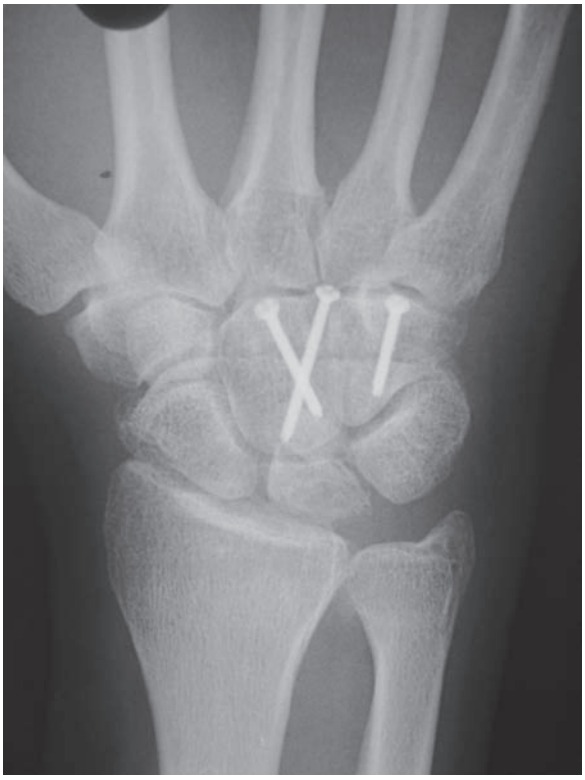

Figure 5: Clinical radiograph following combined capitate and hamate shortening.

Horii, E., et al., Effect on force transmission across the carpus in procedures used to treat Kienbock's disease. J Hand Surg [Am], 1990. 15(3): p. 393-400.

Coe, M.R. and T.E. Trumble, Biomechanical comparison of methods used to treat Kienbock's disease. Hand Clin, 1993. 9(3): p. 417-29.

Peltier, L.F., The classic. Concerning traumatic malacia of the lunate and its consequences: degeneration and compression fractures. Privatdozent Dr. Robert Kienbock. Clin Orthop, 1980(149): p. 4-8.

Almquist, E.E., Capitate shortening in the treatment of Kienbock's disease. Hand Clin, 1993. 9(3): p. 505-12.

Repair of Ulnar Collateral Ligament Injuries of the Thumb Metacarpophalangeal Joint with Pull-out Button and Cast Immobilization Versus Bone Anchor and Early Mobilization

Leonid I. Katolik, M.D. and Thomas E. Trumble, M.D.

Disruption of the ulnar collateral ligament (UCL) of the thumb metacarpohhalangeal (MCP) joint is a common injury. An increasing body of evidence supports surgical repair of complete UCL disruptions as conservative treatment of complete tears of the UCL of the thumb MCP has produced inconsistent results.

Closed treatment treatment may lead to persistent instability, pain, loss of strength, and early arthrosis. This may in part reflect the difficulty of making a definitive diagnosis which accurately distinguishes an incomplete tear from a complete tear. Accurately gauging this degree of instability in the swollen painful thumb requires experience as well as keen clinical acumen (Figure 1). This may also reflect the fact that since the insertion of both collateral ligaments is very close to the articular surface, small degrees of retraction following rupture preclude opposition to a robust healing surface, even without the presence of a Stener lesion (Figure 2).

A variety of surgical approaches to surgical repair of the UCL have been described. These include primary repair of midsubstance tears, repair with a bone anchor, dynamic repair with advancement of the adductor pollicis, repair with a pullout wire (Figure 1,2) , and ligament reconstruction with tendon graft. Each repair method is technically difficult. Techniques which require the placement of external wires and sutures may lead to nerve injury, wound complications, and a prolonged period of immobilization.

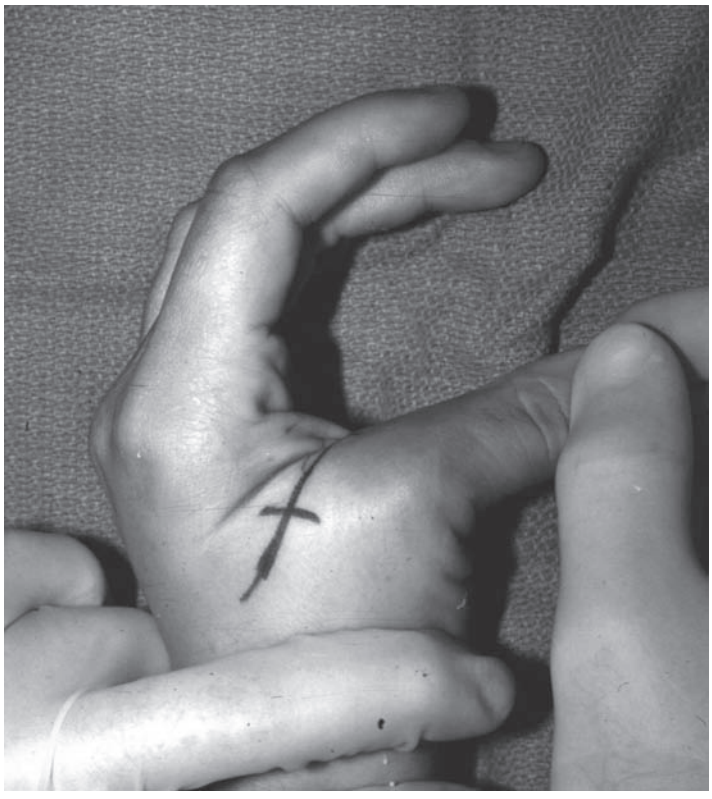

Figure 1: The thumb can be deviated with radial stress over 30° total or more than 10° than the contralateral uninjured thumb.

Intraosseous suture anchors have improved reconstructive options in hand surgery (Figure 3). Their use in the treatment of UCL ruptures in the thumb has been previously described. However, no direct comparisons of UCL repair with bone anchor versus repair with a pull out button and immobilization exist.

We compare two cohorts of patients with complete rupture of the UCL of the thumb MCP joint. Surgical treatment of seventy-three UCL ruptures of the thumb MCP was performed between 1990 and 2002. Diagnosis of a complete rupture was established clinically based on manual stress testing of the thumb MCP in 30° of flexion (Figure 1). Absolute laxity of greater than 30°, or laxity of 10° greater than the contralateral side, without evidence of a firm endpoint were used as confirmatory criteria for diagnosis.

Both repair methods utilize a curvilinear incision over the ulnar border of the thumb MCP. The adductor pollicis aponeurosis was incised longitudinally and reflected to identify the stump of the UCL. In all cases either a Bunnell stitch was placed into the ligament stump with care taken to place the suture as close to the ligament end as possible, since this is the portion of the ligament to be brought into opposition to bone (Figure 4A). Bone tunnels or troughs were not used. Isometric reinsertion of the ligament is crucial to avoid repair laxity and limitations of thumb MCP motion (Figure 4B).

Postoperatively, the pullout button group was immobilized in a thumb spica cast with the interphalangeal (IP) joint free for 6 weeks, followed by a removable hand based thumb spica splint for an additional 6 weeks. Supervised therapy for protected active, active assisted, and passive MCP range of motion was begun at

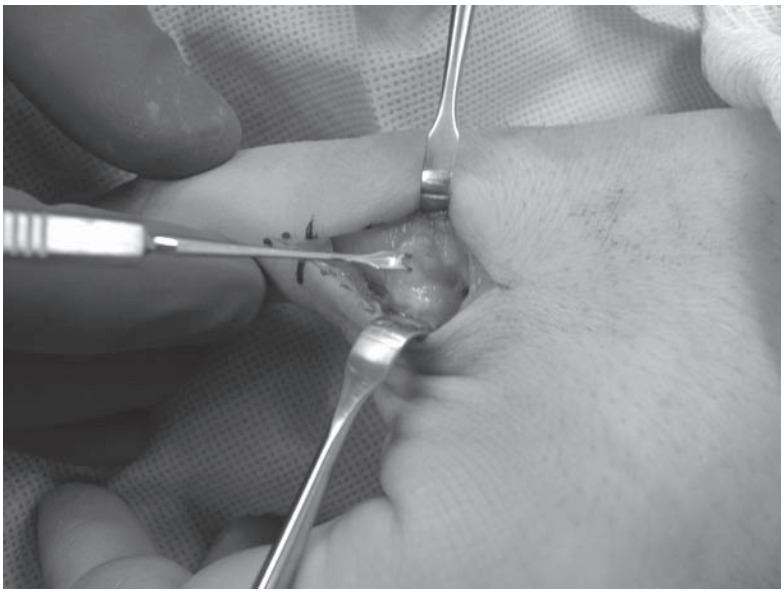

Figure 2: The Stener lesion can be identified with the ULC avulsed from the proximal phalanx and now retracted by the skin hooks.

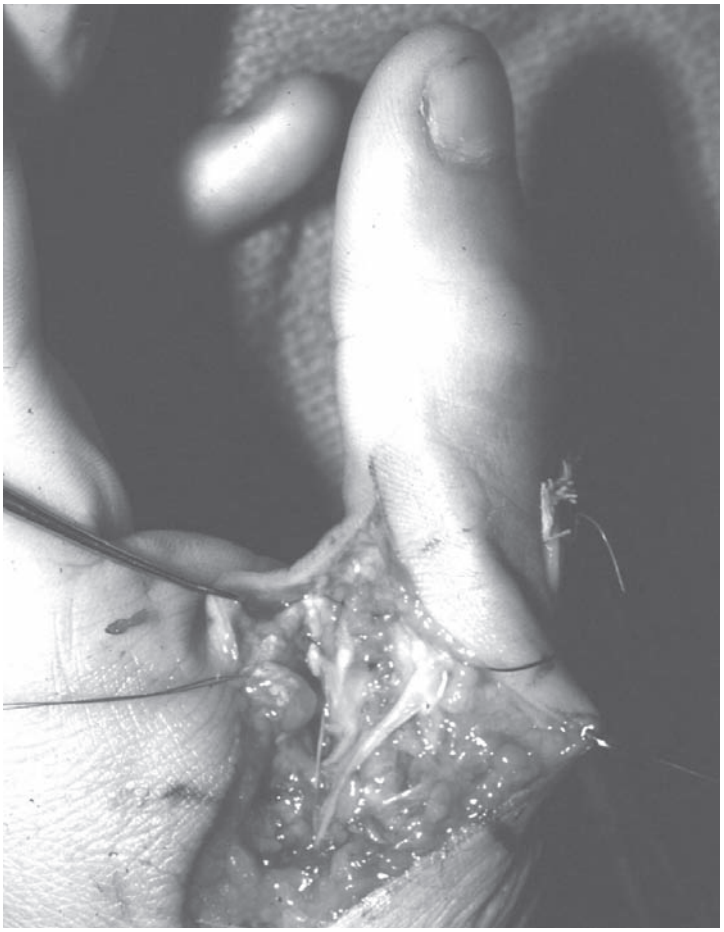

Figure 3: The standard repair of the UCL involved a pullout button that was tied on the skin and frequently caused skin problems and required a cast to protect the button for 6 weeks.

6 weeks. Continued splinting during sports was advised for a total of 10-12 weeks.

For the suture anchor group, patients were placed into a thumb spica splint for two weeks with the IP joint free. At 2 weeks, a removable hand based thumb spica splint was applied and supervised therapy for protected active, active assisted, and passive MCP range of motion was begun.

With the number of patients studied we were not able to detect any significant difference between the two groups with respect to potentially confounding variables such as age (mean 32 years old for both groups), gender, hand dominance, mechanism of injury, or the delay until operation (mean 11.8 days for the button group versus 12.5 days for the anchor group).

At a mean follow up of 29 months, range of motion at the MCP and IP joints for the anchor group averaged 97% of the contralateral side compared to 86% and 87% respectively for the button group. For the anchor group, pinch strength averaged 101% of the contralateral side compared to 95% for the button group. No significant difference was noted between the two groups for grip strength. Average tourniquet time for the anchor group was 28 minutes compared to 43 minutes. Soft tissue complications were present in 21% (8/30) patients in the pull-out button group compared to 7% (2/30) in the anchor group.

Injury to the ulnar collateral ligament of the thumb MCP joint is a common injury. Unpredictable results, with a high rate of failure may be expected from nonsurgical treatment of complete UCL injuries with persistent pain, laxity, and loss of strength reported as reasons for failure. Although early repair of UCL ruptures through a variety of techniques has been previously described as yielding acceptable results, others have noted equally acceptable results following late reconstruction of the ulnar buttress. This work then allows the treating physician perhaps greater latitude in treatment. The logical inference is that the majority patients may be treated with splint immobilization. Those with persistent laxity, pain, and loss of grip, may then be treated with delayed reconstruction. However, this path necessarily prolongs the

A)

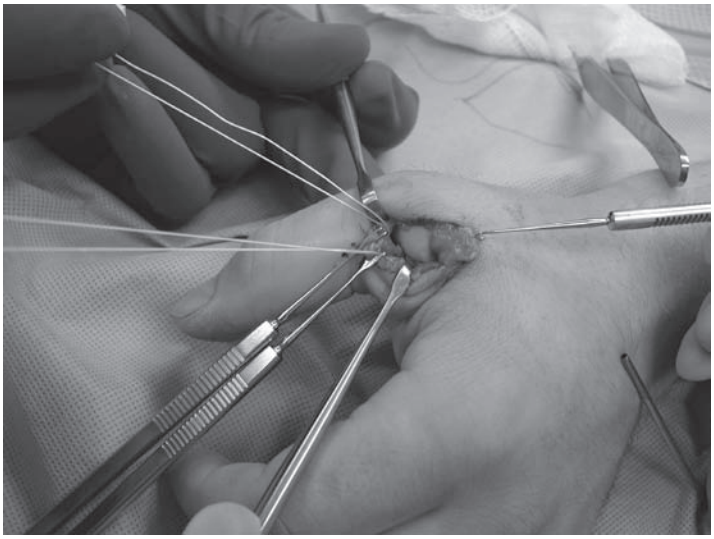

B)

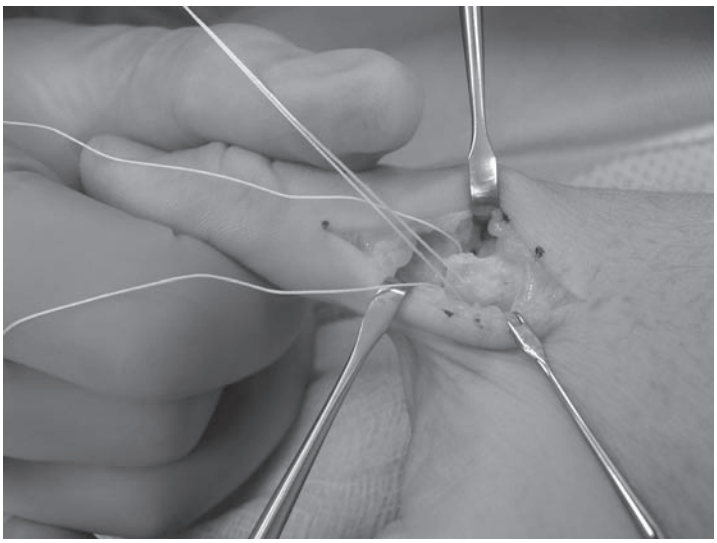

Figure 4: A) The sutures anchors are placed in the base of the proximal phalanx to reattach the UCL to the center point of rotation on the volar aspect of the distal phalanx. B) The bone anchors help to recreate the anatomic site of attachment without the need for a pullout button tied over the skin.

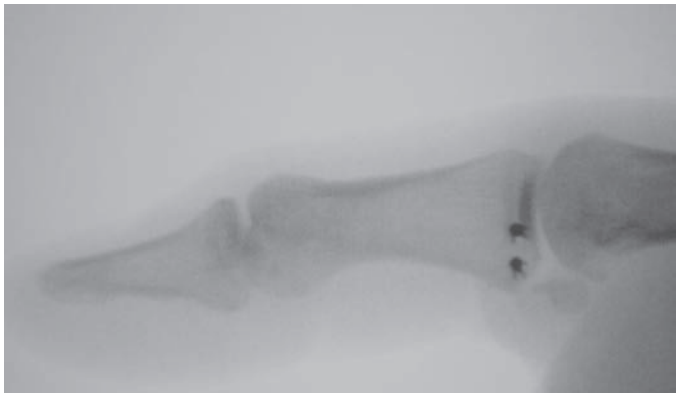

Figure 5: This lateral radiograph of the thumb shows the placement of the bone anchors to attach the ligament at the isometric point on the proximal phalanx.

total treatment time and delays the resumption of full household and occupational activities.

Acute surgical repair should be facile for the surgeon to perform, should minimize operative morbidity, and should yield a return of motion and strength comparable to the uninjured extremity. Repair of the torn thumb UCL must be performed in such a manner than the ligament stump be reinserted into its isometric point. Previous reports of decreased motion or persistent laxity following thumb UCL repair may be attributable to nonisometric reconstruction.

This study demonstrates that both repair methods yield results that are highly acceptable to the patients. The use of osseous suture anchors however required less tourniquet time, and resulted in fewer wound and soft tissue complications. Overall function with respect to range of motion and strength favored the anchor group as well. Logically, fixation methods which allow safe transition to an accelerated rehabilitation course will lead to more favorable results.

Recommended Reading

Arranz Lopez, J., F. Alzaga, and J. Molina, Acute ulnar collateral ligament injuries of the thumb metacarpophalangeal joint: an anatomical and clinical study. Acta Orthop Belg, 1998. 64(4): p. 378-84.

Kozin, S.H., Treatment of thumb ulnar collateral ligament ruptures with the Mitek bone anchor. Ann Plast Surg, 1995. 35(1): p. 1-5.

Bean, C.H., A.F. Tencer, and T.E. Trumble, The effect of thumb metacarpophalangeal ulnar collateral ligament attachment site on joint range of motion: an in vitro study. J Hand Surg [Am], 1999. 24(2): p. 283-7.

Glickel, S.Z., et al., Ligament replacement for chronic instability of the ulnar collateral ligament of the metacarpophalangeal joint of the thumb. J Hand Surg [Am], 1993. 18(5): p. 930-41.

EWS/FLI-1 Inhibits Cellular Senescence and Promotes Proliferation in Ewing's Sarcoma Cells

Hsien-Ming Hu, Ph.D., Karen Munro, B.S., Liu Yang, Ph.D., and Howard A. Chansky, M.D.

Ewing's sarcoma is the second most common malignant bone tumor in children and young adults and nearly one-half of children with Ewing's sarcoma succumb to the disease. The cancerous cells in Ewing's family tumors (EFTs) posess one of several related gene defects that results in the tumor making what is referred to as a chimeric fusion protein. The chimeric fusion proteins contain a portion of two different and normally distinct proteins. These fusion proteins are necessary and sufficient for the development of Ewing's sarcoma. We have sought to understand how these fusion proteins make otherwise normal cells cancerous.

Our laboratory is using a technique, RNA interference, that is based upon an endogenous biological process, to develop a targeted molecular approach to suppress expression of the EWS/FLI-1 fusion protein. We previosuly showed that siRNA delivered via electroporation (shocking cells) can dramatically modify the oncogenic properties of Ewing's sarcoma cells. SiRNA-mediated knockdown of EWS/FLI-1 results in decreased proliferation and invasiveness of Ewing's cells. To further these studies and to develop animal models, we have developed an adenoviral vector to deliver small interfering RNA (siRNA) that in turn disrupts expression of the EWS/FLI1 protein. We believe that this viral construct is a valuable investigative tool that may also have therapeutic applications. Most recently we have begun to use RNAi-mediated knockdown of EWS/FLI-1 expression to explore the role and regulation of cellular senescence in Ewing's sarcoma.

The molecular pathways that lead to EFTs are very complex with disruptions of several pathways involved in turning genes into proteins. It has been difficult to translate the discovery of the primary genetic abnormality of Ewing's family tumors into a clear understanding of how this leads to cancer. One problem that investigators have faced is the absence of an adequate model system to study EFTs. Researchers typically use the normal counterpart of cancerous lines of cells to study tumors. However, it is not known what the the normal cells are that lead to EFT's. This has forced scientists to use cells that are not related to EFTs to study the function of fusion proteins. By using knockdown of EWS/FLI-1 we are able to study actual Ewing's sarcoma cells in the absence of EWS/FLI-1. We hypothesize that this may be a better representation of Ewing's sarcoma precursor cells.

Results and Discussion

Adenovirus-siRNA Constructs Efficiently Infect Ewing's Sarcoma Cells

We generated adenoviral vectors encoding siRNA targeting the oncogenic fusion protein EWS/FLI-1 or the luciferase GL2, a gene not expressed in Ewing's cell lines, as a negative control. The expression of siRNA is driven by the U6 RNA promoter. To monitor the efficiency of gene transduction by siRNA encoding adenovirus, two Ewing's sarcoma cell lines, SK-ES and RD-ES, were infected with the adenovirus and stained for β-galactosidase activity (the recombinant adenovirus contains the LacZ gene in the viral DNA backbone) 36 hours after infection. Nearly 100% of the cells were positive in the x-gal staining, demonstrating efficient delivery of the siRNA-encoding gene into the target Ewing's cells. Efficient delivery of the siRNA targeting EWS/FLI-1 is critical to study the effects of knockdown in a relatively homogeneous population

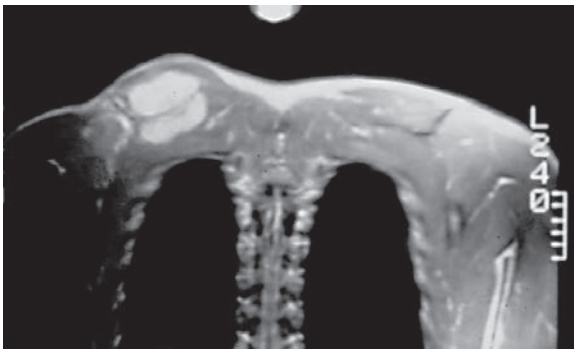

Figure 1: The MRI on the left shows a larger soft tissue mass arising from a Ewing's sarcoma of the scapula. The surgical specimen on the right shows the remaining mass after chemotherapy and resection of the scapula. This young man eventually developed pulmonary metastases.

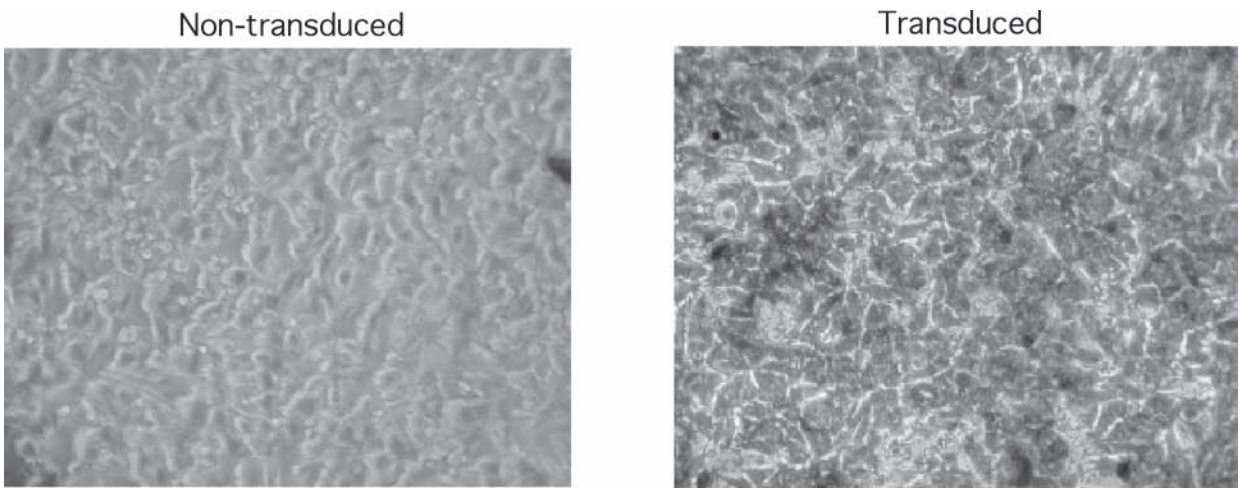

Figure 2: SK-ES cells were either untreated (left panel) or were transduced with adenovirus harboring the β-galactosidase gene (right panel). After 48 hours the cells were stained with the X-gal substrate.

of cells.

Adenovirus-mediated RNAi Knocks Down Expression of EWS/FLI-1

Infection of SK-ES and RD-ES cells with the EWS/FLI-1 siRNA-encoding virus, but not with the GL2 siRNA-encoding negative control virus, resulted in a near complete knockdown of EWS/FLI-1 fusion protein, which lasted for at least 5 days as demonstrated by Western blotting. The efficiency of knockdown is similar to our previously reported results using chemically synthesized siRNA but the effects are longer lasting. Since the control siRNA did not knockdown EWS/FLI-1 and neither siRNA elicited a generalized inteferon response, we believe that the targeting of EWS/FLI-1 is specific.

Knockdown of EWS/FLI-1 Induces Senescence in Ewing's Sarcoma Cells

EWS/FLI-1 expression could be nearly completely suppressed after SK-ES and RD-ES cells were infected with siRNA-encoding adenovirus. These cells showed decreased cell proliferation, consistent with our previous findings with the synthetic siRNA in SK-ES cells. Knockdown of EWS/FLI-1 in these cell lines resulted in distinct morphological changes that we sought to charcaterize. Cells in which EWS/FLI-1 was knocked down assumed a large and flat morphology, with increased granularity in the cytoplasm. These phenotypic changes are similar to those that occur with cellular senescence. To further explore the possibility that EWS/FLI-1 knockdown was leading Ewing's cells to become senescent, we analyzed the activity of SA-β-gal, a marker specific for cellular senescence in our Ewing's cell lines treated with our synthetic siRNA. Approximately 20% of the SK-ES cells treated with the specific siRNA targeting EWS/FLI-1 were positive for SA-β-gal staining at day 6 post-transfection while no positive cells were found after treatment with the negative control siRNA. These results suggest that knockdown of EWS/FLI-1 induces senescence in the Ewing's sarcoma cells.

Discussion

We have shown that synthetic small interfering RNA (siRNA) can be inserted into Ewing's cells to specifically down-regulate the production and function of the cancer-causing fusion protein EWS/FLI-1. This in turn leads to profound changes in the behavior of the Ewing's cells including decreased invasiveness and proliferation as well as an assumption of other features indicating senescence. Cellular senescence is a natural process that limits the proliferative capacity of cells. Inhibition of senescence is recently been implicated in the develoment and progression of several cancers. This is the first evidence that we are aware of indicating that EWS/FLI-1 may in part block the normal senescnece pathways resulting in uncontrolled proliferation of Ewing's cells. All of the changes we have documented indicate the Ewing's cells are less cancerous after treatment with siRNA.

The reduction or "elimination" of the cancer-causing fusion protein from Ewing's sarcoma cell lines has the added benefit of serving as a model of the precursor cells of Ewing's sarcoma. This may permit us to further understand how fusion proteins cause cells to become malignant. This viral vector will allow us to continue our exploration of the feasibility of treating Ewing's sarcoma with RNA interference in mouse models of Ewing's sarcoma. RNA interference is generating much enthusiasm in the medical community and it may represent a real breakthrough for developing gene therapy to target a variety of diseases including cancer.

Recommended Reading

Chansky HA, et. al: Targeting of EWS/FLI-1 by RNA interference attenuates the tumor phenotype of Ewing's sarcoma cells in vitro. J Orthop Res. 2004 Jul;22(4):910.

Martinez N, et. al: The oncogenic fusion protein RUNX1-CBFA2T1 supports proliferation and inhibits senescence in t(8;21)-positive leukaemic cells. BMC Cancer. 2004 Aug 06;4(1):44.

Clinical and Radiographic Outcome of Large Segment Prosthetic Replacement for Tumors of the Distal Femur and Proximal Tibia

Hannah D. Morgan, M.D., Seth S. Leopold, M.D., Douglas S. Hawkins, M.D., Amy M. Cizik, M.P.H., and Ernest U. Conrad III, M.D.

In this current era of chemotherapy, limb salvage remains the standard of treatment for aggressive tumors of the extremities; however, surgical resections leave large defects that must be reconstructed (Figure 1). There are various materials used in limb reconstruction that are available to the sarcoma surgeon, including bulk allografts, large-segment modular prosthetic implants, alloprosthetic composites, and less commonly used methods such as rotationplasty. For tumors involving the distal femur or proximal tibia, oncologic megaprostheses have proven to be the preferred reconstruction technique as they are durable, allow immediate joint range of motion, and do not require prolonged bony healing time (Figure 2). Despite their advantages, these implants are associated with both short- and long-term complications, the most common of which is aseptic loosening.

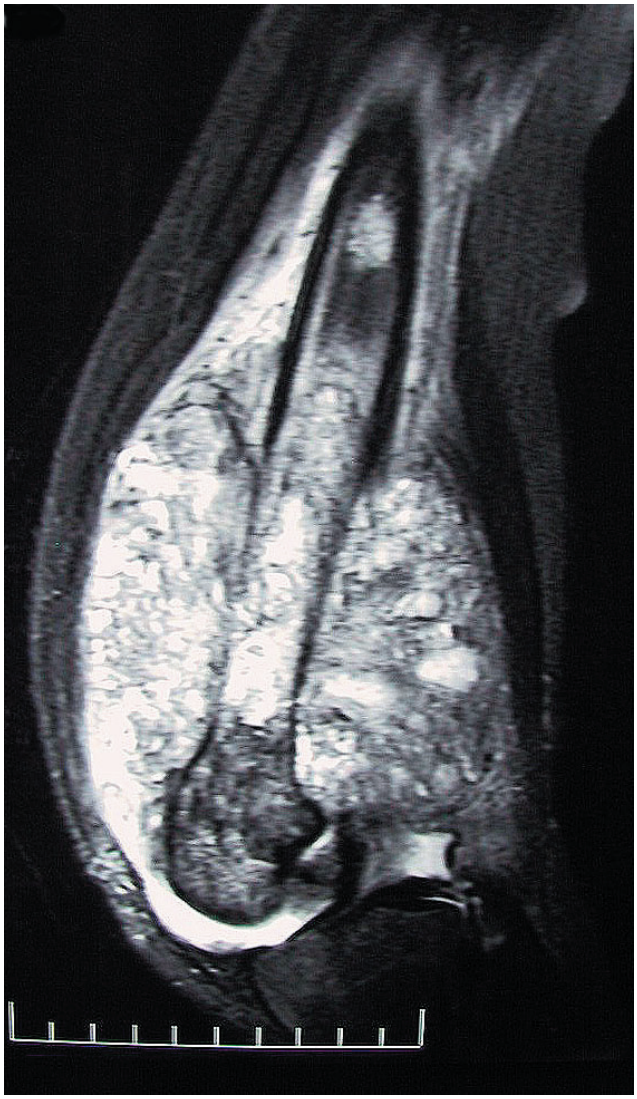

Figure 1: Sagittal MRI view of a very large osteosarcoma of a distal femur. The tumor involves not only bone, but has an expansile soft tissue mass around the entire femur. Also note the "skip lesion" in the femoral canal proximal to the main tumor. The entire tumor, both bony and soft tissue components, must be removed for adequate treatment.

The purpose of this study was to evaluate the clinical and radiographic outcomes of a cohort of patients treated with distal femoral and proximal tibial modular implants placed following the resection of an aggressive lower extremity tumor.

Materials and Methods

We retrospectively reviewed 88 consecutive patients treated between 1985 and 2002 who received distal femoral (61 patients) or proximal tibial (27 patients) modular, large-segment rotating hinge prostheses following resection of malignant or benign aggressive lesions involving bone. Patients were excluded from the study if their prosthesis was placed for a nontumorous condition (trauma, failed total knee arthroplasty), and five patients were lost to follow-up. Eighteen patients died with less than 24 months follow-up; all were known to have intact prostheses at the time of death. The surviving patients all had a minimum follow-up of 24 months, and the mean follow-up for all patients was 70 months. The age range of patients at resection was 9 to 86 years, with a mean age of 33 years. Thirty-one of the 88 patients (35%) were younger than 18 years of age. Forty-nine patients were male, and 39 were female. Seven patients with primary sarcomas presented with metastatic disease.

Femoral components were cemented in all cases except one, and all tibial components were cemented. Since 1996, routine extracortical bone grafting was performed with local autologous bone at the junction of

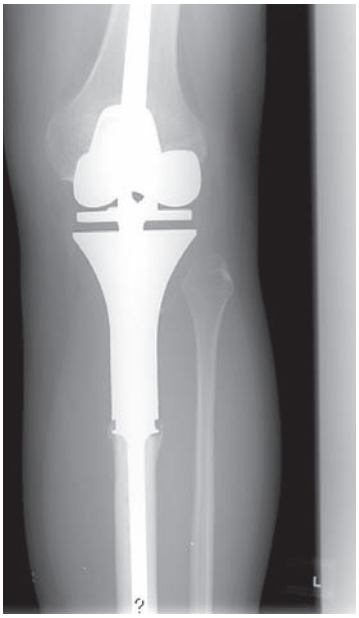

Figure 2: AP radiograph of a proximal tibial replacement rotating hinge knee prosthesis.

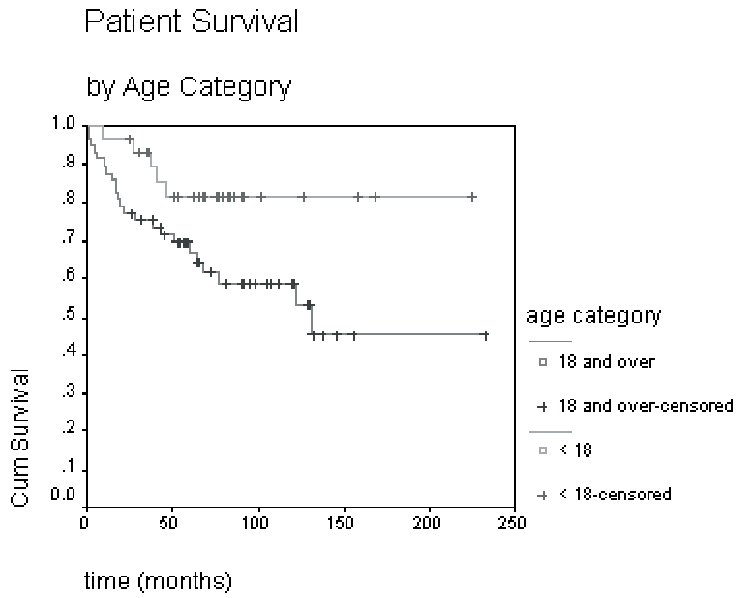

Figure 3: Kaplan Meier survival curve showing overall patient survival for adults (>/= 18 years of age) vs. children (< 18 years). Patients < 18 years had better overall survival that was statistically significant (p = 0.04).

the patient host bone and the porous coated collar of the prosthesis to enhance bony bridging between the patient's bone and the prosthesis and achieve better fixation of the implant.

At each postoperative visit, patients were evaluated clinically by an orthopaedic surgeon. Additionally, a modified Musculoskeletal Tumor Society (MSTS) questionnaire and an SF-36 evaluation were completed. Surgical or postoperative complications were recorded. Subjects had anteroposterior (AP) and lateral radiographs obtained of affected extremities, and the x-rays were graded in three categories thought to represent best adequate implant fixation: cement mantle thickness, lucencies within the cement, and extracortical bridging. Patient survival (following surgery) and prosthetic survival were evaluated.

Results

The minimum follow-up for all surviving patients was 24 months, and the range was 25-233 months, with a mean of 70 months for all 88 patients. The overall patient survival was 85% at two years, 73% at five years, and 67% at ten years. Younger patients had a significantly better overall patient survival than did older patients (p=0.04) (Figure 3).

The prosthetic survival (no femoral or tibial revision) was 81% at two years, 71% at five years, and 59% at ten years, with a mean prosthetic survival time of 119 months. Tibial prostheses tended to have a better survival rate, although this was not statistically significant (p=0.12). Gender, length of resection, diagnosis (osteosarcoma vs. other), and the use of allograft for reconstruction prior to implant placement did not significantly affect implant survival (Figure 4).

Complications

A total of 68 complications occurred in the 88 patients. The most common complication was aseptic

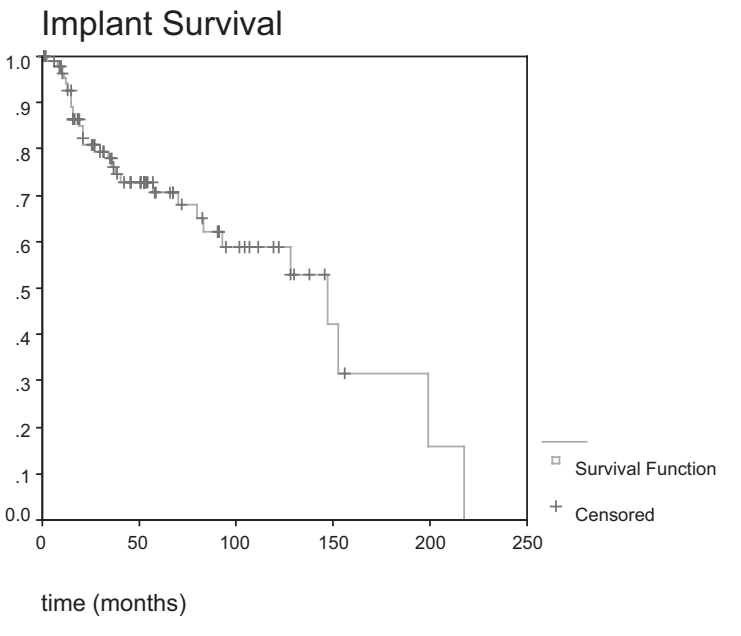

Figure 4: Kaplan Meier survival curve showing implant survival (both distal femoral and proximal tibial prostheses). Implant survival was 59% at 10 years.

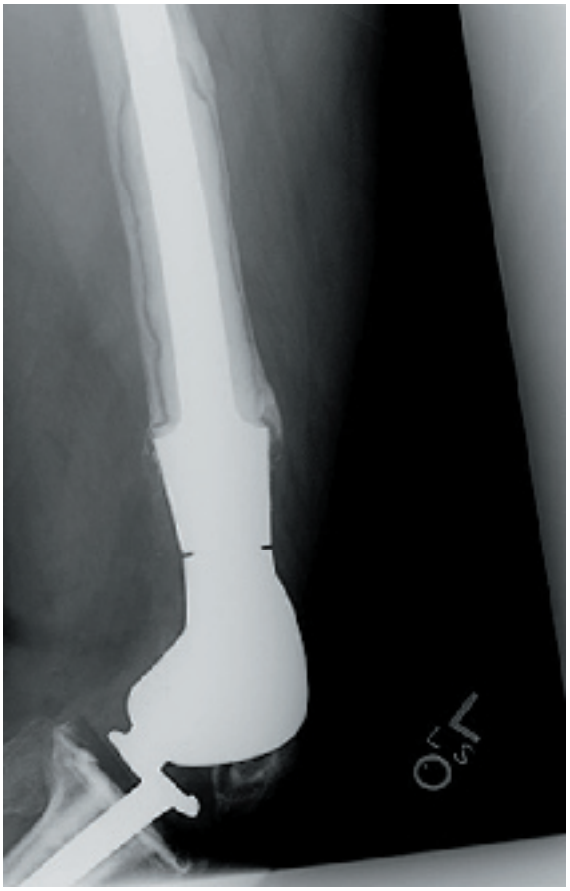

Figure 5: Lateral radiograph of a distal femoral replacement with aseptic loosening. There is a > 1 mm lucent line all the way around the stem, and the proximal portion of the stem has a cement mantle of < 2mm. This patient had a painful prosthesis and required a revision procedure.

loosening (Figure 5), which occurred in 17 patients (19%) and required 36 revision procedures. Seven patients (7%) experienced a deep infection, and underwent five prosthetic revisions, six irrigation and debridement procedures, and one amputation. Seven additional patients had superficial wound-healing problems, requiring six minor procedures. Other complications included: arthrofibrosis in 11 patients (12%), stem fracture (6%), bushing failure (8%), prosthetic disengagement (1%), femoral condyle fracture (1%), periprosthetic fracture (2%), lower extremity malrotation (2%), patellar instability (6%), patellar fracture (2%), patellar tendon avulsion (1%). Eight patients developed nerve palsies following surgery due to the proximity of the tumor to nerve. Three patients suffered a thromboembolic event (3%), and three additional patients developed a secondary malignancy following chemotherapy (3%).

Functional Results

Based on clinical evaluation and Musculoskeletal Tumor Society forms, 35 patients (40%) had an excellent clinical grade, 21 (24%) had a good outcome, 18 (20%) scored fair, and 7 (8%) received a poor grade. Seven patients did not receive a grade because they died before adequate clinical follow-up could be obtained.

Eight standard categories were assessed on the SF-36 forms. These scores were compared to the scores obtained in the general United States population. The scores in the knee implant population were lower in each category, with the largest differences seen in the categories for physical function and bodily pain; however, these results were not statistically significant.

Radiographic Results

In the group of patients who did not undergo revision surgery, 74% had continuous cement mantles of at least 2mm, and 87% had no cement luciencies. In the group of patients who did subsequently require revision surgery, only 27% had continuous 2mm cement mantles, and 64% had significant lucencies around the cement. These differences were significant in each category ($p < 0.0001$). Of the patients with significant radiolucencies, 80% were symptomatic with at least mild pain. Lucencies and pain were both considered to be signs of clinical loosening. An inadequate cement mantle was also predictive of the need for subsequent femoral revision.

Discussion

The survival of patients with sarcomas has increased dramatically since chemotherapy has been employed. Furthermore, studies have shown no significant survival advantage with limb ablation over limb salvage, and the rate of limb salvage procedures has increased. Longer patient survival demands a durable prosthesis; however, both late and early complications following megaprosthetic implantation can make this goal difficult to obtain. Even with improved design features such as larger stems, improved cementation technique, rotating instead of rigid hinges, and porous-coated collars which can accept bone graft, aseptic loosening is still the most common reason for failure of modular prostheses. While the implant performance and patient function is reasonable, making these megaprostheses a viable treatment option for patients with lower extremity sarcomas, a 40% stem revision rate at 10 years would strongly suggest the need to develop better methods of stem fixation. Small patient volumes increase the challenge of this task.

Recommended Reading

Horowitz SM, Glasser DB, Lane JM et al. Prosthetic and Extremity Survivorship after Limb Salvage for Sarcoma: How Long Do the Reconstructions Last? Clin Orthop 293: 280-286, 1993.

Kawai A, Muschler GF, Lane JM, Otis JC, Healey JH. Prosthetic Knee Replacement after Resection of a Malignant Tumor of the Distal Part of the Femur: Medium to Long-Term Results. J Bone Joint Surg 80A(5): 636-647, 1998.

Malawer MM, Chou LB. Prosthetic Survival and Clinical Results with Use of Large-Segment Replacements in the Treatment of High-Grade Bone Sarcomas. J Bone Joint Surg 77A(8): 1154-1165, 1995.

Rougraff BT, Simon MA, Kneisl JS et al. Limb Salvage Compared with Amputation for Osteosarcoma of the Distal End of the Femur: A Long-Term Oncological, Functional, and Quality-of-Life Study. J Bone Joint Surg 76A(5): 649-656, 1994.

Wirganowicz PZ, Eckardt JJ, Dorey FJ et al. Etiology and Results of Tumor Endoprosthesis Revision Surgery in 64 Patients. Clin Orthop 358: 64-74, 1999.

Zeegan EN, Aponte-Tinao LA, Hornicek FJ et al. Survivorship Analysis of 141 Modular Metallic Endoprostheses at Early Followup. Clin Orthop 420: 239-250, 2004.

Patellar Bone Loss Induced by Transient Hindlimb Muscle Paralysis in Mice

Sarah E. Warner, Ph.D., Sundar Srinivasan, Ph.D., and Ted S. Gross, Ph.D.

Muscle function plays an integral role in the achievement and maintenance of robust bone mass and morphology. The varied spectra of mechanically induced bone strains generated by muscle action range from high magnitude locomotion events to low magnitude high frequency vibrations. However, the interaction between muscle and bone remains an area of limited exploration. To address this limitation, we have developed a new murine model in which right hindlimb muscle function is transiently inhibited by intramuscular injections of botulinum neurotoxin A (Botox). Using this model, we tested the hypothesis that inhibition of hindlimb muscle function would rapidly induce bone loss in the patella.

Methods

Forty female C57B6 mice (16 wk) were randomized into four groups (n = 10 each): 1) 3 wk Botox, 2) 3 wk Saline, 3) 6 wk Botox, 4) 6 wk Saline. At day zero all mice received IM injections of Botox (2.0 unit/100 g, 2.5 unit/100 μl dilution) or saline (equal volume, mean: 18.6 μl) in both the quadriceps and gastrocnemius/soleus of the right leg. The 6 wk mice received a second set of injections at d 22. During the experiment the behavioral response of the mice was quantified by whole body weight measurement and by assessment of gait disability via a multi-observer inventory. Following sacrifice, quadriceps wet weights were determined, and the entire patella was imaged using micro-CT at a 10 μm voxel nominal resolution (Scanco μCT 20). Noise was reduced with a low pass filter and bone identified using a fixed threshold (275). Automated contour subroutines were then used to define the bone. The following parameters were characterized for each right patella: 1) total volume (TV, mm^3), 2) bone volume/total volume (BV/TV, %), and 3) patella porosity (PP, mm^3) a parameter that reflected the total porous volume within the patella (PP = TV-BV). Treatment effects were assessed using ANOVA ($p = 0.05$) while linear regression was used to explore correlative relations between quadriceps muscle mass and patellar BV/TV.

Results

Mean body weights were diminished in Botox mice compared to Saline mice at both 3 wk (-11.4%) and 6 wk (-9.8%). Compared to Saline mice, mean (± S.E.) quadriceps wet weight was diminished 47.1% following 3 wk of Botox treatment (0.103 ± 0.031 vs 0.195 ± 0.014 g, $p < 0.001$) and 66.3% by 6 wk (0.068 ± 0.015 vs 0.202 ± 0.014 g, $p < 0.001$). The lameness inventory indicated that maximum limb dysfunction was attained by 3 d post-injection, with gradual restoration of weightbearing occurring within 2 wk. At 3 wk, the mean TV of the patella in Botox mice (0.740 ± 0.014 mm^3) was equivalent to that of the Saline mice (0.740 ± 0.008 mm^3). Mean TV was only slightly reduced at 6 wk between Botox and Saline injected mice (0.752 ± 0.015 vs 0.791 ± 0.015 mm^3, respectively, $p = 0.05$). However, patellar BV/TV in Botox treated mice was diminished 15.8% compared to saline mice at 3 wk (64.1 ± 2.19 vs 76.2 ± 0.69%, $p < 0.001$) and 19.9% at 6 wk (58.8 ± 1.23 vs 77.1 ± 1.01%, $p < 0.001$, Figure 1). Concomitantly, patellar porosity was elevated 49.4% compared to saline mice at 3 wk (0.263 ± 0.015 vs 0.176 ± 0.007 mm^3, $p < 0.001$) and –89.7% at 6 wk (0.327 ± 0.014 vs 0.172 ± 0.008 mm^3, $p < 0.001$). Quadriceps wet weight was not correlated with patellar BV/TV in Saline mice ($r^2 = 0.06$, Figure 2), but was powerfully correlated with patellar BV/TV in Botox mice ($r^2 = 0.83$, $p < 0.001$, Figure 2).

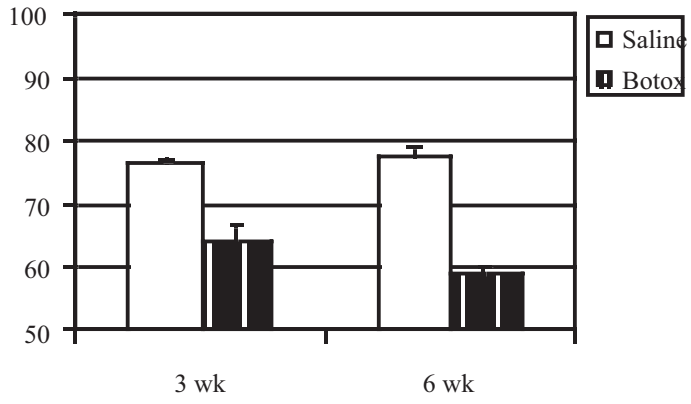

Figure 1: Mean (+ S.E.) patellar BV/TV was significantly reduced by Botox induced muscle paralysis at both 3 wk and 6 wk (*, $p < 0.001$).

Discussion

Intramuscular injection of Botox induces temporary muscle paralysis by blocking the release of acetylcholine into the neuromuscular junction. Here, we observed significant bone loss in response to transient hindlimb muscle paralysis using a dose of Botox within the range approved for human use. As patellar TV was unchanged at 3 wk and diminished only 4.9% by 6 wk in Botox treated mice, we conclude that the bone loss was primarily achieved via enhanced bone resorption. These data also support the conclusion that the amount of muscle loss was proportional to bone loss as 83% of the variance in patellar BV/TV was determined by quadriceps muscle mass alone. These data emphasize the essential, yet poorly understood, role of

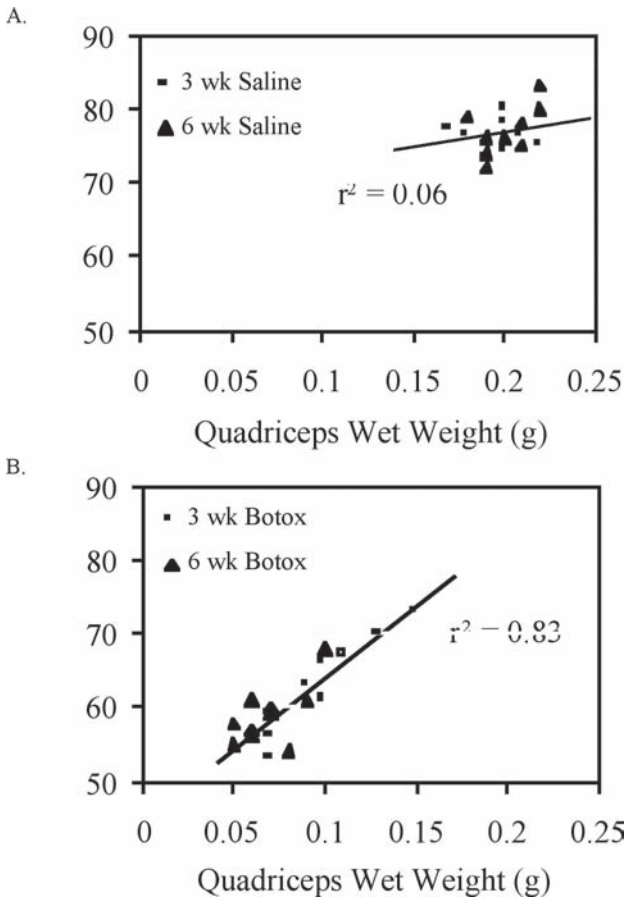

Figure 2: Quadriceps muscle wet weight was not correlated with patellar BV/TV in saline injected mice (A). However, in Botox treated mice, those animals with the lowest quadriceps wet weight (indicative of greatest muscle loss) also demonstrated the least patellar BV/TV (B).

neuromuscular function in maintaining bone mass. We believe that this new model will enable mechanistic exploration of the causal aspect of this relation as well as the delineation of specific mechanical stimuli responsible for enabling bone homeostasis.

Acknowledgements

This work was supported, in part, by NIH AR45665 and the Sigvard T. Hansen, Jr. Endowed Chair for Orthopaedic Traumatology.

Recommended Reading

Parfitt, A.M., Bone, 34: 767-770, 2004.

Kiralti, B.J., et al., J Rehabil Res Dev, 37:225-233, 2000.

Fritton, S.P., et al., J Biom, 33:317-325, 2000.

Adams, D.J., et al., J Biom, 30:671-678, 1997.

Hambleton, P., J Neurol, 239:16-20, 1992.

PEG-grafted Chitosan as an Injectable Thermosensitive Hydrogel for Sustained Protein Release

Narayan Bhattarai, Ph.D., Hassna R. Ramay, Ph.D., Frederick A. Matsen III, M.D., and Miqin Zhang, Ph.D.

It is recognized that many proteins have the ability to stimulate the synthesis of bone, cartilage, fibrous tissue and muscle. Use of these proteins as therapeutic agents requires a means of guided local administration (Figure 1) and a method of retaining the protein in the desired target area so its release is sustained over time. The vehicle in which the protein is administered should not interfere with the activity of the protein and should breakdown slowly leaving only benign products. Ideally, the vehicle would be injectable through a small-bore needle and then set up as a gel once it is *in situ.* In this regard, thermosensitive polymeric hydrogels that undergo a sol-to-gel transition in response to temperature changes are of great interest as injectable depot delivery systems. Chitosan is a polysaccharide derived from abandoned chitin (crab shells) (Figure 2). In this study we prepared a chitosan-based, injectable thermogel by grafting an appropriate amount of poly ethylene glycol (PEG) onto a chitosan backbone and studied its drug release properties *in vitro* using bovine serum albumin (BSA) as our model protein.

Thermoreversibility

We demonstrated that when more than 40 wt % of PEG grafted onto chitosan via covalent bonding, the aqueous solution of the resultant copolymer was an injectable liquid at low temperature and transformed to a semisolid hydrogel at body temperature (Figure 3 and 4). The viscosity of samples G45 and G55 (45 and 55 wt % of PEG grafted on chitosan respectively) increased over time at 37°C and decreased over time at 4°C, establishing a thermoreversible sol-gel transition. There was no apparent phase transition observed for the pure chitosan solution. Samples of PEG-g-chitosan, with 45 and 55 wt % of PEG grafted on chitosan respectively, underwent an apparent sol-to-gel transition in the solutions with polymer concentrations ranging from 1.3 to 3 wt %. Below the transition temperature, the solutions were viscous liquids that flow easily and injectable through a 20-gauze needle. As the solutions were heated to body temperature, they transformed into gels. The gels reverted back to solutions when temperature dropped to 10°C or below. The typical so-to-gel transition time was 10 ± 4 minutes.

Protein release

Hydrogels made from G45 and G55 PEG-g-chitosan were used for the protein (BSA) release study. Figure 5 shows the percent cumulative release profiles of the hydrogel matrices loaded with BSA of different concentrations ranging from 200 to 1000 μg/ml. Two distinctive release characteristics were

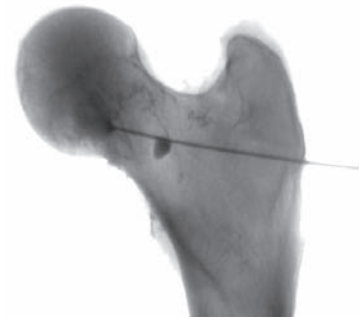

Figure 1: Image guided, minimally invasive topical administration of therapeutic protein to the femoral neck.

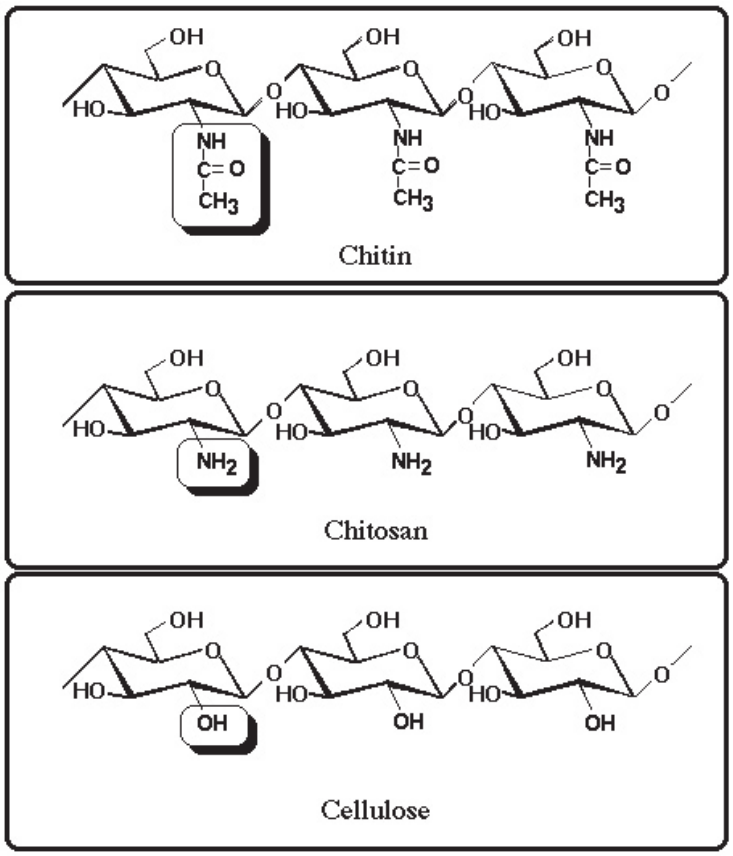

Figure 2: Chitosan, a polysaccharide related to chitin and cellulose.

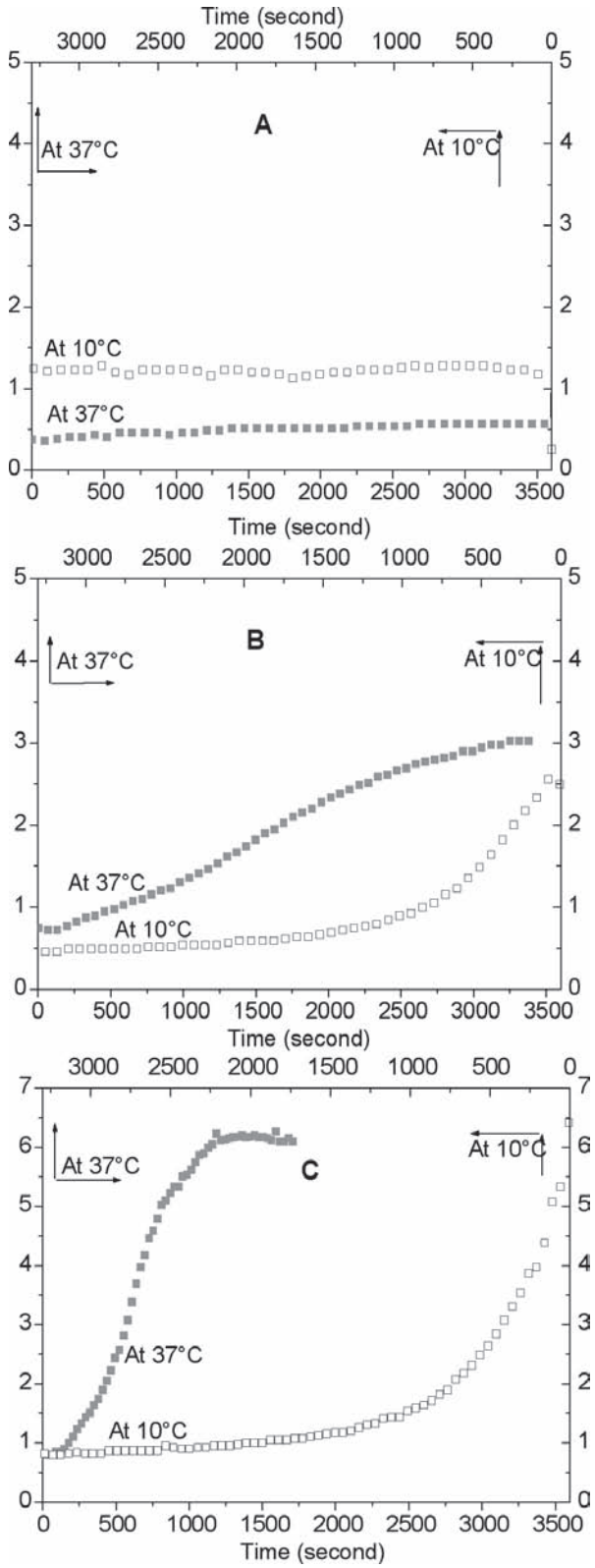

Figure 3: Aqueous solution viscosity of (A) pure chitosan, (B) G45 and (C) G55 of PEG-g-chitosan. The filled symbols refer to the solutions at 37°C and the open symbols refer to the solutions at 10°C. Note that for the latter two preparations (B and C), the viscosity is greater at body temperature (37°) than at 10°C.

seen for hydrogels made from G45 and G55. The G45 gel showed a release of 52-67% of BSA in the first 5 h, whereas the G55 gel showed a release of 10-58% of BSA in the same time period. Both copolymers showed slow BSA release in the period of 5 to 70 h and no apparent release thereafter. After 70 h, the remaining BSA was trapped in the gel matrix and could not be completely released until the gel matrix was dissolved in media. Typically, G55 gels were dissolved in PBS (pH = 7.4) in 1 to 2 weeks and G45 gels in 3 weeks. In general, hydrogels loaded with BSA of different concentrations exhibited a similar trend in accumulative BSA release, except for the initial "burst" release that exhibited an accumulative release proportional to BSA loading. Clearly, hydrogels of this type are suitable for short-term drug release, for examples, in hours or days.

Crosslinking

Genipin has recently drawn a great interest in tissue engineering due to its excellent tissue compatibility. It is estimated that genipin is approximately 5000 to 10,000 times less cytotoxic than commonly used glutaraldehyde. Prolonged quasi-linear release of protein up to 40 days was achieved by crosslinking the hydrogel with genipin *in situ* in a fashion suitable for protein encapsulation while maintaining the injectability of the hydrogel. The crosslinking transformed the copolymer from a physical gel to an insoluble chemical gel and substantially reduced the initial burst release of protein. The hydrogel can be prepared in solutions of physiological pH allowing safe incorporation of bioactive molecules for a broad range of medical applications, particularly, in sustained *in vivo* drug release and tissue engineering.

The addition of genipin did not seem to affect the injectability of the hydrogel solution at 4°C for 24 h. However, the solutions with genipin incorporated lost thermoreversibility at 37°C, and the color of gels changed from transparent to light blue within 2 h. This is not a problem for the intended applications where only injectability of the hydrogel solution at lower temperature and gelation process at body temperature are concerned.

As expected, crosslinking hydrogels with genipin prolonged the BSA release from the hydrogels. The hydrogel without genipin released more than

(A)

(B)

Figure 4: PEG-g-Chitosan is injectable when cooled (A) and a gel when warmed (B).

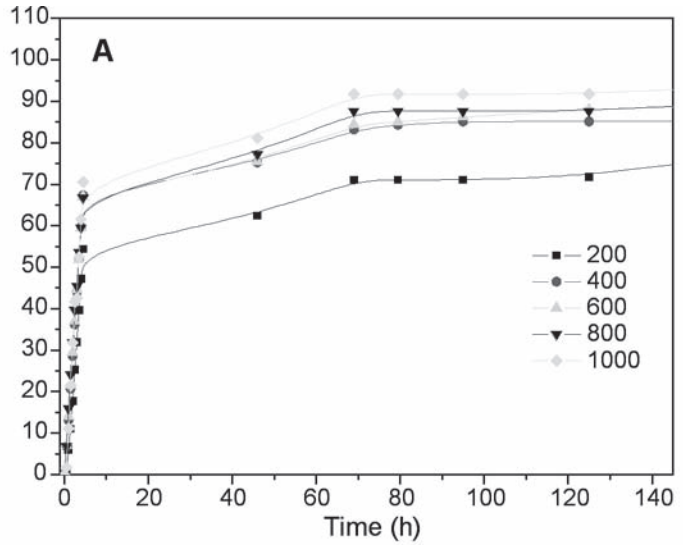

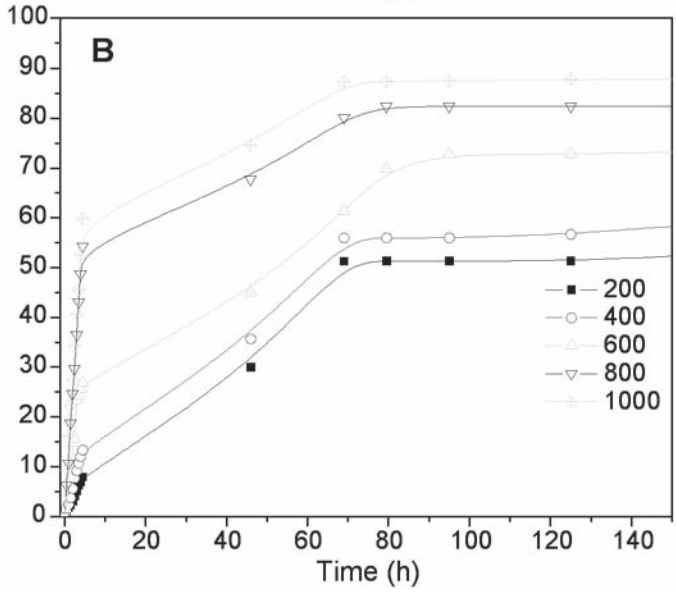

Figure 5: In vitro cumulative percent release of BSA from thermoreversible hydrogels of (A) G55 and (B) G45 loaded with different concentrations of BSA. Each point represents the mean value ± SEM (n = 3).

70% of BSA in the first 5 h, while the one cross linked with genipin for 24 h released only ~12% of BSA in the first day and another 30% in a week. For the hydrogel treated with genipin for only 10 minutes, ~15% of BSA was released within the first day and another ~25% of BSA in two days. (Figure 6). In contrast to unlinked PEG-g-chitosan hydrogels, the cross-linked hydrogels may be potentially suitable for long-term drug release applications.

Conclusion

We fabricated an injectable, thermoreversible hydrogel by chemically grafting monohydroxy PEG on chitosan backbone. The copolymer solution prepared at low temperature transforms to a gel at body temperature. The hydrogel can be prepared and gels under physiological pH, which allows safe incorporation of proteins or other bioactive agents. When the PEG-g-chitosan copolymer was cross-linked *in situ* with genipin, prolonged drug release with a "quasi-linear" release profile up to 6 weeks were achieved. Although present research is targeted at controlled drug release, the hydrogels developed also find application in tissue engineering, such as tissue repair and regeneration. Since all the component materials involved have been proved to be biocompatible, the copolymer hydrogel is potentially suitable for a wide range of *in vivo* biomedical applications.

We have shown that this new approach has the following advantages compared to previous techniques: (1) it provides the flexibility to easily prepare the hydrogel in solutions of a wider range of pH, particularly at physiological pH (7.4) under which bioactive species can be safely incorporated; (2) the produced hydrogel has gelation temperature well below, and thus gels readily at, body temperature, making it ideally suitable to serve as an injectable depot for sustained drug delivery; (3) the hydrogel has favorable and controllable drug release profiles: after an initial short burst release, virtually linear release profiles can be obtained for all the protein loadings studies. We achieved a short-term (a few days) drug release for non-cross linked PEG-g-chitosan. We achieved a quasi-linear long-term (a few weeks) drug release

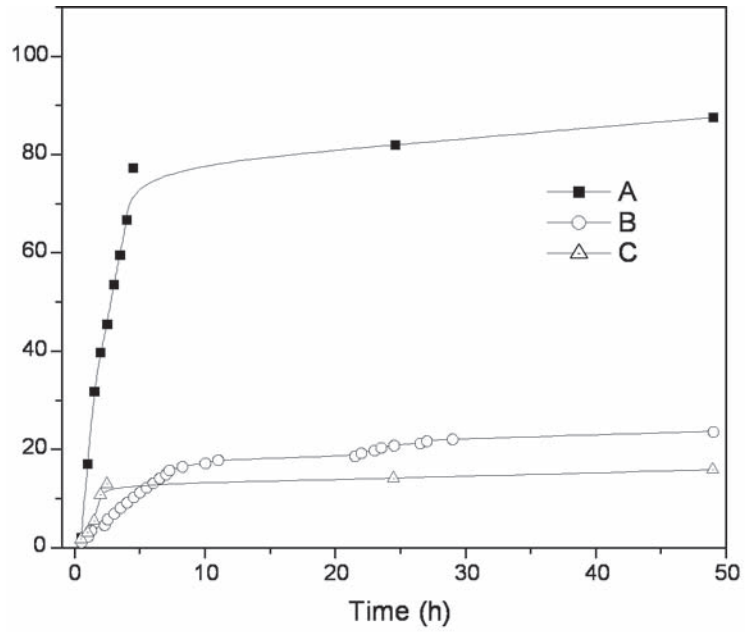

Figure 6: In vitro percent cumulative release of BSA from PEG-g-chitosan hydrogels: (A) G55, (B) G55 treated with genipin for 10 minutes, and (C) G55 treated with genipin for 24 h. All the hydrogels contain the same amount of BSA, and BSA was released in PBS with pH = 7.4. The concentration of genipin was 0.5 mM. Triplicates for each hydrogel were analyzed and each data point represents the mean value ± SEM.

for a cross-linked PEG-g-chitosan was achieved using genipin.

Recommended Reading

N. Bhattarai, D. Edmondson, O. Veiseh, F. A. Matsen, and M. Zhang "Electrospun chitosan-based nanofibers and their cellular compatibility", Biomaterials, in press.

N. Bhattarai, H. R. Ramay, J. Gunn, F. A. Matsen, and M. Zhang "PEG-grafted chitosan as an injectable thermosensitive hydrogel for sustained protein release", Journal of Controlled Release, 103, 609-624 (2005).

N. Bhattarai, F. A. Matsen, and M. Zhang "PEG-grafted chitosan as an injectable thermoreversible hydrogel", Macromolecular Bioscience, 5, 107-111 (2005).

Proteoglycans Influence The Assembly Of Type II N-Procollagen Into Fibrils

Russell J. Fernandes, Ph.D., Thomas M. Schmid, Ph.D., and David R. Eyre, Ph.D.

Cartilage is a unique tissue characterized by an extensive extracellular matrix. The molecular mechanisms that enable chondrocytes to assemble a functional cartilage matrix from a complex mix of collagens, proteoglycans and matrix proteins in the correct proportions are not well understood. Clarifying these mechanisms of assembly is important for future efforts to engineer functional cartilage.

We have been using a chondrocyte cell line as an experimental system to study matrix assembly *in vitro*. We have shown that this cell line, RCS-LTC, established from the Swarm rat chondrosarcoma tumor, maintains a cartilage phenotype in long-term monolayer culture. The cells synthesize and assemble collagen type II/IX/XI heteropolymers and the proteoglycan aggrecan in the extracellular matrix. This cell line fails to process type II procollagen beyond the stage of N-procollagen molecules. Although the type II N-procollagen molecules are stabilized by pyridinoline cross-links, collagen fibrils in the extracellular matrix were not evident by electron microscopy. The aggrecan rich, highly hydrated and fragile matrix of the cell line presents a system to test if high proteoglycan content could influence assembly of collagen fibrils.

Here we investigated the properties of the collagenous matrix when the content of proteoglycans in the extracellular matrix was depleted.

Materials and Methods

Cell culture

The RCS-LTC cell line was maintained as monolayer or micromass cultures in DMEM containing bovine calf serum and ascorbate in the presence of 100 ug/ml porcine testicular hyaluronidase for 2 weeks. Controls were cultured in the absence of hyaluronidase. Porcine hyaluronidase degrades both hyaluronic acid and the glycosaminoglycan chains of aggrecan.

Estimation of Collagen and Proteoglycan content

Proteoglycan content in samples was measured by a modification of the dimethyl methylene blue dye binding assay. Determination of hydroxyproline as a measure of collagen content was performed by the dimethyl amino benzaldehyde assay.

Microscopy

For light microscopy, micromass cultures were fixed, sectioned and treated with Mallory's stain. For electron microscopy, cultures were post fixed in osmium, embedded in plastic and thin sections stained with uranyl and lead.

Metabolic radiolabeling

Medium was supplemented with 20 uCi/ml [^{3}H]-proline, ascorbate and β-APN for 24 hours. The medium was removed, radiolabeled collagen in the cell layer was extracted in 0.15M potassium phosphate buffer, pH 7.6 and the residue solubilized in 1% SDS. Radioactivity incorporated into collagen was determined by liquid scintillation counting.

Electrophoresis

Cell layer collagen was extracted sequentially with 0.15M potassium phosphate buffer, pH 7.6 or 1M NaCl, 50mM Tris, pH 7.5, and 100 ug/ml pepsin in 3% acetic acid. Collagen chains were resolved by Laemmli SDS-PAGE and visualized by western blots using a monoclonal antibody (1C10) that detects type II collagen.

Results

The total collagen and proteoglycan production by RCS-LTC chondrocytes the first five days in monolayer culture is shown in Figure 1. These cells produce 7 - 8 times more proteoglycan than collagen on a weight basis for all the days in culture. 85% of the proteoglycans accumulated in the cell layer.

The high proteoglycan content of the extracellular matrix was further evident when the cells were cultured in the presence of hyaluronidase for 2 weeks. A marked difference in the size of the treated and control cultures is observed. As shown in Figure 2, light micrographs of 1 um thin sections of RCS-LTC micromass cultures cultured in the absence of hyaluronidase (A), showed cellularity in multilayers and an extensive translucent matrix between the cells. When the cells were cultured in the presence of hyaluronidase (B), there is a marked reduction in the volume of extracellular matrix as would

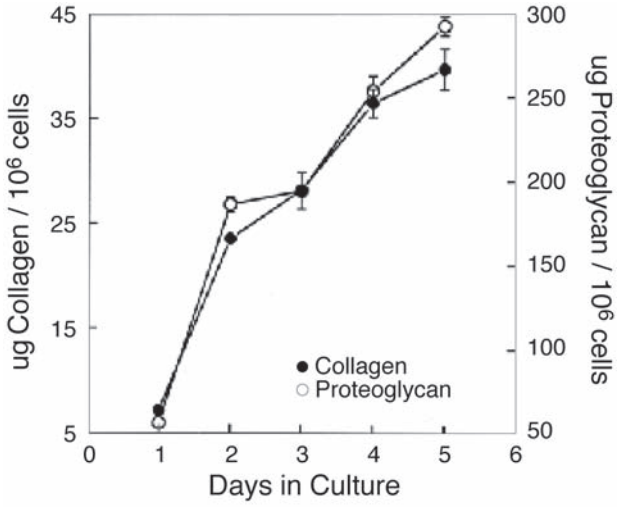

Figure 1: Total collagen and proteoglycan production by RCS-LTC chondrocytes in monolayer culture; collagen, proteoglycan. Values are expressed as the mean ± SD obtained from duplicate cultures.

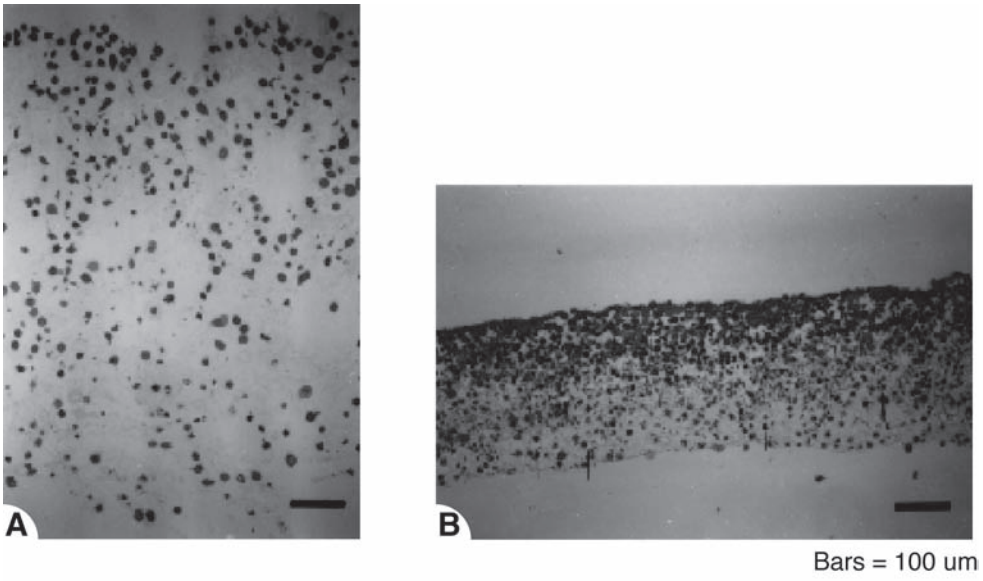

Figure 2: Light micrographs of 1 um thin sections of RCS-LTC micromass cultures cut perpendicular to the cover slip. A. Cultured in the absence of hyaluronidase. B. Cultured in the presence of hyaluronidase.

be expected when the proteoglycan content of the matrix is depleted. The cells were still present in multilayers and the presence of 'lacunae' around cells was more prominent. The full height of the cultures are shown. The thickness of the cell-matrix layer in hyaluronidase treated cultures was about 1/3 that in control cultures.

The effect of hyaluronidase on collagen production was also studied. Equal numbers of chondrocytes were cultured in the presence or absence of hyaluronidase for 14 days. The cells were labeled with [^{3}H]-proline in the presence of β-APN and hyaluronidase on day 14. The labeling data showed that even after 14 days of treatment with enzyme the cells were still metabolically active, synthesizing [^{3}H]-proline-labelled proteins (Table 2). Highest hydroxyproline contents (20-22%) were found in the extracts of the cell layer in both treated and untreated cultures (Table 1 and 2), suggesting most of the collagen had accumulated in the matrix. Total [^{3}H]-hydroxyproline incorporated into the labeled proteins of the cell layer of treated and untreated cultures showed a similar incorporation of newly synthesized collagen into the matrix.

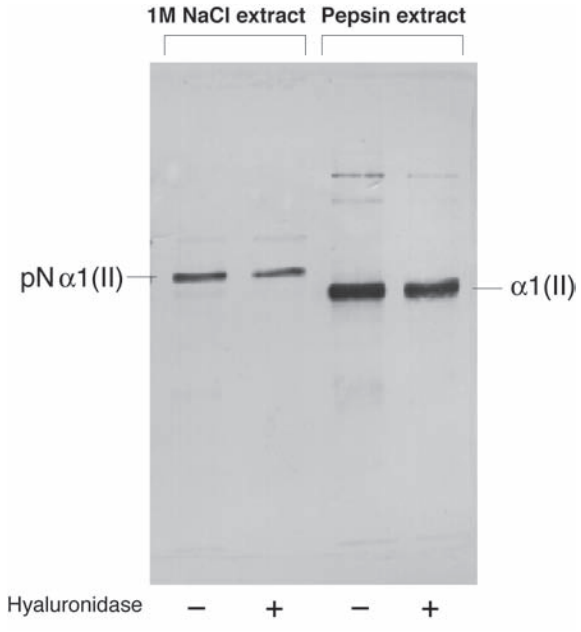

Figure 3: Western blot showing type II N-procollagen deposited in the matrix of hyaluronidase treated and control cultures. The cross-linked type II N-procollagen is extracted using pepsin.

After 14 days in culture only type II N-procollagen is detected in the matrix of both treated and control cultures as seen in Figure 3. Pepsin effectively solubilized the cross-linked type II N-procollagen.

Electron micrographs (Figure 4) of the matrix surrounding the RCS-LTC chondrocytes cultured in the absence of hyaluronidase, showed a characteristic lack of typical banded collagen fibrils and linear arrays of flocculent material that could represent fine fibrils of type II N-procollagen associated with proteoglycans. When cultured with hyaluronidase, a pericellular distribution of thin, laterally associated collagen fibrils, approximately 10 nm in diameter was seen in the matrix. The fibrils were often in groups of three or more giving the impression of lateral association into larger fibrils. The fibrils seemed to be oriented tangentially to the surface of the cell and associated with amorphous electron dense material. Since collagen synthesis was unaffected, the high proteoglycan production appears to

Collagen Pool	Total ^{3}H-hydroxyproline cpm x 10^{-6} / plate	Total ^{3}H-proline cpm x 10^{-6} / plate	% ^{3}H-hydroxyproline
Medium	0.21 ± 0.03	1.8 ± 0.29	11.5
0.15M PO_4 Extract	0.19 ± 0.03	0.9 ± 0.12	22.3
Residue (SDS)	0.16 ± 0.01	5.9 ± 0.42	2.7

Table 1: Cultures without hyaluronidase treatment. Incorporation of ^{3}H-proline into ^{3}H-hydroxyproline.

Collagen Pool	Total ^{3}H-hydroxyproline cpm x 10^{-6} / plate	Total ^{3}H-proline cpm x 10^{-6} / plate	% ^{3}H-hydroxyproline
Medium	0.34 ± 0.04	3.7 ± 0.45	9.1
0.15M PO_4 Extract	0.17 ± 0.01	0.8 ± 0.07	20.7
Residue (SDS)	0.16 ± 0.01	6.4 ± 0.41	2.4

Table 2: Cultures with hyaluronidase treatment. Incorporation of ^{3}H-proline into ^{3}H-hydroxyproline.

be one factor influencing collagen fibril assembly in these cultures.

Discussion

The ratio of total proteoglycan to total collagen produced by the cell line (approximately 7:1) remains constant during the 5 days in culture (Figure 1). This ratio is much higher than the ratio of 1:1 calculated from proteoglycan and collagen synthetic rates observed in studies of chick chondrocytes and the ratio of 1:2 for canine articular cartilage. The high proportion of proteoglycans can explain the highly hydrated matrix that is characteristic of these cells. We have previously shown that the type II N-procollagen in the extracellular matrix of the RCS-LTC cultures forms pyridinoline crosslinks, indicating an ordered packing of collagen molecules into microfibrils. These fibrils are too thin to identify as collagen by electron microscopy. We hypothesized that the high proteoglycan content may interfere with the lateral growth of microfibrils into thin collagen fibrils thus contributing to the fragility of the cell layer.

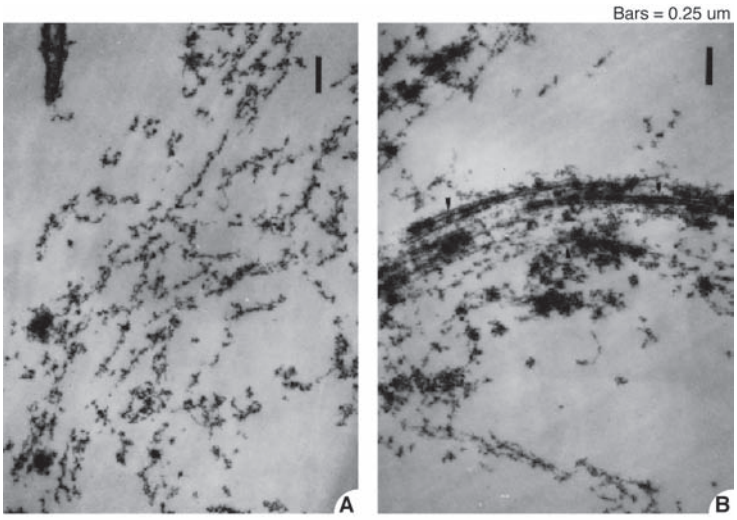

Figure 4: Electron micrographs of the matrix surrounding the RCS-LTC chondrocytes. A. Cultured in the absence of hyaluronidase, showing a characteristic lack of typical banded collagen fibrils. B. Cultured with hyaluronidase, showing thin, laterally associated collagen fibrils.

To test this hypothesis we cultured the RCS-LTC cells in the presence of hyaluronidase to reduce the proteoglycan content of the matrix. Even after 14 days, these cells were metabolically active, synthesizing but still not able to process type II collagen beyond the stage of N-procollagen molecules. The synthesis of the other collagens types IX and XI (data not shown) also did not seem to be affected. When the matrix of the treated cultures was examined by electron microscopy, collagen fibrils were detectable, leading us to conclude that the assembly into fibrils must be due to lateral aggregation of type II N-procollagen microfibrils made possible by the decrease in proteoglycan content. The collagen network was not as extensive as that

in the RCS parental tumor chondrocyte matrix, but clearly modified from that of the non-treated cultures. A similar conclusion was reached by Kuhn and von der Mark who showed that the treatment of epiphyseal cartilage with hyaluronidase *in vitro* resulted in a rearrangement of the collagen network, where thin filaments had grown together to fibrils with larger diameters.

The results show that depletion of proteoglycans from the assembling matrix resulted in thicker type II N-procollagen fibrils. The culture system further offers the potential to study early stages in the assembly of types II, IX and XI collagens into the heterotypic polymer.

Recommended Reading

Fernandes, R. J., Schmid, T. M. & Eyre, D. R. (2003) Assembly of collagen types II, IX and XI into nascent hetero-fibrils by a rat chondrocyte cell line, Eur J Biochem. 270, 3243-50.

Kuijer, R., van de Stadt, R. J., De Koning, M. H. M. T., van Kampen, G. P. J. & van der Korst, J. K. (1988) Influence of cartilage proteoglycans on type II collagen fibrillogenesis, Connective Tissue Research. 17, 83-97.

Vogel, K. G. & Trotter, J. A. (1987) The effect of proteoglycans on the morphology of collagen fibrils formed in vitro, Collagen and Related Research. 7, 105-114.

Kuhn, K. & von der Mark, K. (1978) The influence of proteoglycans on the macromolecular structure of collagen, Suppl Thromb Haemost. 63, 123-6.

van de Breevaart Bravenboer, J., In der Maur, C. D., Bos, P. K., Feenstra, L., Verhaar, J. A., Weinans, H. & van Osch, G. J. (2004) Improved cartilage integration and interfacial strength after enzymatic treatment in a cartilage transplantation model, Arthritis Res Ther. 6, R469-76.

A Distinctive Type V/XI Collagen Phenotype In The Intervertebral Disc

Jiann-Jiu Wu, Ph.D., Mary Ann Weis, B.S., and David R. Eyre, Ph.D.

The intervertebral disc has a hybrid collagen architecture that embodies features of ligament and cartilage in its structure and function. Nucleus pulposus (Figure 1), the gel-like central zone of the young intervertebral disc, has a similar collagen phenotype to that of hyaline cartilage, with types II, IX and XI collagens being the principal fibrillar components. In fetal cartilage, type XI collagen consists of molecules containing three genetically distinct chains, α1(XI), α2(XI) and α3(XI) in a 1:1:1 ratio. The molecules are cross-linked by lysyl oxidase-mediated bonds, which exhibit distinct chain specificities . However, from mature articular cartilage, the isolated type XI collagen fraction includes a significant proportion of the α1(V) chain, the chain ratios suggesting the existence of type V/type XI hybrid molecules in the tissue. It is possible that the type V/type XI hybrid molecules also exist in disc tissue. To test this possibility, we identified the molecular isoforms of type V/XI collagen present in the nucleus pulposus with a view to understanding how the type V/type XI chains are organized in the intervertebral disc matrix. Since collagen V/XI in general appears to act as a template in regulating the overall fibril architecture of a tissue, the unique organization of disc collagen may in part depend on a novel type V/XI phenotype.

Materials and Methods

Nucleus pulposus was dissected from lumbar spines of 3-month-old calves. Tissue slices were extracted in 4M guanidine HCl, 0.05M Tris-HCl, pH 7.4 containing protease inhibitors, at 4°C for 24 h to remove proteoglycans and other matrix proteins, then washed thoroughly with water and freeze-dried. Cross-linked collagens were solubilized by digesting the washed residues with pepsin at 4°C. Pepsin digests were fractionated into collagen types II, XI and IX by precipitation at 0.7M, 1.2M and 2.0M NaCl, respectively. The individual type XI/V chains were then resolved by HPLC on a C4 reverse-phase column with a linear gradient (18-28%) of solvent B in A over 40 min followed by SDS-PAGE. Mass spectrometry was performed on a ThermoFinnnigan LCQ Deca XP with electrospray ionization source and in-line C8 RP-HPLC. Individual protein bands after Coomassie Blue staining on SDS-PAGE were digested in-gel by trypsin. The resulting peptides were subjected to microbore column liquid chromatography (μLC) interfaced directly to a tandem mass spectrometer equipped with a micro-electrospray ionization source. For protein identification, peptide fragments were compared with the FBSC non-redundant protein database using SEQUEST, an automated database search algorithm designed for use with tandem mass spectrometry data.

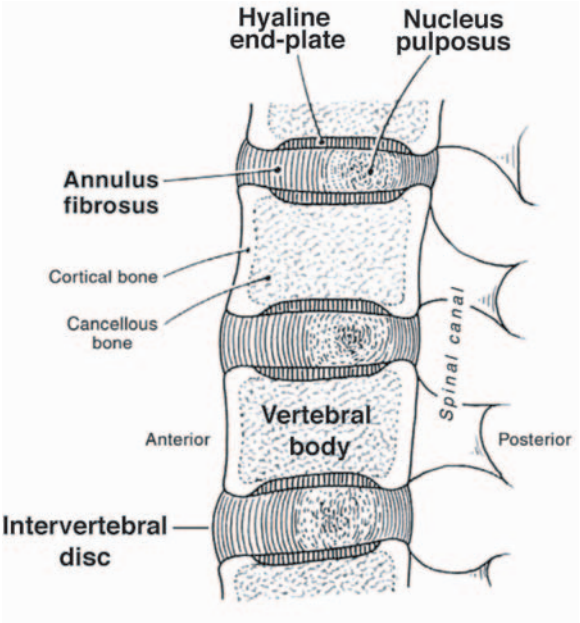

Figure 1: Diagram of disc architecture.

Results and Discussion

Using the two dimensional HPLC/SDS-PAGE method, we are able to resolve all five type V/XI gene products, α1(V), α2(V), α1(XI), α2(XI), and α3(XI) chains, from each other. An unexpected pattern was found in the nucleus pulposus. Instead of the 1:1:1 ratio of α1(XI): α2(XI): α3(XI) chains found in developing hyaline cartilage, two collagen V chains, α1(V) and α2(V), were also prominent in nucleus, despite the tissue being collagen type II-based (Figure 2). The chain identities, assigned from their elution on reverse-phase HPLC and migration on SDS-PAGE, were established beyond doubt by in-gel trypsin digestion, and microbore LC/mass spectrometry with data base matching (Figure 3).

Collagen type V/XI gene products are best considered as members of the same collagen subclass. In cartilage, the α1(V) chain becomes an integral component, increasing in proportion with increasing tissue maturity. Similarly in bone, the α1(XI) chain accumulates with developmental age in the type V collagen fraction in which it is incorporated with α1(V) and α2(V) chains to form an [α1(V) α1(XI) α2(V)]

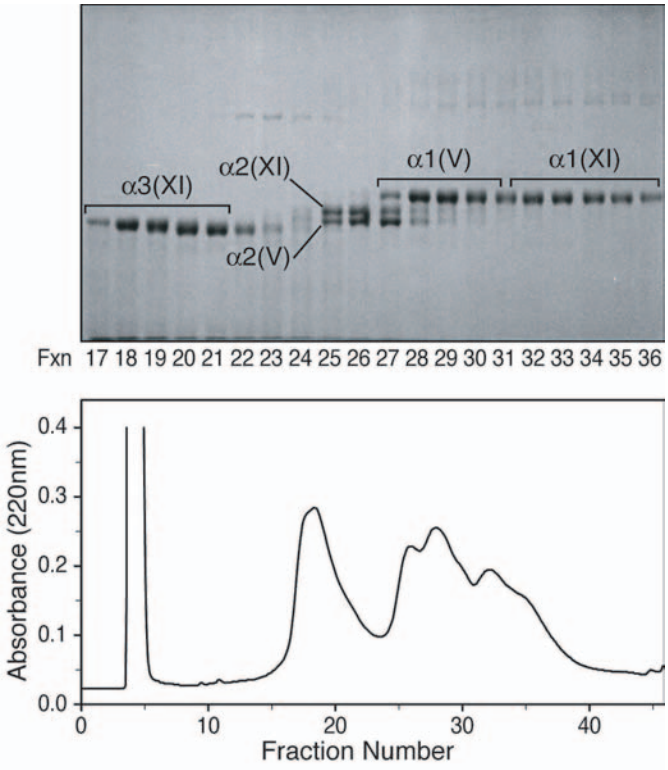

Figure 2: Reverse phase HPLC and SDS-PAGE two dimensional resolution of chain components of the collagen V/XI fraction from pepsin-digested bovine calf nucleus pulposus.

hybrid molecule. Hybrid molecules assembled from α1(XI) and α2(V) chains are also characteristic of bovine vitreous, an extracellular structure with similar physical properties to nucleus pulposus. Type I collagen is absent from nucleus pulposus, so the α1(V) and α2(V) chains are not simply due to a fibrocartilage collagen phenotype. Another difference between nucleus pulposus and hyaline cartilage is the expression of the short form of the α1(IX) chain in nucleus, a product of an alternative promoter which lacks the NC4 globular domain. This short form of the α1(IX) chain is also expressed in the vitreous but not hyaline cartilage. The present findings indicate that several heterotrimeric chain combinations are represented in the type V/XI collagen pool of the disc.

Collagen Chain	Sequence	Mass [M+H]+
α1(II)	GAQGPP*GATGFP*GAAGR	1501.6
(α3(XI))	GFTGLQGLP*GPP*GPSGDQGASGPAGPSGPR	2706.9
α1(XI)	TGPVGPQGPAGKP*GPEGLR	1789.0
	GPQGKPGLAGLP*GADGPP*GHP*GK	2111.3
α1(V)	TGPIGPQGAP*GKP*GPDGLR	1805.0
	GPNGPQGPTGFP*GPK	1424.6
α2(XI)	TGPVGPAGPAGKP*GPDGLR	1717.9
	LGVP*GLP*GYP*GR	1231.4
α2(V)	GLTGNP*GVQGPEGK	1327.4
	GDRGDP*GPAGLP*GSQGAP*GTP*GPVGAP*GDAGQR	3005.1

Figure 3: Tryptic peptides identified by in-gel trypsin digestion and mass spectrometry.

Conclusion

A unique molecular form of type V/XI collagen is revealed in the nucleus pulposus. Given the emerging role of type V/XI collagen in providing a template for the collagen macro-architecture of a tissue, this implies that the unusual organization and properties of disc collagen governed in part by the distinctive collagen V/XI phenotype.

Recommended Reading

Wu JJ and Eyre DR. (1995) Structural analysis of cross-linking domains in cartilage type XI collagen: Insights on polymeric assembly. J. Biol. Chem. 270(32):18865-18870.

Wu JJ and Eyre DR. (1995) Age-related changes in the chain isotypes of type XI collagen of articular cartilage. Trans. Ortho. Res. Soc. 20(2):406.

Niyibizi C and Eyre DR (1989) Identification of the cartilage alpha 1(XI) chain in type V collagen from bovine bone. FEBS Lett. 242:314-318.

Mayne R, Brewton RG, Mayne PM, and Baker JR. (1993) Isolation and characterization of the chains of type V/type XI collagen present in bovine vitreous. J. Biol. Chem. 268:9381-9386.

Wu JJ and Eyre DR (2003) Intervertebral disc collagen: usage of the short form of the α1(IX) chain in bovine nucleus pulposus. J. Biol. Chem. 278, 27521-27525.

Graduating Residents
Class of 2005

Anthony Buoncristiani, MD

Tony will begin a Sports Medicine Fellowship at University of Pittsburgh's Medical Center in August. Afterwards, he and his wife, Carina, plan on practicing in either Sun Valley Idaho or California. Tony's free time is spent with his wife, traveling, skiing, scuba diving, or going to the gym.

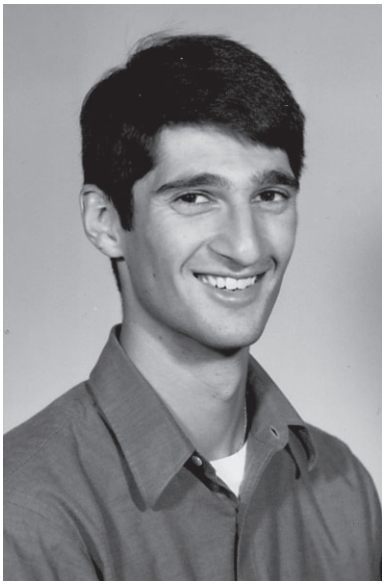

Waqqar Khan-Farooqi, MD

Following residency, Waqqar plans to pursue a fellowship in foot and ankle surgery in Charlotte, North Carolina. Waqqar, Thea, and their daughter Laila plan to return to the West Coast after fellowship.

Wren McCallister, MD

After residency, Wren will complete a fellowship in Hand and Microvascular Surgery here at the University of Washington. Thereafter, he will enter private practice with Stevens Orthopedic Group in Edmonds, Washington. Wren enjoys baseball, golf and reading but the activity he enjoys most is the one he shares with his wife Erika raising their son, Jackson Ryan.

Tim O'Mara, MD

Tim will stay in Seattle next year to spend a year as an ACE at Harborview Medical Center in orthopaedic traumatology. He will then travel to Sydney, Australia for a one-year fellowship in pediatric orthopaedics. Tim plans to return to his hometown to join the Reno Orthopaedic Clinic upon completion of his fellowship training.

David Stevens, MD

David will be continuing his training as a spine ACE here at the University of Washington affiliated hospitals. David will then practice at Mountain Orthopaedics in Bountiful, Utah upon completion of his fellowship.

Incoming Residents

Jason King

Jason attended the University of Washington where he received his Bachelor of Science degree in Chemical Engineering in 1992. He completed his Masters in Public Health UCLA in 2000 prior to medical school to gain a broader prospective of healthcare and acquire epidemiologic skill. He received his MD degree from Georgetown University School of Medicine, in Washington, DC in 2004. Free time is spent with his son and wife, but when there is opportunity, he loves to play golf, running, and shoot hoops.

Rajshri Maheshwari

Becoming a doctor was a goal for Raj. She received her Bachelor of Science degree in Biochemisty and Molecular Biology and graduated cum laude from Trinity University in San Antonio, Texas in 2000. She completed her MD from Baylor College of Medicine in Texas in 2004. She finds orthopaedic diseases and injuries intellectually challenging, but also finds the evaluation and treatment of the patients incredibly fulfilling.

Annie Links

Annie completed her Bachelor of Science degree in Zoology from the University of Washington in 1991 and at the same time exploring an interest in art by taking theater, drawing, and poetry classes. She received her MD from the University of Washington in 2004. She feels very fortunate to be in medicine, and grateful for the opportunity to pursue this rewarding career. She enjoys travel, drawing and painting and spending time with her family.

Soren Olson

Soren obtained his BS degree in Biomedical Engineering from the University of Southern California in 1999. He received his MD degree from the University of Washington School of Medicine in 2004. Soren states that in athletics, academics, medicine, or in any other arena of life, success begins with personal dedication, commitment, and passion. Soren enjoys volleyball, golf, skiing, playing guitar, backpacking, fly fishing, mountain biking, and reading.

Incoming Residents

Karen Perser

Karen's ultimate goal is to help people, and she can think of nothing more rewarding than caring for a person by restoring function, relieving pain, or correcting a deformity. Karen received her bachelor degree in Biological Sciences, Religious Studies from Southern Methodist University in 2000. She completed her MD from the University of Texas Medical School at Houston in 2004. She enjoys scuba diving, auto racing, cycling, camping, skiing, motorcycle riding, travel, and intramural sports.

Addison Stone

Addison obtained his BS degree in Biology from University of Vermont in 1997. He received his MD from the University of Wisconsin Medical School in 2004. He has many interests outside of medicine including woodworking, traveling, alpine skiing, mountain biking, canoeing, and backpacking. His involvement in extracurricular activities has fostered a solid work ethic, and taught him strong leadership and communication skills.

Scott Ruhlman

What attracts Scott most about orthopaedic surgery is the opportunity to operate, the spectrum of disease, and the personalities of the people in the profession. Scott completed his Bachelor of Science in Biology from Cedarville University in 2000. He received his MD from Medical College of Ohio in 2004. Scott enjoys golf, basketball, football, running, financial planning, cars, guitar, and piano.

Jason Wilcox

Jason obtained his BS degree in Pre-professional studies from the University of Norte Dame in 1998. He completed his MD from the University of Tennessee College of Medicine in 2004. Jason enjoys intramural softball and football, whitewater kayaking, rafting, mountain biking, and snow skiing.

ACEs

Foot/Ankle

Wesley P. Bevan, M.D.

Mark T. Gould, M.D.

Joel A. Moore, M.D.

Spine

Gavin J. Button, M.D.

Jason H. Thompson, M.D.

Trauma

Joseph M. Conflitti, M.D.

Gregory J. Della Rocca, M.D.

Arturo Gomez, M.D.

Greg M. Osgood, M.D.

David B. Weiss, M.D.

ACEs

Hand

Nikolaos Zagoreos, M.D.

Oncology

Andrew G. Howlett, M.D.

Shoulder/Elbow

Amy K. Franta, M.D.

Tim R. Lenters, M.D.

Fellows

Hand

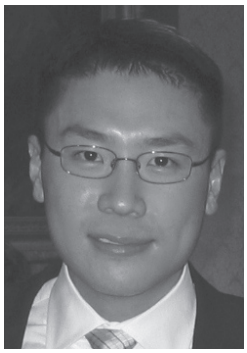

Thomas S. C. Lu, M.D.

Brian Miller, M.D.

Wayne M. Weil, M.D.

2005 Department of Orthopaedics and Sports Medicine New Faculty

Leonid I. Katolik, M.D.

A native of Philadelphia, Dr. Katolik graduated from the University of Pennsylvania with a degree in International Relations. He was inducted into the Alpha Omega Alpha National Medical Honor Society while at Hahnemann University School of Medicine, where he graduated with honors in 1998. Following his internship in general surgery at Hahnemann University Hospital in Philadelphia, he completed his training in Orthopaedic Surgery at Rush-Presbyterian-St. Luke's Medical Center in Chicago. Dr. Katolik spent a year as a Fellow in Hand and Microvascular Surgery at the University of Washington before accepting a position as Assistant Professor of Orthopaedic Surgery at the University of Washington School of Medicine. His clinical interests include sports injuries of the upper extremity, wrist arthroscopy, degenerative conditions of the elbow, and the treatment of complex fractures of the wrist and hand. He has contributed to numerous textbooks and journals on the treatment of upper extremity injuries. In his spare time, Dr. Katolik enjoys tennis, road bicycling, and snowboarding. Dr. Katolik sees patients at the University of Washington Bone and Joint Center, the Sports Medicine Center and the Eastside Specialty Clinic.

Department Photo

Left to right

Fourth Row: Jason King, 'Chappie' Conrad, Leo Katolik, Doug Smith, Evan Ellis, Rick Bransford, Ted Wagner, Mark Freeborn, Mel Wahl, M.L. 'Chip' Routt

Third Row: Sohail Mirza, Gregg Nicandri, Seth Leopold, Eric Klineberg, Joe Lynch, Howard Chansky, Bill Montgomery, Burt Yaszay, Christopher Howe, Jeremiah Clinton, Greg Schmale

Second Row: Sigvard Hansen, Carol Teitz, Drew Fehsenfeld, Mary Cunningham, Nancy Kadel, Jamie Antoine, Heidi Ambrose, John Howlett, Michael Lee, Allison MacLennan, Stacey Donion

Front Row: David Stevens, Tony Buoncristiani, Waqqar Khan-Farooqi, Frederick Matsen, Wren McCallister, Tim O'Mara

Research Grants

National Institutes of Health (NIH)

Augmentation of Peak Bone Mass
Ted S. Gross, Ph.D.

Chondrocyte, Chondrogenesis, and Histone Modification Enzymes
Liu Yang, Ph.D.

Collagens of Cartilage and the Intervertebral Disc
David R. Eyre, Ph.D.

Disuse Induced Osteocyte Hypoxia
Ted S. Gross, Ph.D.

Imaging of Molecules by Oscillator-Coupled Resonance
John A. Sidles, Ph.D.

Pathology of Inborn Skeletal Diseases
David R. Eyre, Ph.D.

Safety of Lumbar Fusion Surgery for Chronic Back Pain
Sohail K. Mirza, M.D.

Skeletal Dysplasias
David R. Eyre, Ph.D.

TLS and TLS Fusion Proteins in Leukemia
Liu Yang, Ph.D.

Veterans Affairs Rehabilitation Research and Development Service

Ewing's Sarcoma Fusion Proteins and mRNA Splicing Factors
Howard A. Chansky, M.D.

The Effect of Foot Morphology on Foot Function
Bruce J. Sangeorzan, M.D.

The Epidemiology of Foot Structure and Ulceration in Diabetic Veterans
Bruce J. Sangeorzan, M.D.

Transtibial Amputation Management Strategies
Bruce J. Sangeorzan, M.D.

VA Center of Excellence in Amputation Prevention and Prosthetic Engineering
Bruce J. Sangeorzan, M.D.

Orthopaedic Research and Education Foundation (OREF)

Overcoming Nerve Defect by Growth Factor Stimulated Regeneration Along Intact Nerves
Ben Dubois, M.D.
Thomas E. Trumble, M.D.

Reduction of Total Knee Arthroplasty Risk in Morbidly Obese Patients Using Laparoscopic Bariatic Surgery: A Prospective, Controlled Trial
Seth S. Leopold, M.D.

Splicing Factors Effect Chondrocyte Differentiation and Collagen Synthesis
Howard A. Chansky, M.D.
Eric O. Klineberg, M.D.
Liu Yang, Ph.D.

A.O. North America

AO Spine North America Fellowship
Carlos Bellabarba, M.D.

Stability After Pin Versus Dorsal Plate Fixation of Simulated Interarticular Distal Radius Fractures: A Biomechanical Investigation
Thomas E. Trumble, M.D.
Wren V. McCallister, M.D.

Amgen, Inc.

Inhibition of Muscle Paralysis Induced Bone Loss by OPG
Ted S. Gross, Ph.D.

Centers for Disease Control

Chest Injuries Due to Motor Vehicle Side Impacts
Allan F. Tencer, Ph.D.

Defense Advanced Research Projects Agency

Achieving Molecular Observation in Four Years
John A. Sidles, Ph.D.

Research Grants

Genetics Institute

A Feasibility and Safety Study of rhBMP-2/ACS and Allograft Compared to Autogenous Bone Graft for Patients with Severe Tibial Shaft Fractures
Sohail K. Mirza, M.D.

Integra Lifesciences Corporation

Comparison of Bioabsorable Tubes for Repair of Nerve Injury
Thomas E. Trumble, M.D.

International Business Machines

System Control for Magnetic Resonance Force Microscopy
John A. Sidles, Ph.D.

National Science Foundation

Direct 3D Imaging of Molecular Structure: Quantum Sensing and Control
John A. Sidles, Ph.D.

Tissue-Engineered Digit Replacement
Christopher H. Allan, M.D.

Novartis Pharmaceuticals Corporation

Cartilage Collagen Study
David R. Eyre, Ph.D.

Orthopaedic Trauma Association

Immediate vs. Delayed Closure of Type II and IIIA Open Tibia Fractures
M. Bradford Henley , M.D.

Percutaneous Pinning versus Open Reduction and Internal Fixation of Proximal Humeral Fractures: A Prospective and Randomized Comparison of Outcomes
Sean E. Nork, M.D.

Ostex International, Inc.

Molecular Markers of Connective Tissue Degradation
David R. Eyre, Ph.D.

Synthes Spine Co.

PRODISC-C Versus Anterior Cervical Discectomy and Fusion (ACDF)
Jens R. Chapman, M.D.

Spine End-Results Research Fund
Frederick A. Matsen III, M.D.

The Boeing Company

Randomized Clinical Trial of Open versus Endoscopic Carpal Tunnel Release and Hand Therapy Comparing Patient Satisfaction: Functional Outcome and Cost Effectiveness
Thomas E. Trumble, M.D.

Tyco Healthcare

Interdiscal Electrothermography (IDET) in Cervical Discs
Allan F. Tencer, Ph.D.

US Army Research Office

UW Team-Advance on Single Nuclear Detection and Atomic-Scale Imaging
John A. Sidles, Ph.D.

Washington Woman's Foundation

Strengthening the Femoral Neck to Prevent Hip Fractures caused by Osteoporosis
Frederick A. Matsen III, M.D.

Whitaker Foundation

Examining Processes Underlying the Dramatic Osteogenic Response Elicited by Rest-Inserted Loading
Sundar Srinivasan, Ph.D.

Zymogenetics, Inc.

Recombinant Human Thrombin Trial
Sohail K. Mirza, M.D.

Resident Research Awards

VICTOR FRANKEL RESIDENT RESEARCH AWARD

Presented to these residents in Orthopaedic Surgery for Excellence in Clinical or Basic Science Research

Timothy P. Lovell- 1990
Mohammad Diab- 1992
P. Brodie Wood- 1994
William J. Mills, Jr., M.D.- 1995
Peter T. Simonian, M.D.- 1996
Daniel J. Stechshulte, Jr. M.D. Ph.D.- 1997
Ben DuBois, M.D.- 2002

THE EDWIN L. LAURNEN AWARD

Established in 1993 by Edwin L. Laurnen for the Best Resident Paper in Spine Research

Sohail K. Mirza- 1994
Peter T. Simonian, M.D.- 1995
Randall W. Viola, M.D.- 1996
Jason Thompson, M.D. - 2003

THE ESTHER WHITING AWARD

Established in 1977 by J. Irving Tuell, M.D. for the Best Resident Paper with an Historical Orientation

William Oppenheim- 1977
Stuart Hutchinson- 1978
John M. Clark- 1981
Joseph Zuckerman- 1981
Marc Swiontkowski- 1982
Marc Swiontkowski- 1983
Richard Barry- 1984
James Crutcher- 1987
James Crutcher- 1988
Nancy Ensley- 1988
Eric Vanderhooft- 1990
Curt Rodin – 1992
James W. Vahey- 1993
Timothy C. Beals- 1994
David J. Belfie- 1997
Andrew Howlett - 2003

Contributors to Departmental Research and Education

April 2004 Through March 2005

We express our appreciation to all who have contributed to the work of the Department of Orthopaedics and Sports Medicine over the past year. Your assistance makes possible special research activities, educational programs, and other projects that we could not offer without this extra support from our alumni, faculty, and friends in the community. We owe a special thanks to the University of Washington Resident Alumni who have made significant contributions to help further the education of our current residents. We have tried to include in this list all who contributed; if anyone was overlooked, please be sure to let us know!

Friends of Orthopaedics

Elizabeth Abu-Haydar
Aircast
Jeffrey Akeson
Christopher Allan
Nancy Allan
Arnold Altamirano
Noemi Altamirano
Franklin Alvine
Marilyn Alvine
American Society of Biomechanics
AO North America
Dheera Ananthakrishnan
Gilbert Anderson
Mary Anderson
Douglas Armintrout
Elizabeth Armintrout
Michael Aronow
Allan Bach
Carol Bach
Martha Baker
Samuel Baker
Ballard Orthopedic and Fracture Clinic
Bank of America Foundation
David Barei
Lauren Barrett
William Barrett
Richard Barry
Timothy Beals
Christian Bean
Carlo Bellabarba
Ron Beman
Stephen Benirschke
Colleen Bergman
Gary Bergman
Bill Blackburn
Kathy Bloomer
Jonathan Braman
Stephanie Braman
Richard Bransford
John Brown
Kay Brown
Shirley Burbach
Michael Cero
Susan Cero
Howard Chansky
Kari Chansky
Jens Chapman
Gary Clancey
Paula Clancey
John Clark
Burnet Clarke
Crissy Clarke
Joseph Clifford
The C.F. Sauer Company
Sheldon Cober
Chappie Conrad
Marjolyn Conrad
Richard Conrad
Gilbert Contreras
Jay Crary
James Crutcher
Jill Crutcher
Dorothy Davis
Frederick Davis
Susan DeBartolo
DePuy Orthopaedics
Richard Dimond
Oriente Ditano
Brady and Anne Elliott
Leonard Ely
Karl Engdahl
Donald Ericksen
Sara Ericksen
Larry Erickson
Virginia Erickson
David Eyre
Susan Eyre
Cynthia Farrar
Edward Farrar
F.J.D. Enterprises
Cheryl Flugstad
Daniel Flugstad
Trygve Forland
Elizabeth Forney
Harold Forney
Cynthia Franklin
Jonathan Franklin
Candice Frias
Michael Gannon
Park Gloyd
Loeta Goodnight
Janet Grant
William Grant
Richard Greaves
Nanci Green
Patrick Green
Thomas Green
Green Mountain Orthopedic Surgeons
Sandra Greenlee
Ted Greenlee
Karen Gritzka
Thomas Gritzka
Ted Gross
Doug Hanel
Margaret Hanel
Dalia Hansen
Jeffrey Hansen
Sigvard Hansen
Susan Heckbert
Helena Orthopaedic Clinic
John Hendrickson
Brad Henley
Amy Hirasawa
Joel Hoekema
Karin Hoekema
George Hopwood
Bill Hoglund
Lannie Hoglund
Scott Hormel
Shari Hormel
Frederick Huang
Jennifer Hubbert
Frances Huisman
Larry Hull
Illinois Orthopaedic and Hand Center
Judith Irons
Sarah Jackins
Colleen Johnson
Janet Johnson
Nancy Kadel
David Karges
Gail Karges
Susan Karnezis
Tom Karnezis
Carleton Keck
Betsy Kirby
Richard Kirby
Jonathan Knight
Elizabeth Krengel
Walter Krengel
Gladys Kretzler
Harry Kretzler
Wanda Ledbetter
William Ledbetter
Elizabeth Leedom
William Leedom
Seth Leopold

Friends of Orthopaedics

David Levinsohn
George Luck
Jean Mainelli
Deborah Malestky
John Malestky
Diane Mankey
Martin Mankey
Judith Matchett
William Matchett
Anne Matsen
Frederick Matsen
Gregory May
Heather McAdam
Michael Metcalf
Becky Mezistrano
Joseph Mezistrano
Jean Michele
John Michelotti
Microsoft Corporation
Midwest Orthopaedic Center
Ralph Miller
Carey Mills
William Mills
Atiyya Mirza
Sohail Mirza
Leslie Morris
Michael Morris
Vince Mosca
Furman Moseley
Susan Moseley
Marr Mullen
Mark Murphy
Gary Glancey Nelson
Neuromusculoskeletal Center
Nevada Community Foundation
Kathy Nguyen
Sean Nork
Edward North
Jan Northrop
Northwest Biomet
Northwest Orthopaedic Physicians
William Oppenheim
Pacific Medical
Pacific Orthopaedics
Pacific Rim Orthopaedic Surgeons
Lawrence Page
Jennifer Patriarche
Michael Patriarche
Susan Peters
Mary Pleger
Proliance Surgeons
Linda Quan
Shawn Quigley
Gregory Rafijah
Marijo Ratcliffe
Steven Ratcliffe
Victoria Reed
William Reed
Reliable Furniture Service
Mark Remington
Robert Ripley
Kearney Robert
Kristine Roberts
Rodney Roberts
Charles Rockwood
M.L. Chip Routt
Ann Rutledge
STH Foundation
Michael Sailer
Shelly Sailer
Bruce Sangeorzan
Mary Sangeorzan
Shanon Sara
Kenichi Sato
Sarah Sato
C.F. Sauer III
C.F. Sauer IV
Matthew Sauer
Greg Schmale
Sarah Schmale
Kevin Schoenfelder
The Seattle Foundation
Seattle Hand Surgery
Andrea Semon
Richard Semon
Wolfram Shulte
Geoffrey Sheridan
Constance Sidles
John Sidles
Patricia Simonian
Peter Simonian
Simonian Sports Medicine Clinic
Smith & Nephew Richards Inc
Carla Smith
Doug Smith
Kathryn Smith
Kevin Smith
Patricia Sobeski
Kit Song
Debbie Southern
Larry Southern
Robert Stack
Staheli Inc
Lana Staheli
Lynn Staheli
Susan Stephens
Jeffrey Stickney
Kathleen Stickney
Edward Stokel
Donald Striplin
Stryker
Stryker Biotech
Surg-Elite Inc
Marc Swiontkowski
Synthes USA
Harriette and Charles Tabas
Lisa Taitsman
Carol Teitz
Allan Tencer
David Thayer
Dorna Theaman
Mark Theaman
Arrol Thieme
William Thieme
Karen Thomas
Steven Thomas
Michael Thorpe
Sonja Thorpe
Delvin Tingwall
Christian Treuer
Cynthia Tronsrue
George Tronsrue
Dawn Trudeau
Maureen Trumble
Thomas Trumble
Diane Tullus
Martin Tullus
United Way of King County
A.P. Van Meter
Mary Van Meter
J. Eric Vanderhooft
Sheryll Vanderhooft
Nicholas Vedder
Robert Veith
Iris Wagner
Ted Wagner
William Wagner
Charles Wahtola
Michael Walsh
Washington Hand Surgery
Edward Weinberger
Neil Wells
John West
Maureen West
Janet Wierenga
Sarah Wilder
Thomas Wilder
Doris M. Wilkinson
Georgia Rae Williams
Judith Winquist
Robert Winquist
Jay Winzenried
Emma Woodhouse
Jiann-Jiu Wu
Hansjoerg Wyss
Xelan Foundation
Yancey & Associates
Liu Yang
Pam Young
Ralph Young
Jane Younge
Zimmer
Zimmer Northwest
Tom Zorich

Alumni

1952
Park W. Gloyd, M.D. ★

1954
Trygve Forland, M.D. ★

1955
Robert W. Florence, M.D.

1956
J. Michael Egglin, M.D. ★
John E. Goeckler, M.D.
Robert L. Romano, M.D.

1957
John H. Aberle, M.D. ★
John R. Beebe, M.D.

1958
Harry H. Kretzler, Jr., M.D. ★
James R. Friend, M.D. ★
Kenneth L. Martin, M.D. ★
Samuel L. Clifford, M.D.

1959
James W. Tupper, M.D.

1960
Irving Tobin, M.D. ★
William V. Smith, M.D. ★

1961
Robert C. Colburn, M.D.

1962
Arthur Ratcliffe, M.D.
Marr P. Mullen, M.D. ★

1963
Alfred I. Blue, M.D.
Robert A. Kraft, M.D.

1964
David E. Karges, M.D. ★★★
Harold J. Forney, M.D. ★
Theodore K. Greenlee II, M.D. ★★★★★
Thomas E. Soderberg, M.D.

1966
F. Richard Convery, M.D. ★
Joseph S. Mezistrano, M.D. ★
William A. Reilly, Jr., M.D.

1967
Ivar W. Birkeland, M.D.
J. Conrad Clifford, M.D.
Robert F. Smith, M.D. ★★★★★

1968
Lynn T. Staheli, M.D. ★
Stewart M. Scham, M.D. ★
William T. Thieme, M.D. ★

1969
Edward E. Almquist, M.D. ★★
Edward L. Lester, M.D.
Hugh E. Toomey, M.D. ★★★
Sigvard T. Hansen, Jr., M.D. ★★★

1970
John C. Brown, M.D. ★
John M. Coletti, Jr., M.D. ★
Malcolm B. Madenwald, M.D. ★
Michael T. Phillips, M.D. ★
Robert D Schrock, Jr., M.D.

1971
Bruce E. Bradley, Jr., M.D.
Franklin G. Alvine, M.D. ★★★
Jerome H. Zechmann, M.D.
Louis A. Roser, M.D. ★
Nils Fauchald, Jr., M.D.

1972
David J. LaGasse, M.D.
David R. Nank, M.D. ★★
Donald D. Hubbard, M.D. ★
John A. Neufeld, M.D. ★
Thomas L. Gritzka, M.D. ★

1973
Frederick J. Davis, M.D. ★
Larry D. Hull, M.D. ★
Robert P. Watkins, Jr., M.D. ★
Theodore A. Wagner, M.D. ★★★★★

1974
Richard A. Dimond, M.D. ★★
Ronald B.H. Sandler, M.D. ★★★
Samuel R. Baker, M.D. ★★
Robert A. Winquist, M.D. ★★★★★

1975
Donald L. Plowman, M.D. ★★★
Frederick A. Matsen III, M.D. ★★★★★
Gunter Knittel, M.D.
Larry R. Pedegana, M.D. ★
Thomas M. Green, M.D. ★★★★
William M. Backlund, M.D., P.S. ★

1976
Douglas K. Kehl, M.D.
Douglas T. Davidson III, M.D. ★
John F. Burns, M.D.
Peter Melcher, M.D.
Richard A. Zorn, M.D. ★

1977
Carl A. Andrews, M.D. ★
Geoffrey W. Sheridan, M.D. ★★
Larry D. Iversen, M.D. ★
Mark C. Olson, M.D. ★
Steven T. Bramwell, M.D.

1978
Arnold G. Peterson, M.D. ★★★★
Gary J. Clancey, M.D. ★★★
John W. Brantigan, M.D.
Richard S. Westbrook, M.D. ★★
Robert J. Strukel, M.D.
William Oppenheim, M.D. ★

1979
Allan W. Bach, M.D. ★★★★
Gregory M. Engel, M.D. ★★
Jonathan L. Knight, M.D. ★★
Richard L. Semon, M.D. ★★★

1980
Carol C. Teitz, M.D. ★★
Douglas G. Norquist, M.D.
John M. Hendrickson, M.D. ★★
Michael A. Sousa, M.D. ★★
Stuart R. Hutchinson, M.D. ★

1981
Dennis J. Kvidera, M.D. ★
John M. Clark, Jr., M.D., Ph.D. ★★★
Martin S. Tullus, M.D. ★★★★
Robert G. Veith, M.D. ★★★★★

1982
John L. Thayer, M.D. ★
Richard M. Kirby, M.D. ★★★★★
Steven S. Ratcliffe, M.D. ★★
William D. Burman, M.D.

1983
E. Anne O. Elliot, M.D. ★
Edward L. Farrar III, M.D. ★★★★
Henry K. Yee, M.D.
Joseph D. Zuckerman, M.D. ★★★★
Keith A. Mayo, M.D. ★★★
Robert M. Berry, M.D.

1984
Jeffrey C. Parker, M.D. ★
Jeffrey W. Akeson, M.D. ★★★
Kevin P. Schoenfelder, M.D. ★
Marc F. Swiontkowski, M.D. ★★★★★
Thomas J. Fischer, M.D. ★★★★

1985
Daniel L. Flugstad, M.D. ★★★
Jeffrey N. Hansen, M.D. ★★★
Paul J. Abbott, M.D. ★★★
Richard J. Barry, M.D. ★
William P. Barrett, M.D. ★★★★★

1986
Carleton A. Keck, Jr., M.D. ★★★
Gary Bergman, M.D. ★★★★★
Lawrence E. Holland, M.D. ★
Michael E. Morris, M.D. ★★★★

1987
Craig T. Arntz, M.D. ★★
Herbert R. Clark, M.D. ★★
Michael K. Gannon, M.D. ★
Steven L. Reed, M.D. ★

1988
Jonathan L. Franklin, M.D. ★★★★
Michael A. Thorpe, M.D. ★★★★★
Richard V. Williamson, M.D. ★

1989
James P. Crutcher, M.D. ★★★★
Lawrence V. Page, D.O. ★
Martin G. Mankey, M.D. ★★★
Nancy J. Ensley, M.D.
Steve C. Thomas, M.D. ★★★

1990
David M. Kieras, M.D. ★
J. Roberto R. Carreon, M.D.
Jay A. Winzenried, M.D. ★★
Ken Fujii, M.D. ★
Walter F. Krengel III, M.D. ★★

1991
David H. Bishop, M.D. ★★
Kit M. Song, M.D.
Mark Remington, M.D. ★★★
Mark E. Murphy, M.D., Ph.D. ★
Tim P. Lovell, M.D. ★★

1992
Curt Rodin, M.D.
Don Striplin, M.D. ★★
Eli Powell, M.D. ★
Jeff Stickney, M.D. ★
John D. West, M.D. ★
Michael Sailer, M.D. ★★

1993
J. Eric Vanderhooft, M.D. ★★★★
Lyle S. Sorensen, M.D. ★★★★★
Philip J. Kregor, M.D. ★★
Susan R. Cero, M.D. ★★★

1994
Brodie Wood, M.D. ★★
Eric Bowton, M.D. ★
Jim Vahey, M.D. ★
Sohail K. Mirza, M.D.
William Obremskey, M.D. ★★

1995
Ron Kristensen, M.D. ★
Scott Hormel, M.D. ★★
Timothy Beals, M.D. ★
Todd Clarke, M.D. ★★
William J. Mills III, M.D. ★

1996
David Deneka, M.D. ★
Peter Mitchell, M.D. ★★
Peter T. Simonian, M.D. ★★★
Vernon Cooley, M.D. ★
William Wagner, M.D. ★★★

1997
Daniel Stechschulte, Jr., M.D.
David Levinsohn, M.D. ★
L. Anthony Agtarap, M.D. ★
Mohammad Diab, M.D.
Randall W. Viola, M.D.

1998
Colin Poole, M.D. ★
David Belfie, M.D. ★
Don Ericksen, M.D. ★★★
Jay Crary, M.D. ★★
Oriente DiTano, M.D. ★

1999
Craig Boatright, M.D.
Jeffrey Garr, M.D.
John Michelotti, M.D. ★
Julie A. Switzer, M.D.
Thomas D. Chi, M.D. ★

2000
Brett Quigley, M.D. ★
Cara Beth Lee, M.D.
Daniel Jones, M.D. ★
Joel Hoekema, M.D. ★
Patrick McNair, M.D.

2001
Eric Novack, M.D.
Frederick Huang, M.D. ★
Matthew Camuso, M.D.
Michael Metcalf, M.D. ★
Richard Bransford, M.D.

2002
Timothy DuMontier, M.D.
Scott Hacker, M.D.
Timothy Rapp, M.D.
William Sims, M.D. ★
Carla Smith, M.D. ★

2003
Ben DuBois, M.D.
Andy Howlett, M.D.
Guy Schmidt, M.D. ★
Brian Shafer, M.D.
Emma Woodhouse, M.D. ★

2004
Jon Braman, M.D. ★
Alexis Falicov, M.D.
Mike McAdam, M.D. ★
Jason Thompson, M.D.
Thea Khan-Farooqi, M.D.

2005
Tony Buoncristiani, M.D.
Waqqar Khan-Farooqi, M.D.
Wren McCallister, M.D.
Tim O'Mara, M.D.
David Stevens, M.D.

STARS INDICATE TOTAL DONATIONS IN SUPPORT OF THE RESIDENCY

★★★★★ = $10,000 and over
★★★★ = $7,500 - $9,999
★★★ = $5,000 - $7,499
★★ = $2,500 - $4,999
★ = $1 - $2,499

Endowments

We express our appreciation to all who have contributed to the endowments of the Department of Orthopaedics and Sports Medicine. Your assistance makes possible special research activities, educational programs, and other projects that we could not offer without this extra support from our alumni, faculty, and friends in the community. Additional Contributions to these and new endowments are most welcome! If you have any questions, please contact our Chair, Rick Matsen, or our Administrator, Ken Karbowski.

Hansjoerg Wyss Endowed Chair

Ernest M. Burgess Endowed Chair for Orthopaedics Investigation

Sigvard T. Hansen Jr. Endowed Chair in Orthopaedic Traumatology

Jerome H. Debs Endowed Chair in Orthopaedic Traumatology

Endowed Chair for Women's Sports Medicine and Lifetime Fitness

Surgical Dynamics Endowed Chair for Spine Research

Douglas T. Harryman II/DePuy Endowed Chair for Shoulder Research

Synthes Spine End Results Endowed Chair

Zimmer Fracture Fixation Biology Endowed Professorship

Ostex Bone and Joint Research Endowment

Orthopaedic Traumatology Endowed Lectureship

John F. LeCocq Lectureship in Orthopaedic Surgery

Don and Carol James Research Fund in Sports Medicine and Fitness

James G. Garrick Lectureship in Sports Medicine

Regenerative Spine Surgery Endowed Professorship

Victor H. Frankel Award

Esther Whiting Award

Ed Laurnen Award

Spine Research Endowment